PRODUCTION OF FUELS AND CHEMICALS FROM BIOMASS-DERIVED OIL AND LARD

A Thesis Submitted to the College of Graduate Studies and Research
in partial fulfilment of the requirements for the degree of
Master of Science
in the Department of Chemical Engineering
University of Saskatchewan
Saskatoon, Saskatchewan

By

Adenike Adebanjo

COPYRIGHT

ABSTRACT

Biomass derived oil (BDO) reforming with CO_2 was carried out at 800^oC under atmospheric pressure in a tubular fixed bed vertical reactor packed with quartz particles. The feed gas was a mixture of CO_2 and N_2 at various compositions with a flow rate of 30 to 60 cm^3/min. The BDO flow rate was 5 g/h. The product gas consisted mostly of H_2, CO, CO_2, CH_4 and C_2H_4.

The maximum production of synthesis gas (~76 mol%) was observed at a total carrier gas flow rate of 60 cm^3/min and a mole fraction of CO_2 in carrier gas of 0.1. Maximum hydrogen (42 mol%) and H_2 to CO molar ratio (1.44) were obtained while using only N_2 as the carrier gas at a flow rate of 50 cm^3/min. In the range of residence time considered, CO_2 was not consumed in BDO gasification at 800^oC but helped to increase gas production at the expense of the char.

Pyrolysis of lard was performed to produce a diesel-like liquid and a high heating value gaseous fuel. Lard was fed into the reactor at 5 g/h using N_2 (10-70 cm^3/min) as carrier gas. Two particle size ranges of quartz particles (0.7-1.4 and 1.7-2.4 mm) were used as reactor packing material. The liquid product essentially consisted of linear and cyclic alkanes and alkenes, aromatics, ketones, aldehydes and carboxylic acids. The maximum yield for diesel-like liquid product (37g/100g lard) was obtained at 600^oC, residence time of 1.5 s and packing particle size of 1.7- 2.4 mm. The liquid product obtained at 600^oC, carrier gas flow rate of 50 cm^3/min and quartz packing particle size of 0.7-1.4 mm has a cetane index of 46, specific gravity of 0.86, a heating value of 40 MJ/kg and cloud and pour points of 10 and -18 respectively. The heating value of the

product gas ranged between 68 and 165 MJ/m^3. This study shows that there is a potential for producing diesel-like liquid from pyrolysis of lard. It also identifies the pyrolysis of animal fats as a source of high heating value gaseous fuel.

Steam reforming of lard was performed at 500, 550, 600 and 800^oC and at steam to lard mass ratios of 0.5 to 2.0. The maximum diesel-like liquid yield from the steam reforming process (39 g/100g of lard) was obtained at a steam to lard ratio of 1.5 and a temperature of 600^oC. Higher cetane index (52) and lower viscosity (4.0 mPa.s at 40^oC) were obtained by addition of steam. The net energy recovered from pyrolysis and steam reforming processes were 21.7and 21.9 kJ/g of lard respectively. Thus, the processes are energy efficient.

In comparison, lard is a better feedstock for the production of hydrogen, char, high heating value gas and high H_2/CO ratio than BDO. On the other hand, BDO is the preferred feedstock for the production of synthesis gas with H_2/CO in the vicinity of 1.

ACKNOWLEDGEMENT

I would like to express my sincere appreciation to Prof. A. K. Dalai whose guidance throughout my graduate program has contributed immensely to the success of this work. I am also indebted to my co-supervisor Prof. N.N Bakhshi for his guidance, understanding and the fatherly role he played in the course of this program. My special thanks go to the remaining members of my advisory committee, Profs. D.Y. Peng and Hui Wang for their helpful discussions and suggestions.

I am also grateful to Messrs. T. Wallentiny, R. Blondin and D. Cekic of the Chemical Engineering Department for their technical assistance at various stages of this work and K. Thoms of Saskatchewan Structural Science Center for his help with the GC-MS studies. I appreciate the cooperation and useful discussions of Drs. H. K. Mishra, D. D. Das and M. Kulkani. Many thanks go to my friends (Janny Bos, Bimpe Akinlade and others) for their understanding, cooperation and support through out the period of my graduate program. I am especially grateful to my mother, sisters, and brothers for their enthusiastic support which encouraged me throughout my academic pursuits. I am also grateful to Dr I. Oguocha, Mr T. Ajala and E. Gikunoo, all of Mechanical Engineering department and to Crystal Stadnyk of the Information Technology Services for their useful information and suggestions on the use of MS Word. The research was made possible by the financial assistance from the Canada Research Chair program to Prof. A. K. Dalai. Above all, I am grateful to the Almighty God for His preservation of life, grace and good health towards the completion of this program.

DEDICATION

This work is dedicated to

My mother, Mrs G.A. Adebanjo

TABLE OF CONTENTS

LIST OF TABLES

LIST OF FIGURES

NOMENCLATURE

amu	atomic mass unit
CI	Cetane index
i.d.	Internal diameter (mm)
G	specific gravity at room temperature
MSDS	Material Safety Data Sheet
NIST	National Institute of Standard and Technology
T_{50}	mid boiling temperature (^{o}C)

1. INTRODUCTION

The massive energy crunch triggered by the 1973 oil price hike led to the revival of interest in non-conventional and renewable energy sources worldwide. Thus, along with the solar and the wind energy, the long neglected but potentially rich biomass became the focus of intensive utilisation for energy generation (Robertson, 1981). The increase in greenhouse gas emissions and the resulting climatic changes have understandably caused worldwide concern. According to an assessment by the Intergovernmental Panel on climate change (Watson, 2001); the rise in the average temperature by the end of the next century, i.e., 2100 will be between 1 - 3.5^{o}C. This has serious implications on the entire ecosystem. This fact has led to a series of initiatives at the international level to develop eco-friendly alternatives that would meet the needs of the present generation without compromising the abilities of future generations. This calls for urgent measures for minimizing, if not replacing, the reliance on fossil fuels to meet the increasing energy requirements. Therefore, the non-conventional renewable sources of energy have become the focus of research.

Wood and other forms of biomass are one of the main renewable energy sources available and provide liquid, solid and gaseous fuels. The global potential of primary biomass (in about 50 years) is very broad, quantified at 33-1135*10^{15}Jy^{-1} (Hoogwijk *et al*, 2003). But for biomass to effectively compete with fossil fuel there is need to explore more economic sources of biomass. Biomass waste is really cheap; in fact millions of dollars are used for its disposal annually. It is therefore of great interest to present one of

the possibilities of converting these problematic wastes into ecologically friendly fuels. The use of biomass as fuels help to reduce the greenhouse gas emission because the CO_2 released during combustion or conversion of biomass to chemicals is that removed from the environment by photosynthesis during the production of the biomass (i.e. plant growth).

1.1 Problem Identification

The initial objective of this research was to maximize the consumption of CO_2 in biomass-derived oil (BDO) reforming to syn-gas and other value added chemicals. This objective was coined from an earlier study on BDO gasification in CO_2/N_2 environment (Panigrahi, 2003). In that study, it was observed that there was a significant decrease in the mole fraction of CO_2 in the product gas due to increase in the mole fraction of CO_2 in the feed gas. However, in this present research, it was observed that increasing CO_2 in the feed rather increased its mole fraction in the product gas.

From this observation, the focus of the research was changed. Another feed stock was considered for the second phase. The justifications for considering these two phases are explained below.

1.1.1 CO_2 reforming of biomass derived oil

At present, technologies exist to pyrolyse biomass to produce a liquid product, namely, biomass-derived oil (BDO). But this BDO is quite unstable. Its physical properties have been shown to change over time (Adjaye *et al*, 1992; Meier *et al*., 1997). Therefore there is need to convert it to more stable fuels and chemicals such as syn-gas. Syn-gas plays an important role as intermediate in the production of several industrial

products such as Fischer-Tropsch liquids, methanol, and ammonia (Bharadwaj and Schmidt, 1995).

Greenhouse gases such as CO_2 in the atmosphere decrease the escape of terrestrial thermal infrared radiation. With the industrial growth, the burning of coal, oil and natural gas keeps increasing, and thus results in increased quantities of CO_2 released into the atmosphere (Rathi, 1994). Increasing CO_2 release into the atmosphere definitely caused an increase in radiative energy retained within the atmosphere. CO_2 reforming (Snoeck and Froment, 2002), has been proposed as a promising technology because of the use of the greenhouse gas CO_2. By using CO_2 in BDO reforming to value added products, an increased sink is found for the greenhouse gas.

1.1.2 Diesel fuel production from animal fats

Saskatchewan's livestock industries continue to grow and expand at a competitive rate with the rest of the nation. According to a release from Statistics Canada in July 2004, Saskatchewan now contributes 28.1 % of the Canadian beef cow head (Russell and Cannon, 2004). Also, pork production continues to increase as more hog production facilities are built throughout the province. Because meats cannot be produced without the simultaneous production of fat, a large amount of animal fat is unavoidably produced in the process of supplying meat.

Formerly, about 80% of the global animal fats production was consumed by humans (Gunstone, year unknown) but because of the health problems associated with the overuse of saturated fat in the diet, this percentage has fallen (Sanford and Allshouse, 1998). Also due to the recent bovine spongiform encephalopathy (BSE) crisis, the use of animal derived products to feed cattle is now severely restricted (Chaala

and Roy, 2003). This implies that a huge amount of animal fat is unavoidably available as waste.

Using animal fat as fuel could help to solve the problem of waste disposal (Wiltsee, 1998). The transesterification process for the production of biodiesel from vegetable oils is not very efficient with animal fats (GOE, 1999) due to high water content and free fatty acids. Pyrolysis is more efficient in converting animal fats into diesel fuel (Zhenyi *et al*, 2004).

In this present investigation, lard was used as a representative feed material for animal fats. The choice of lard was based on the fact that it is readily available in a pure form. Lard is a waste product of pork production. It is produced from the fatty or otherwise unusable parts of pig carcasses.

1.2 Research Objectives

1.2.1 CO_2 reforming of biomass derived oil

The intent here was to investigate the role of CO_2 in BDO reforming to syn-gas and gaseous fuels and to maximize the consumption of CO_2. The experiments were conducted at 800^oC in a fixed bed reactor based on earlier studies (Panigrahi, 2003). The mole fraction of CO_2 in N_2 was varied from 0 to 1 and the total gas flow rate was varied from 30 to 60 cm^3/min (STP).

1.2.2 Pyrolysis of lard

The aim here was to optimise the production of diesel-like liquid from lard pyrolysis. The possibility of producing syn gas from lard at higher temperature was also investigated. The reaction temperature was varied from 500 to 800^oC while the carrier

gas (N_2) flow rate was varied from 10 to 70 cm^3/min. These experiments were conducted in the same fixed bed reactor used for CO_2 reforming of BDO.

1.2.3 Steam reforming of lard

In this stage, the role of steam in pyrolysis of lard was investigated. The experiments were conducted in the temperature range of 500 to 800^oC. The aim was to further optimize the diesel-like liquid production and to improve on syn gas production.

The properties of the total liquid products obtained for lard pyrolysis and steam reforming such as density, viscosity, cetane index and heating value were determined using standard methods used for characterizing diesel fuel. These properties were compared to that of the conventional diesel fuel.

2. LITERATURE REVIEW

This section reviews studies on thermal treatment of biomass-derived oil (BDO) and animal fat. Emphasis is placed on BDO preparation, characterization, pyrolysis and CO_2 reforming and fats and oils pyrolysis, and reaction pathway.

2.1 Biomass-Derived Oil

2.1.1 Production of BDO via pyrolysis of biomass

The pyrolysis of biomass is a thermal treatment which results in the production of char, liquid and gaseous products. Pyrolysis is the general term to describe the process whereby organic material is heated essentially in the absence of oxidizing agents (Diebold and Bridgwater, 1997). Biomass conversion into oil and gas has been achieved by thermo-chemical technologies such as vacuum pyrolysis, fast pyrolysis, flash pyrolysis and gasification.

Fast pyrolysis has made significant advances in the past 20 years (Scott *et al.*, 1985; Graham *et al.*, 1988; Diebold and Scahill, 1988; Janse *et al.*, 1997). It requires rapid heating of biomass to temperatures between 450 and 550°C and short residence times of 0.5 to 1 second of the volatile vapors in the reaction zone in order to prevent secondary cracking. In such conditions the yield of the liquid product (BDO) can reach up to 80 wt% (Piskorz *et al*. 1988).

2.1.2 Characterization of BDO

Analysis and characterisation of liquids from fast pyrolysis processes is an important area of research. Data on the physical and chemical properties of the liquids provide important indications about process parameter, quality, toxicity and stability of the BDO (Meier *et al*., 1997). BDO is a mixture of simple aldehydes, alcohols, and acids as well as more complex carbohydrate and lignin-derived oligomeric materials emulsified with water (Bighelli *et al.*, 1994; Milne *et al*., 1997; Sipila *et al*., 1998). Its physical properties have been shown to change over time and also depend on the nature of biomass used (Adjaye *et al.*, 1992; Meier *et al*., 1997). Table 2.1 gives a list of the physical and chemical properties of the BDO used in this research as obtained from DynaMotive Energy Systems Corporation, Vancouver.

2.1.3 Pyrolysis of BDO

Due to instability of BDO, it is necessary to recover valuable chemicals from it. One of the methods of converting BDO to value added chemicals is pyrolysis. Only a few studies have been carried out on pyrolysis of BDO. In their work, Panigrahi *et al.* (2002) used a fixed bed micro reactor for thermo-chemical conversion of BDO to syn-gas and medium heating value gaseous fuels. They found that the conversion of BDO was increased from 57 to 83 wt% as the reactor temperature increased from 650 to 800^{o}C at a nitrogen (carrier gas) flow rate of 30 cm^{3}/min. The heating value of the product gases ranged between 49-64 MJ/Std.m^{3}. The volume of the product gas also increased from 73 to 104 L/100g of BDO with increase in reaction temperature from 650 to 800^{o}C. They concluded that by adjusting the parameters such as inert gas flow rate

Table 2.1 Physical and chemical properties of biomass-derived oil (DynaMotiveTM, 1999)

Physical properties	
pH	2.4
Solids content, wt%	<0.10
Ash content, wt%	<0.02
Density, g/cm^3	1.2
Heating value, MJ/kg	16.4
Kinematic Viscosity @20ºC, cSt	40
Kinematic Viscosity @80ºC, cSt	6
Chemical composition (wt%)	
Water	23.4
Methanol insolvable solids	24.9
Cellubiosan	1.9
Glyoxal	1.9
Hydroxyacetaldehyde	10.2
Levoglucosan	6.3
Formaldehyde	3.0
Formic acid	3.7
Acetic acid	4.2
Acetol	4.8

and the reactor temperature, the composition of the product gas can be tuned in the desired direction.

In another work by Panigrahi *et al.* (2003), syn-gas was produced by steam gasification of BDO while still using N_2 as the carrier gas. A similar experiment was carried out using mixture of CO_2 and N_2, and H_2 and N_2. They found that the conversion of BDO was decreased from 75 to 68 wt% at 800^oC with addition of CO_2 by 40 % in nitrogen as a carrier gas. The gas product consisted of H_2, CO, CO_2, CH_4, C_2, C_3 and C_{4+} hydrocarbons. The total volume of gas increased with increase in CO_2 percentage in carrier gas. They concluded that syn-gas production can be improved by increasing the percentage of CO_2 in the carrier gas. The conversion of BDO increased from 67 to 81 wt% with steam whereas it was unaffected with H_2.

In the report prepared for a bio-energy development program, Chaudhari and Bakhshi (2002) also studied pyrolysis of BDO with and without steam using N_2 and He as the carrier gas in a fixed bed reactor. Conversion of 89.4 % was obtained at 800^oC for pyrolysis in the presence of steam and the gas product had a heating value of 37 - 48 MJ/ m^3. Also the gas product contained a large amount of light hydrocarbons. With pyrolysis in the absence of steam, they carried out the experiments in the temperature range of 650-800^oC, BDO flow rate of 4 g/h and N_2 flow rate of 50 cm^3/min. They observed that the conversion increased from 70 to 77 wt% as the reaction temperature increased from 650 to 700^oC and then gradually decreased to 71 wt% with an increase in temperature from 700^oC to 800^oC. This slightly differs from the report by Panigrahi *et al.* (2002) where conversion was found to increase with temperature from 650 to 800^oC. The volume of the product gas increased from 29.7 mL to 46.5 mL/100g of BDO. This agrees well with the work of Panigrahi *et al.* (2002). The heating value of the product

gases ranged between 35 and 60 MJ/Std.m^3, slightly lower than those by Panigrahi *et al.* (2002). This might be due to different residence times used for the two studies. A comparison of the results obtained for a run at 800^oC by Chaudhari and Bakhshi (2002) and Panigrahi *et al.* (2002) is given in Table 2.2. The ratio of H_2 to CO for Chaudhari and Bakhshi (2002) was about 1:2 whereas that of Panigrahi *et al*. (2002) was 2:1. The mole percent of H_2, CO, C_2H_4 and C_2H_6 produced by Chaudhari and Bakhshi (2002) were significantly different from that of Panigrahi *et al.* (2002). For the other gases such as CO_2, CH_4, C_{4+}, C_3H_6 and C_3H_8, the quantities produced were comparable.

2.2 Triglycerides Based Fuels

Fats and oils are composed of molecules called triglycerides. Each triglyceride is composed of three long-chain fatty acids of 8 to 22 carbons attached to a glycerol backbone. The structure of a typical triglyceride is shown in Figure 2.1 Although triglycerides can fuel diesel engines, their high viscosities, low volatilities and poor cold flow properties have led to the investigation of various derivatives (Srivastava and Prasad, 2000). Dilution, micro emulsification, pyrolysis and transesterification are the four techniques applied to solve the problems encountered with the high fuel viscosity (Karaosmonoglu, 1999). Dilution with solvents and micro emulsification lowers the viscosity, but some engine performance problems still exist (Demirbas, 2003). The transesterification process converts triglycerides to fatty acids alkyl esters called biodiesel (Figure 2.2). The oils or fats used in transesterification should be substantially anhydrous (≤ 0.06% w/w) and free of fatty acids (>0.5% w/w) (Ma and Hanna, 1999). This implies high cost of raw material.

Table 2.2 Comparison of results obtained for pyrolysis of bio-oil in a fixed bed reactor at 800°C (Chaudhari and Bakhshi, 2002 and Panigrahi et al., 2002)

Component	mol% (Panigrahi *et al.*, 2002)*	mol% (Chaudhari and Bakhshi, 2002)**
H_2	43.8	14.5
CO	18.7	27.6
CO_2	5.1	5.8
CH_4	20.4	20.4
C_2H_4	6.9	22.2
C_2H_6	0.3	2.9
C_3H_6	0.3	1.3
C_3H_8	0.2	0.0
C_4+	4.4	5.3
Total	99.9	100

* Nitrogen flow (54mL/min) ** Nitrogen flow (50mL/min)

$$H_2\underset{l}{C}-O-CO-(CH_2)_{16}CH_3$$
$$H\underset{l}{C}-O-CO-(CH_2)_7CH=CH(CH_2)_7CH_3$$
$$H_2C-O-CO-(CH_2)_7CH=CHCH_2CH=(CH_2)_4CH_3$$

Figure 2.1 Structure of a typical triglyceride molecule

$$\begin{array}{lcl} H_2\underset{l}{C}-O-CO-R_1 & & H_2\underset{l}{C}-OH \quad R_1COO-R' \\ H\underset{l}{C}-O-CO-R_2 \quad + \quad 3R'OH & \xleftrightarrow{Catalyst} & H\underset{l}{C}-OH \quad + \quad R_2COO-R' \\ H_2C-O-CO-R_3 & & H_2C-OH \quad R_3COO-R' \end{array}$$

Triglyceride Alcohol Glycerol Ester

Figure 2.2 Transesterification of triglycerides with alcohol to alkyl esters

The cost of raw materials accounts for 60 to 75% of the total cost of biodiesel fuel (Krawczyk, 1996). Pyrolysis is an efficient way of producing less expensive alternative diesel fuel from lower quality raw materials such as waste fryer grease (Zhenyi *et al.*, 2004) and especially animal fats in which high levels of free fatty acids and water negatively affect the yield of biodiesel from its transesterification (Ma *et al.*, 1998).

2.2.1 Alternative fuels via thermal treatment of triglycerides

Considerable research has been done on pyrolysis of vegetable oils to produce chemicals and diesel-like fuel (Alencer *et al.*,1983; Schwab *et al.*, 1987; Idem *et al.*, 1996; Lima *et al.*, 2004). These studies were carried out using oils extracted from soybean, castor, palm tree, babassu, pequi and canola. The studies included the effects of temperature on the type of products obtained, effects of co-feeding steam and the characterization of the gas and liquid products. Some of these studies were conducted in batch and fixed-bed flow reactors whereas others were conducted in a standard ASTM distillation apparatus in which case, cracking and distillation occur simultaneously in the same unit. Different types of vegetable oils produce large differences in the composition of the thermally decomposed oil. Chemicals such as alkanes, alkenes, alkadienes, aldehydes, ketones, aromatics and carboxylic acids were found in the products.

The properties of the liquid fractions of the thermally decomposed vegetable oil are similar to those of diesel fuels. For example, pyrolysed soybean oil contains 79% carbon and 11.88% hydrogen, has low viscosity and a high cetane number compared to pure vegetable oils. The cetane number of pyrolysed soybean oil is enhanced to 43 from 37.9. Its viscosity is reduced to 10.2 from 32.6 mm^2/s at 38°C (Schwab *et al.*, 1987). But it

exceeds the specified value of 7.5 mm^2/s for diesel fuel. The pyrolysed vegetable oils possess acceptable amounts of sulphur, water and sediment and give acceptable copper corrosion values but unacceptable ash, carbon residue amounts and pour point.

Pyrolysis, assisted by solid catalysts, has also been reported (Dandik and Aksoy, 1998, Prasad *et al.*, 1986, Katikaneni *et al.*, 1998) and it was noted that the product selectivity is strongly affected by the presence and nature of heterogeneous catalysts. The liquid product however is similar to gasoline. Marquevich *et al.* (2000) studied the production of hydrogen by catalytic steam reforming of sunflower oil. The study was performed in a fixed bed reactor with a commercial nickel based catalyst for steam reforming naphtha. Sunflower oil was completely converted to hydrogen, methane and carbon oxides, except for the runs performed at the lowest temperatures and a steam to carbon ratio (S/C) of 3. The hydrogen yield ranged from 72% to 87% of the stoichiometric potential, depending on the S/C and the catalyst temperature.

Pyrolysis of animal fats however, has not been studied to the same extent as vegetable oils. Green Oasis EnviroEconomics Inc. (1999) employed a one-step process of thermal cracking and distillation to convert animal tallow into a diesel-like product having a flash point of 60^oC, perfect distillation curve, and a pour point of -28^oC.

2.2.2 Mechanism of triglycerides pyrolysis

The variety of reaction path and intermediates makes it difficult to describe the reaction mechanism of triglycerides. Besides, the multiplicity of possible reactions of mixed triglycerides make pyrolysis reaction more complicated (Schwab *et al.*, 1988). According to Alencer *et al*. (1983), formation of homologous series of alkanes and alkenes is accountable from the generation of the RCOO radical from the triglyceride

cleavage and subsequent loss of carbon dioxide. The R radical, upon disproportionation and ethylene elimination, gives the odd-numbered carbon alkanes and alkenes. The presence of double bond in the triglyceride molecule enhances cleavage at a position β to the unsaturation (see Figure 2.3). The formation of aromatics is supported by a Diels–Alder addition of ethylene to a conjugated diene formed in the pyrolysis reaction. Their mechanism was based on that originally proposed by Chang and Wan (1947). In addition to the possible reaction pathways explained above, Chang and Wan (1947) also proposed that alkynes are formed from alkene decomposition. The reaction mechanism in Figure 2.3 was proposed by Schwab *et al.* (1988). This mechanism is actually a simplified form of that proposed by Chang and Wan (1947).

Idem *et al*. (1996) also proposed further mechanisms that account for the formation of other observed compounds. According to them, elimination of heavy oxygenated hydrocarbons as esters, carboxylic acids, ketones and aldehydes are dominant step in the cracking reactions of triglycerides and begins at 240 – 300°C for vegetable oils. CO_2 is formed from the decarboxylation of saturated and unsaturated carboxylic acids while CO is produced by the decarbonylation of oxygenated hydrocarbons. Hydrogen is produced by formation of cycloolefins and aromatics, polymerisation of olefins and aromatics, polycondensation of triglyceride, splitting of hydrocarbons and dehydrogenation of olefins. Char is formed by decomposition of long-chain hydrocarbon radicals, polymerisation of olefins and aromatics, polycondensation of triglyceride and heavy oxygenated hydrocarbons and dehydrogenation of aromatics. Heavy hydrocarbons are produced by polymerisation and polycondensation reactions.

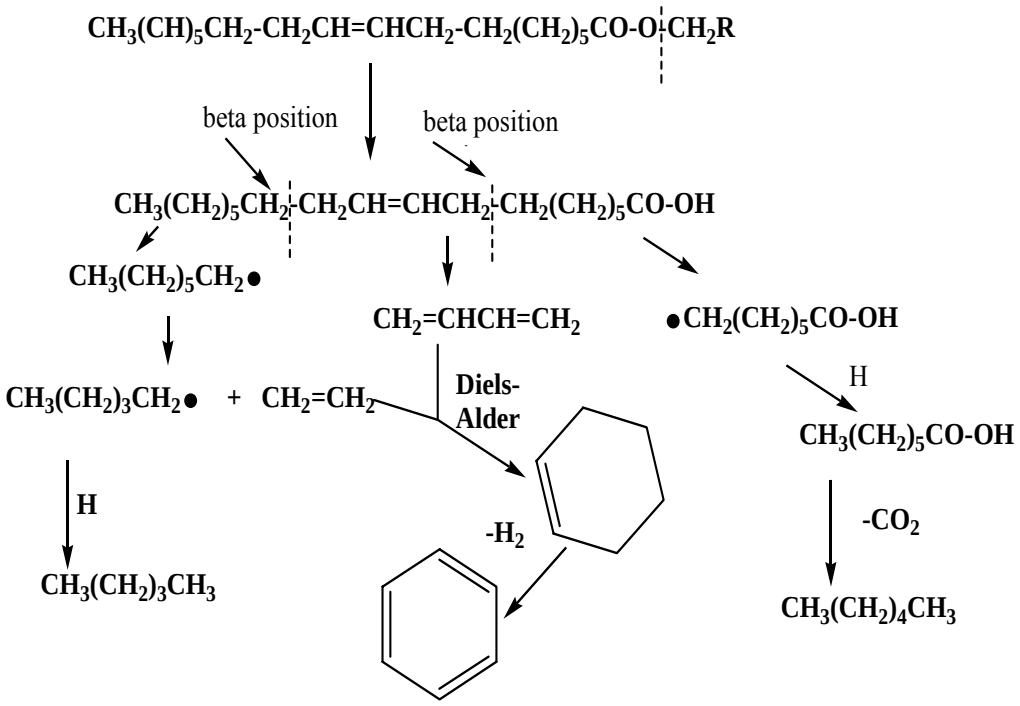

Figure 2.3 The proposed mechanisms for thermal decomposition of triglycerides (Schwab *et al.*, 1988).

Zhenyi *et al.* (2004) showed by thermodynamics calculation that the initial decomposition of vegetable oils occurs with the breaking of C-O bond at lower temperature (< 400^{o}C). At this temperature, fatty acids are the main products. They further advised that in order to get maximum yield of diesel fraction, the pyrolysis temperature should be higher than 400^{o}C.

From the literature review, no study has been done on pyrolysis of lard. The proposed mechanisms as shown in Figure 2.3 were based on pyrolysis products of vegetable oils such as soybean, canola and safflower. No such mechanism has been proposed for studies on animal fats. Also, Panigrahi (2003) did not consider the use of pure CO_2 in BDO reforming.

3. EXPERIMENTAL

This chapter describes the experimental design and procedures for CO_2 reforming of biomass derived oil (BDO), pyrolysis of lard, steam reforming of lard and the analysis and characterization of the reaction products.

3.1 Pyrolysis and CO_2 Reforming of BDO

The BDO used for this study was obtained from DynaMotive Energy Systems Corporation, Vancouver, Canada where it was produced by fast pyrolysis technology of wood. The BDO was mixed thoroughly before any sample was taken for analysis or for the experiment. This was done to ensure uniformity of sample.

3.1.1 The experimental set-up

The experiments were conducted at atmospheric pressure in a continuous down flow fixed-bed micro reactor operated at 800^{o}C. The experimental set up is shown in Figure 3.1. The reactor was a 310 mm long, 10 mm i.d. Inconel® alloy tube placed co-axially in a furnace. Quartz particles (5g, 1.7-2.4 mm size), with a height of 70 mm in the reactor, were held on a plug of quartz wool placed on a supporting mesh inside the micro reactor. The reactor was heated by a furnace with temperature controlled by a series SR22 microprocessor-based autotuning PID temperature controller (Shimaden Co. Ltd., Tokyo, Japan) using a K-type (~2.5 mm diameter) thermocouple placed on the furnace side of the annulus between the furnace and the reactor. A calibration of the

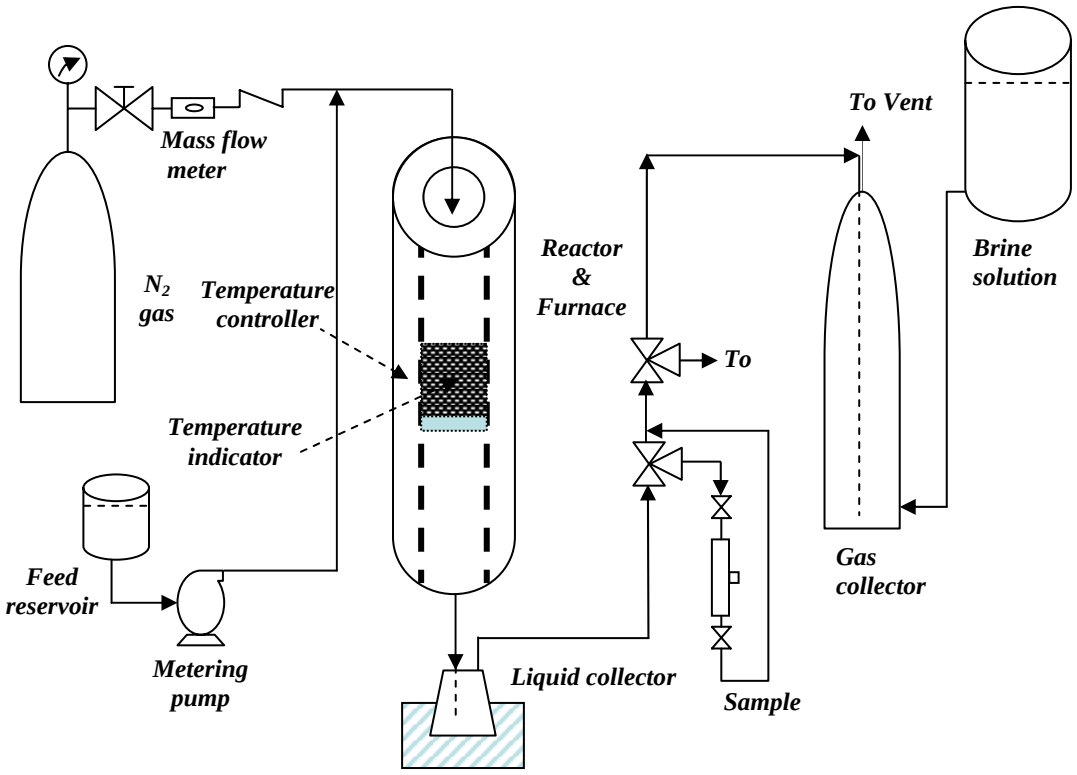

Figure 3.1 The experimental set-up for CO_2 reforming of BDO, pyrolysis and steam reforming of lard

temperature profile in the reactor at different furnace temperatures was done (Figures A-1 and A-2, Appendix A). BDO was introduced into the reactor using an Eldex (Model A-10-S) metering pump (see calibration curve in Figure A-3, Appendix A) at the rate of 5g/h. The desired flow rate of the gases (CO_2 and/or N_2) was maintained by using mass flow meters (Top-trak model 822, Sierra Instrument Inc. California, USA). The calibrations of these mass flow meters for N_2 and CO_2 are given in Figures A-4 and A-5, respectively (Appendix A). The liquid products were collected with the help of a condenser attached at the bottom of the reactor outlet. The gaseous products were collected in a gas collector by the downward displacement of brine solution of NaCl.

3.1.2 A typical run

In a typical experiment, the reactor was cleaned, dried, packed with quartz particles, weighed and mounted inside the furnace. Nitrogen was allowed to flow through the set up at ~ 10 cm^3/min while the reactor was been heated up. After attaining the desired operating temperature (a period of about 60 minutes), the flows of BDO and CO_2 were started while that of N_2 was increased to the desired rate. BDO was fed at a fixed rate of 5 g/h and each experiment was run for 0.5 h. After the completion of a run, the flow of N_2 was allowed to run for an additional 10 minute to clear the line. The reactor was then cooled and weighed to determine the amount of retained products (char). The condensate was also weighed.

3.1.3 Analysis of products

The product gas was analyzed for its composition using two GCs (Hewlett Packard 5890 series II and Carle GC-500 series). The Hewlett Packard 5890 II was

equipped with a thermal conductivity detector (TCD) and CarboSieve S II column (3000 mm, 3.18 mm i.d.) and it analysed H_2, CO, CO_2 and CH_4, whereas the Carle GC equipped with a flame ionization detector and a capillary column was used to analyse for hydrocarbons. The programs used in the GCs are given in Table 3.1. The calibrations of the GCs for the gases are given in Figures A-6 to A-17, Appendix A). Standard gas mixtures were used for the calibration. After normalization of the components, the weight of the gas product was calculated from the moles of the components and the total volume of gas evolved during the run (see Appendix B). The condensate was not analysed.

3.1.4 Determination of spray pattern into the reactor

For effective cracking of the feed, it is necessary to have the feed introduced into the reactor as fine droplets. This is one of the functions of the carrier gas. In order to have an approximate idea of what the spray pattern will be into the reactor, a study was done on the feed line to the reactor at two carrier gas temperatures (25 and 50^{o}C) and flow rates (30 and 60 cm^3/min). The BDO flow rate was kept constant at 5g/h. The BDO was not heated directly because of its tendency to polymerize at high temperature when exposed to air. The carrier gas was used to spray the feed (BDO). The spray patterns at different carrier gas temperatures and flow rates were obtained (in 30 seconds) on white papers placed at a distance of approximately 2 cm below the discharge point. The papers were allowed to dry in a fume hood overnight as BDO has a pungent smell. The droplet sizes of the sprays were then measured approximately with a scale.

Table 3.1 Temperature program for the GCs and GC/MS

	GC HP 5890	Carle GC-500	GC/MS	SDGC
Initial temperature ^{o}C	40	40	40	40
Initial hold time, min	0	3	5	5
Heating rate, ^{o}C/min	12	10	10	10
Final temperature, ^{o}C	200	200	250	300
Final hold time, min	1	2	15	5
Detector temperature, ^{o}C	250	250	280	400

3.2 Pyrolysis and Steam Reforming of Lard

3.2.1 Feed analysis

The lard used in this study was produced by Sobeys in Toronto, and was obtained from a retail outlet. The elemental analysis of the lard was performed on a CHN analyser (Perkin Elmer 2400). Traces of nitrogen known to be present in animal fats could not be detected by the CHN analyzer. Therefore, the ANTEK 9000 Combustion analyzer coupled to an ANTEK 738 Robotic Auto-sampler was used to analyze for sulphur and nitrogen. The wt% of O_2 in the lard was obtained by difference. The lard's fatty acid composition was determined by POS Pilot Plant Corporation, Saskatoon, using gas chromatography. This was done by converting the fatty acids in the lard to their corresponding methyl esters and analyzing the resultant liquid with GC equipped with DB-FFAP column and flame ionization detector. The determination was according to AOCS standard method Ca 5a-40 (1997).

In order to determine a reasonable temperature at which significant pyrolysis can occur, a TG/DTA analysis of the lard was done to estimate its boiling point. The analysis was done by Perkin Elmer Pyris Diamond TG/DTA by Seiko Instrument Inc. About 10 mg of lard was placed in the sample pan inside the analyzer. The analyzer read the

weight of the sample automatically. The sample was heated in flowing nitrogen (10 cm^3/min) from 40 to 800^oC with a heating rate of 10^oC/min.

3.2.2 Pyrolysis of lard

The reactor set-up used for the BDO experiments was also used for the lard pyrolysis experiments. Lard is a solid at room temperature however it melts at about 37^oC. It was therefore preheated to 40^oC before pumping. The Eldex A-10-S pump was used for a few of the experimental runs. Due to difficulties in pumping, the pump was changed to a programmable syringe pump (Genie model YA-12, Kent Scientific Corporation, USA). All the results presented in the next chapter are those from the syringe pump runs except otherwise stated. The lard flow rate was maintained at ~ 5 g/h for all runs. N_2 was used as carrier gas for all pyrolysis experiments. The purpose of the carrier gas was to bring about a uniform distribution of the feed in the reactor. The carrier gas also helps to limit the residence time of the volatiles (products) in the reactor and thereby prevents secondary reactions. The lard feed line was maintained at 40^oC using heating tape. Apart from the thermocouple placed in the furnace, another K-type (~ 1.0 mm diameter) thermocouple (in a thermowell) was used to monitor the temperature at the centre of the reactor. All experiments were conducted for 30 min except for a particular experiment which was conducted for 225 min in order to collect enough liquid products for the determination of pour and cloud points.

3.2.3 Steam reforming of lard

The reactor set-up used for the pyrolysis experiment was also used for the steam reforming process. But since lard is not miscible with water a second syringe pump

(Genie model YA-12, Kent Scientific Corporation, USA) was used to introduce the water. In addition, during the steam reforming process no carrier gas was used. The N_2 flow was stopped after the desired reactor temperature was attained.

3.3 Gas Product Analysis

GC Hewlett Packard 5890 II (described in section 3.1.3) was used to analyze for H_2, CO and CO_2 while Hewlett Packard 5880A equipped with a flame ionization detector and a Chromosorb102 column (1800 mm, 3.18 mm i.d.) was used to analyse for hydrocarbons. The same programming used for Carle GC 500 was used for Hewlett Packard 5880A. The calibrations of the GC HP 5880 A for the hydrocarbons are given in Figures A-18 to A-26, Appendix A)

3.4 Liquid Product Analysis

3.4.1 Gas chromatographic analysis

The liquid product was first injected into an FID Varian 3400 GC equipped with a capillary column (DB-1, 100% dimethylpolysiloxane, 26 m x 0.32 mm) to obtain analytical chromatograms. Over 240 peaks were observed. The compounds present in the liquid product were then identified using a VG70-250-VSE mass-spectrometer (VG Analytical, Manchester, England) coupled to a Fisons GC 8000 series, Model 8060 (Fisons Instrument, Italy) which was equipped with a DB 5/MS (5% diphenyl, 95% dimethyl polysiloxane) capillary column (30 mm long and 0.25 mm i.d.). The GC/MS program is also given in Table 3.1. The MS detector was operated in the scan mode (2 scans/s) and its mass range was 25 to 450 amu. The identification was done with NIST library containing 60,000 compounds. The composition of the liquid product was

estimated from the observed total ion chromatogram. All quantifications were relative to the total sample and based upon the mass spectral peak areas with an assumed relative response factor of unity.

3.4.2 Cetane index

Cetane number (CN) is a measure of ignition quality or ignition delay, and is related to the time required for a liquid fuel to ignite after injection into a compression ignition engine. CN is determined from real engine test. Cetane index (CI) is a calculated value derived from the density (see below) and volatility obtained from boiling characteristics of the fuel. CI usually gives a reasonably close approximation to real cetane number (Song, 2000). ASTM D976-91 was used to calculate CI as a function of mid-boiling point and density of the liquid according to the formula below.

$$CI = 454.74 - 1641.416(G) + 774.74(G)^2 - 0.554(T_{50}) + 97.803(\log T_{50})^2 \qquad (3.1)$$

3.4.3 Density

Density is the mass per unit volume of any liquid at a given temperature. Density has importance in diesel engine performance, since fuel injection operates on a volume metering system (Song, 2000). Also, the density of the liquid product is required for the estimation of the Cetane index (Srivastava and Prasad, 2000). The densities were determined using a density meter (DMA 35, PARR Instruments Company Inc., USA,) at 25^{o}C according to ASTM D5002-94. The density meter was calibrated using reverse osmosis water at room temperature.

3.4.4 Distillation range

The distillation range of a fuel affects its performance and safety. It is an important criterion for engine's start and warm up. It is also needed in the estimation of cetane index. The distillation range of the liquid product was determined by Simulated Distillation Gas Chromatography (SDGC). SDGC is a test method (ASTM D2887-97) that covers the determination of the boiling range distribution of liquid fuels. Using a calibration curve obtained by chromatographic analysis of a mixture of hydrocarbons with known boiling points (calibration standard), boiling temperature were assigned as a function of residence time. The temperature at which specified percentages of the total sample have eluted from the column were calculated and reported. Additional information may be extracted from the results to provide more information about the sample's properties. This method can be used to compliment or replace conventional distillation methods.

The initial boiling point (IBP) is the temperature (corresponding to the retention time) at which a cumulative corrected area count equals to 0.5% of the total sample area under the chromatogram is obtained. The final boiling point (FBP) is the temperature (corresponding to the retention time) at which a cumulative corrected area count equals to 99.5% of the total sample area under the chromatogram is obtained. A Varian model CP 3800 GC (specially configured for simulated distillation) coupled to a Varian CP 8400 Auto-sampler was used. The SDGC was equipped with a capillary column (HP-1 100% Dimethylpolysiloxane, 5000 mm x 0.53 mm i.d.).

3.4.5 Viscosity

Viscosity is a measure of the internal fluid friction, which tends to oppose any dynamic change in the fluid motion (Song, 2000). Proper viscosity of fuel is required for proper operation of the engine. It is also important for flow of oil through pipelines, injector nozzles and orifices (Radovanovic et al, 2000). The lower the viscosity of the oil, the easier it is to pump and atomize and achieve finer droplets (Islam et al, 2004). The viscosities of the total liquid products were determined using a digital cone and plate viscometer (Brookfield, Model LVDV-1+, Brookfield Engineering Laboratories, Stoughton, MA) at 40^{o}C. The temperature of the sample was maintained within ±0.5^{o}C with a constant temperature bath. Brookfield standard fluid 100 was used to calibrate the viscometer.

3.4.6 Heat of combustion

Heat of combustion measures the energy content in a fuel. This property is also referred to as calorific value or heating value. Although cetane number determines the combustion performance, it is the heating value along with thermodynamic criteria that sets the maximum possible output of power (Song, 2000). Combustion with oxygen in a sealed bomb is a very effective and reliable method for releasing all heat energy obtainable from a fuel (Parr, 1997). The heats of combustion of the liquid products were measured using an oxygen bomb calorimeter (Parr 1341, PARR Instruments Company Inc. Moline, IL) according to ASTM D240-92 using benzoic acid as the primary standard.

3.4.7 Cloud and pour points

The cloud point is the temperature at which a cloud of crystals first appears in a liquid when cooled under conditions as described in ASTM D2500-91. The pour point is the lowest temperature at which the oil specimen can still be moved. It is determined according to ASTM D97-96. These two properties are used to specify cold temperature usability of a fuel. Two cooling baths with different cooling temperatures were used. The first bath was maintained at about -2^{o}C by mixing crushed ice with NaCl. The second one was maintained around -20^{o}C by using ice and $CaCl_2$. For the case of pour point determination, the thermometer was positioned so that just its bulb was immersed in the fuel.

3.4.8 Water content

The water content of the fuel is required to accurately measure the net volume of actual fuel in sales, taxation, exchanges and custody transfer (Srivastava and Prasad, 2000). The analysis was done with 950 Ross® FASTQC^{TM} Titrator (Orion Research Inc., Beverly, MA, USA). Three steps were followed in the water content analysis, blank preparation, standardization with distilled water and analysis of sample. The reagent used for titration was Aquastar® Comp 5 containing 2-methoxyethanol. The solvent used was Aquastar® methanol which is a special anhydrous reagent for moisture determination.

4. RESULTS AND DISCUSSION ON CO_2 REFORMING OF BIOMASS DERIVED OIL

The results obtained from the spray test on the reactor inlet and the study on CO_2 reforming of biomass derived oil (BDO) are presented and discussed in this chapter. The discussion was based on the effects of residence time and mole fraction of CO_2 in the carrier gas on products distribution.

4.1 Determination of Spray Pattern into the Reactor

The feed inlet was designed to allow the feed to spray on the quartz bed as described in Chapter 3. Figure 4.1 shows the spray pattern obtained at two carrier gas temperatures and flow rates. It is observed from Figure 4.1 that the flow rate of carrier gas has a significant effect on spray pattern and droplet size of the reactant. The droplet size was obtained by taking the average of the sizes of any five spots taken at random from the pattern created. As the carrier gas flow rate was increased from 30 to 60 cm^3/min at 25^oC (Figures 4.1a and b), the droplet size of the reactant reduced from approximately 2.5 to 1.5 mm. At 50^oC and 30 cm^3/min (Figure 4.1c), the droplet size was decreased further to 0.5 mm. At 50^oC and 60 cm^3/min (Figure 4.1d), the central broad spot completely disappeared and the droplet size was reduced to approximately 0.2 mm. Since the temperature at the reactor entrance during each run was higher than 50^oC (approximately 200^oC), the droplet size would definitely be finer than the observed size in this spray test. The broad area covered by the spray might suggest that the

Figure 4.1a. Spray obtained at 25°C and carrier gas flow rate of 30 cm^3/min

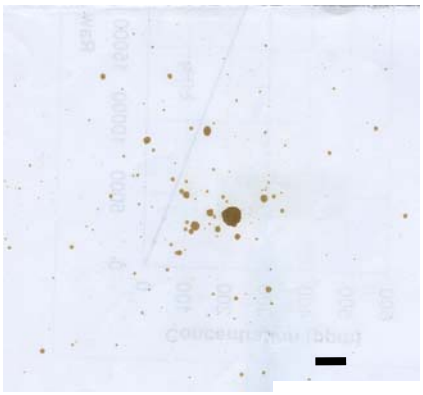

Figure 4.1c. Spray obtained at 50°C and carrier gas flow rate of 30 cm^3/min

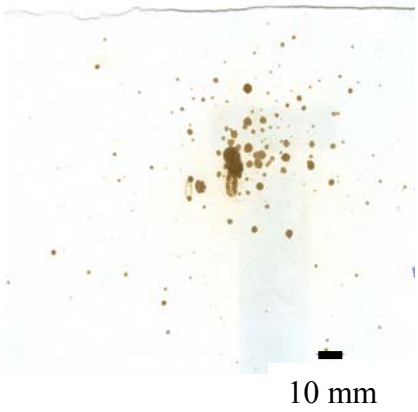

Figure 4.1b. Spray obtained at 25°C and carrier gas flow rate of 60 cm^3/min

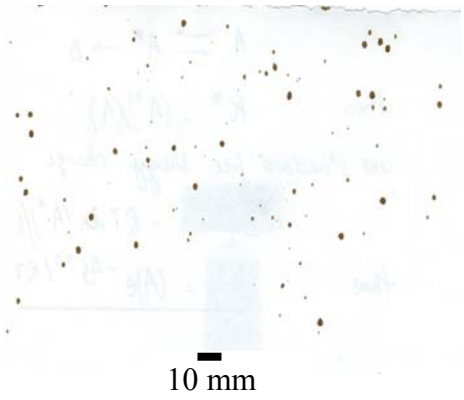

Figure 4.1d. Spray obtained at 50°C and carrier gas flow rate of 60 cm^3/min

Figure 4.1 Spray pattern of BDO (5 g/h) generated by carrier gas

droplets could also fall on the wall of the reactor. However, due to the high temperature in the reactor, the droplets are more likely to be gasified before reaching the quartz bed or the wall of the reactor.

4.2 Characterization of BDO

As obtained from the supplier's MSDS, the BDO contains 25 wt% water, 25 wt% lignin and a balance of 50 wt% of other oxygenated compounds. Its specific gravity and pH are 2.2-3.5 and 1.1-1.25, respectively. The viscosity was not given and thus was obtained using Brookfield Digital Viscometer model DV-1+. The result is given in Table 4.1. It is observed that the viscosity of the BDO ranged from 5.2 to 16.2 cSt over a temperature range of 25 to 80^{o}C. A viscosity of 6 cSt at 80^{o}C was given on DynaMotive website. The carbon (C), hydrogen (H) and nitrogen (N) analysis of the BDO was performed on a CHN analyser (Perkin Elmer 2400) and the results are given in Table 4.2. The wt% of O_2 in the BDO was obtained by difference.

4.3 Pyrolysis and CO_2 Reforming of BDO in a Fixed Bed Reactor

This section describes the effects of residence time and CO_2 mole fraction in the carrier gas on product yields, gas composition and heating value. In the study by Panigrahi et al. (2003), they observed highest conversion at 800^{o}C for pyrolysis of BDO. Therefore, all the runs here were done at a temperature of 800^{o}C. The observed material balance was in the range of 90 – 96 wt%. The complete data of the experimental runs are presented in Appendix C.

In order to check the reproducibility of the experiment, one of the runs was chosen at random and repeated twice. The reproducibility was observed to within ± 2%.

Table 4.1 Viscosity of BDO

Temperature (^{o}C)	Viscosity (cP)	Viscosity (cSt)*
25	18.6	16.2
40	16.9	14.7
80	6.0	5.2

* obtained at a specific gravity of 1.15

Table 4.2 CHN analysis of the BDO

Component	wt%
C	35.3
H	8.3
N	0.4
O*	56.0

*obtained by difference

The statistical analysis was done with SAS V8 program. There is no significant difference in the result at error level of 5%.

4.3.1 Effects of residence time on CO_2 reforming of BDO

The residence time is defined as packing volume divided by the carrier gas volumetric flow rate at the reactor temperature (see Appendix D for detailed calculation). The contribution to volumetric flow rate by the feed was assumed to be negligible. This is because the flow rate of the feed is very small as compared to that of the carrier gas. The discussion here is based on the use of the two gases (CO_2 and N_2) separately i.e. the use of pure N_2 and CO_2.

Figure 4.2 shows the effect of residence time on product yield and heating value of product gas when pure N_2 was used as carrier gas. The gas yield increased almost linearly from 31 to 40 wt% as the residence time increased from 1.4 to 2.8 s. The increase in gas yield is at the expense of the char as the char was seen to take the reverse trend 31 to 24 wt%. This implies that at higher residence time, the char formed is gasified by some compounds (CO and/or H_2O) in the volatiles, thereby yielding more gas (equation 4.1, Corella *et al*., 1998). The condensate yield is almost independent of the residence time. The heating value of the product gas was observed to increase slightly from 19 to 22 MJ/m^3 with increase in residence time. The calculation of the heating value is based on gas composition (see Appendix E) therefore; the observed trend in the heating value of the gas is due to variation in gas composition (explained in the next section). Equation 4.1 also confirms the increase in heating value with increase in residence time since more high heating value methane is produced.

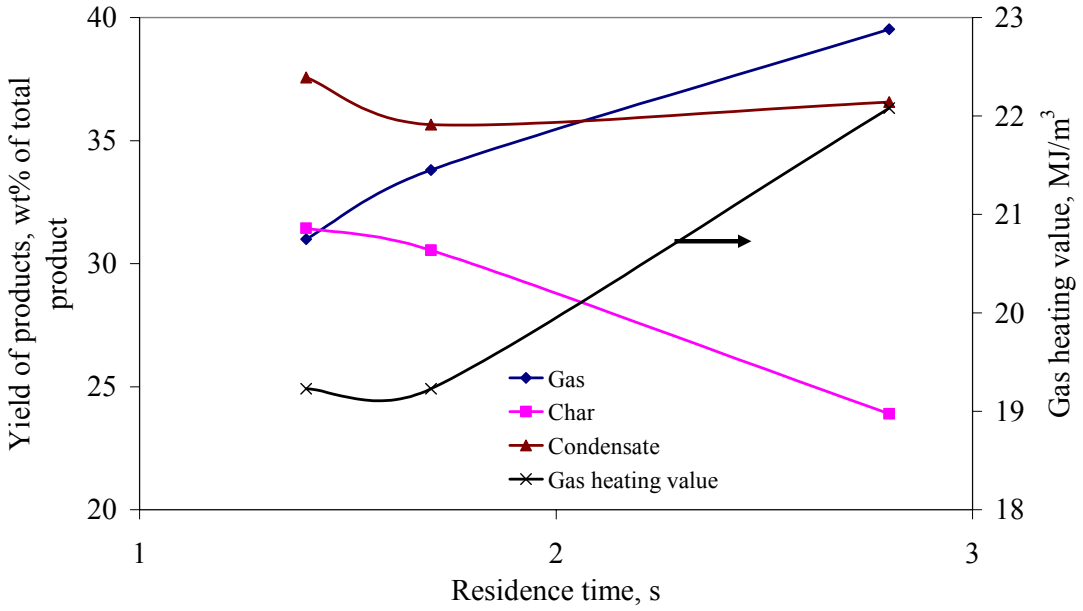

Figure 4.2 **Effects of residence time on product yield and heating value of product gas (carrier gas N_2 only: BDO: 4.5-5.5g/h; temperature 800°C, reaction time: 30 min)**

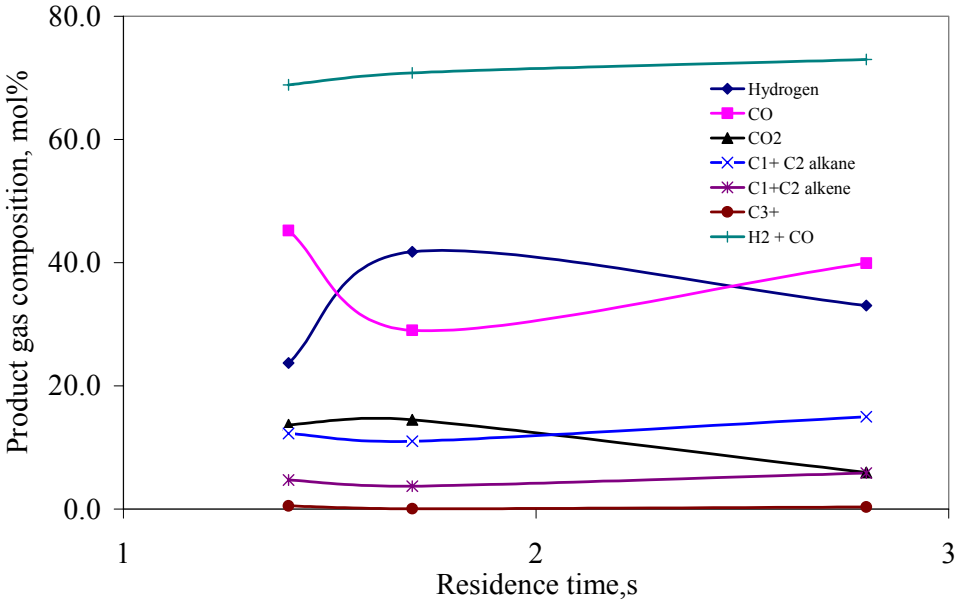

Figure 4.3 **Effects of residence time on product gas composition (carrier gas: N_2 only, BDO: 4.5-5.5g/h, temperature 800°C, reaction time: 30 min)**

$$Char + \left\{ \frac{H_2O}{CO_2} \right\} = H_2 + CO + \bullet\bullet\bullet + CH_4 \qquad (4.1)$$

The effects of residence time on product gas composition are shown in Figure 4.3. It is observed that the production of hydrogen increased from 24 to 42 mol% as the residence time increased from 1.4 to 1.7 s. A further increase in residence time to 2.8 s caused a decline in hydrogen production to 33 mol%. This indicates that H_2 is a primary product during pyrolysis (Panigrahi *et al.*, 2002) and that it (H_2) is being consumed to other products at high residence time. Ferdous *et al.* (2001) have reported that hydrogen produced during pyrolysis reacts with carbonaceous material to form methane. This also explains why methane production (combined in $C_1 + C_2$ alkanes) increased slightly with the decrease observed with H_2 and char (see Figure 4.2). The opposite trends observed between CO and CO_2 might be due to CO_2 reforming of hydrocarbons and/or char to CO (Caballero *et al.*, 1997). This can also explain why hydrocarbon compositions are low in all cases. The synthesis gas ($CO + H_2$) production was high (~73 mol%) and observed to be almost independent of residence time.

The effects of residence time on products yield and the heating value of product gas during CO_2 reforming of BDO are shown in Figure 4.4. The gas yield was observed to decrease from 34 to 31 wt% as the residence time increased from 1.4 to 1.7 s but remained constant with increase in residence time further to 2.8 s. This might be due to attainment of equilibrium in gas composition (Chaudhari *et al*., 2001). The char yield was observed to decrease slightly from 31 to 29 wt% as the residence time increase from 1.4 to 1.7 s but increased rapidly to 36 wt% when the residence time was increased to 2.8 s. The trend observed with the char was almost opposite to that of the condensate.

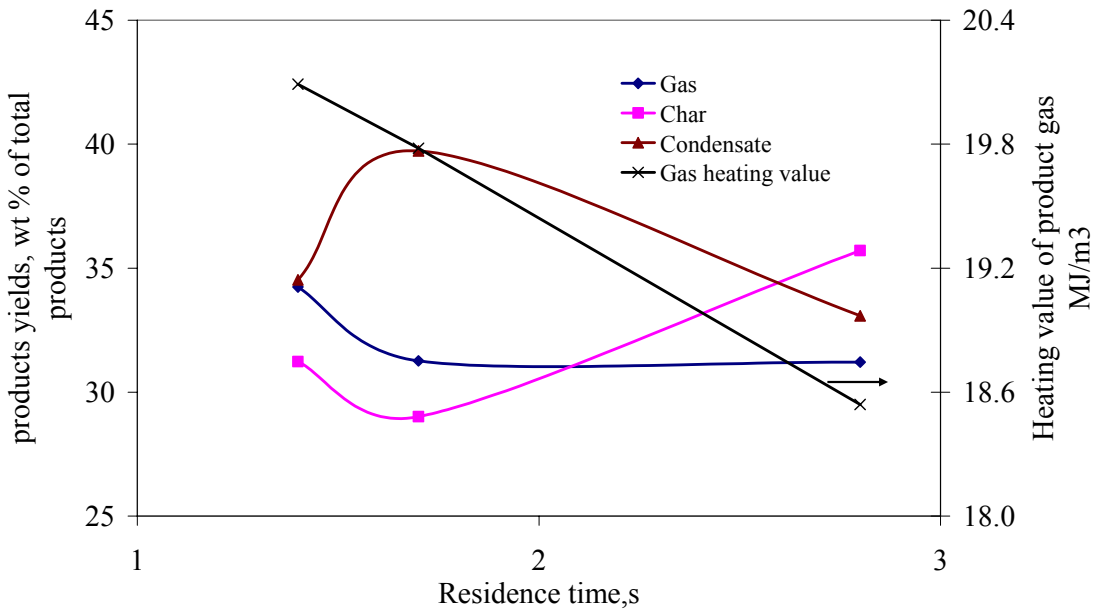

Figure 4.4 **Effects of residence time on products yield and heating value of product gas (carrier gas CO_2 only: BDO: 4.5-5.5g/h; temperature 800^{o}C, reaction time: 30 min)**

This implies that the components of the liquid were converted into char rather than gas at high residence time when the reacting atmosphere is dominated by CO_2. The heating value of the product gas decreased slightly from 20 to 18 MJ/m^3.

The effects of residence time on product gas composition during CO_2 reforming of BDO are given in Figure 4.5. It is observed that an initial increase in residence time increased the mol% of H_2, CO and consequently that of synthesis gas slightly and decreased that of CO_2. A further increase in residence time did not affect the concentration of CO and H_2. This is due to equilibrium achieved in the gas phase as stated above. The concentrations of the hydrocarbons were not affected at all.

4.3.2 Effects of CO_2 concentration in the feed gas on products distribution

The effects of CO_2 in carrier gas on gas and char yields and product gas composition for reforming of BDO were studied by changing the mole fraction of CO_2 in total gas from 0 to 1 and total gas flow rate from 30 to 60 cm^3/min. The reaction temperature was kept constant at 800^oC. It should be noted that the analysis of the product gas was on carrier gas free basis, which implies that the amounts of CO_2 and N_2 fed to the experiment were deducted from the total gas collected over the run period.

The effects of mole fraction of CO_2 in feed gas on product distribution into gas char and condensate and also on gas composition are given in Tables 4.3 to 4.5. As can be observed in these tables, the gas compositions seem not to follow a defined pattern. The same observation was made by Panigrahi *et al*. (2003). The hydrogen production was observed to decrease while those of the hydrocarbons increased with increase in mole fraction of CO_2 in the carrier gas from 0 to 0.4 when the total carrier gas flow rate was 30 cm^3/min (Table 4.3). However when the carrier gas flow rate was increased,

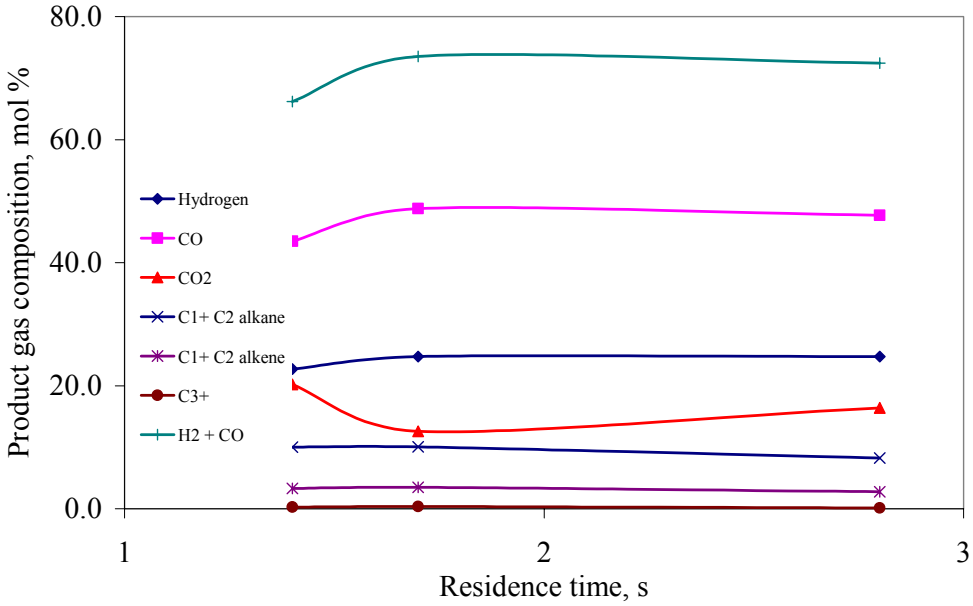

Figure 4.5 **Effects of residence time on product gas composition (carrier gas CO_2 only: BDO: 4.5-5.5g/h; temperature 800^{o}C, reaction time: 30 min)**

Table 4.3 Effects of CO_2 in the feed gas on products distribution and gas composition (N_2 + CO_2: 30 cm^3/min, BDO: 4.5-5.5g/h, temperature: 800^oC, reaction time: 30 min)

Gas composition (mol%)*	Mole fraction of CO_2 in N_2			
	0	0.2	0.4	1.0
H_2	33.1	28.4	27.0	24.7
CO	39.9	33.4	38.0	47.7
CO_2	5.9	15.0	9.9	16.4
C_1 + C_2 alkanes	15.0	16.3	17.7	8.3
C_2 + C_3 alkenes	5.8	6.5	7.0	2.8
C_{3+}**	0.3	0.4	0.5	0.1
Total	100	100	100	100
Calorific value MJ/Std. m^3	22.1	24.5	24.9	18.5
Synthesis gas (H_2 + CO)	73.0	61.8	65.0	72.4
H_2/CO molar ratio	0.83	0.85	0.71	0.52
Product distribution wt% of total product				
Gas	34.8	51.3	48.7	31.2
Condensate	41.6	23.1	28.3	33.1
Char	23.6	25.6	23.0	35.7

*Carrier gas (CO_2 + N_2) free basis ** excluding propylene

Table 4.4 Effects of CO_2 in the feed gas on products distribution and gas composition (N_2 + CO_2: 50 cm^3/min; BDO: 4.5-5.5g/h; temperature 800^oC, reaction time: 30 min)

Gas composition (mol%)*	Mole fraction of CO_2 in N_2			
	0	0.2	0.5	1.0
H_2	41.8	22.8	33.2	24.7
CO	29.0	45.9	38.2	48.8
CO_2	14.5	19.2	5.6	12.6
C_1 + C_2 alkanes	11.0	8.7	16.1	10.1
C_2 + C_3 alkenes	3.7	3.2	6.5	3.5
C_{3+}**	0.03	0.3	0.4	0.4
Total	100	100	100	100
Calorific value MJ/Std. m^3	19.2	19.4	22.0	19.8
Synthesis gas (H_2 +CO)	70.8	68.6	71.4	73.5
H_2/CO molar ratio	1.44	0.50	0.87	0.51
Product distribution wt% of total product				
Gas	33.8	39.8	41.7	31.3
Condensate	35.7	38.2	40.0	39.7
Char	30.5	22.0	18.2	29.0

*Carrier gas (CO_2 + N_2) free basis ** excluding propylene

Table 4.5 Effects of CO_2 in the feed gas on products distribution and gas composition (N_2 + CO_2: 60 cm^3/min, BDO: 4.5-5.5g/h, temperature: 800°C, reaction time: 30 min)

Gas composition (mol%)*	Mole fraction of CO_2 in N_2			
	0	0.1	0.2	1.0
H_2	23.7	28.4	25.9	22.7
CO	45.2	47.2	45.8	43.5
CO_2	13.7	8.4	12.5	20.2
C_1 + C_2 alkanes	12.3	11.7	11.4	10.0
C_2 + C_3 alkenes	4.7	4.0	4.3	3.3
C_{3+} **	0.5	0.2	0.3	0.3
Total	100	100	100	100
Calorific value MJ/Std. m^3	19.2	18.7	20.6	20.1
Synthesis gas (H_2 +CO)	68.9	75.6	71.6	66.2
H_2/CO molar ratio	0.52	0.60	0.56	0.52
Product distribution wt% of total product				
Gas	31.0	28.8	30.3	34.2
Condensate	37.6	34.4	36.5	34.5
Char	31.4	36.8	33.2	31.2

*carrier gas (CO_2 + N_2) free basis ** excluding propylene

corresponding to reducing the residence time (Tables 4.4 and 4.5), the trend was not retained. Probably, the secondary thermo-chemical reactions were affected by the addition of CO_2 and due to the higher residence time at 30 cm^3/min (2.8 s). For example methanation (Mleczco *et al*., 1997) and other reactions might occur consuming H_2 (see equations 4.2 and 4.3, Panigrahi, 2003).

$$CO + 3H_2 = CH_4 + H_2O \quad (4.2)$$

$$C + 2H_2 = CH_4 \quad (4.3)$$

The synthesis gas production was high (> 60 mol%) in all cases, with or without addition of CO_2. The maximum production of synthesis gas (~76 mol%) was observed at a total carrier gas flow rate of 60 cm^3/min and a mole fraction of CO_2 in carrier gas of 0.1. The char formation decreased with increase in mole fraction of CO_2 in the carrier gas (50 cm^3/min) from 0 to 0.5 but increased as the mole fraction of CO_2 increased to one (Table 4.4). Snoeck and Froment (2002) observed a reduction in char formation during CO_2 reforming of methane. The minimum char formation (18 wt%) for all the experiments conducted was observed at a total carrier gas (N_2 + CO_2) flow rate of 50 cm^3/min containing 50 mol% CO_2. The maximum olefin (C_2+ C_3) production (6.5 mol%) was also observed at these conditions.

Other observations from Tables 4.3 to 4.5 and from all the runs conducted on CO_2 reforming of BDO are given below. The maximum gas production (51 wt%) was observed at a total carrier gas flow rate of 30 cm^3/min containing 20 mol% of CO_2. The maximum product gas heating value (25 MJ/m^3) and alkanes production (18 mol%)

were obtained at a total carrier gas flow rate of 30 cm^3/min containing 40 mol% CO_2. Maximum hydrogen (42 mol%) and H_2 to CO molar ratio (1.44) were obtained while using only N_2 as the carrier gas at a flow rate of 50 cm^3/min. This molar ratio is a good one for Fischer-Tropsch synthesis (Chaudhari *et al*., 2001). From the results presented in this chapter, it is glaring that CO_2 was not consumed in BDO reforming. Therefore, the term CO_2 reforming is not appropriate for the process.

5. RESULTS AND DISCUSSION ON PYROLYSIS AND STEAM REFORMING OF LARD

The results obtained from lard analysis and its pyrolysis and steam reforming experiments are presented in this chapter. A discussion on the comparison of the products obtained from BDO and lard pyrolysis is also presented.

5.1 Physical and Chemical Properties of Lard

The physical properties of the lard as well as its fatty acid composition are given in Table 5.1. The techniques used to obtain these properties were discussed in section 3.5.2. The data in Table 5.1 indicate that the feed has a high heating value (39.6 MJ/kg) and viscosity (36.4 mPa.s). Also, the lard contained large quantities of palmitic, stearic, oleic and linoleic acid moieties. The elemental analysis of the lard gave 77.3 wt% C, 12.2 wt% H, 10.5 wt% O. Traces of sulphur (~ 32 wppm) and nitrogen (~ 8 wppm) were also found. These trace amounts of sulphur and nitrogen in the feed is important criteria for its application for fuel. It means that the produced fuel will not be responsible for SO_x and NO_x emission both of which are undesirable in combustion processes.

In order to determine a reasonable temperature at which significant pyrolysis can occur, a TG/DTA analysis of the lard was done to estimate its boiling point. The profile observed is shown in Figure 5.1. The endothermic peak was observed at about 450^{o}C. Significant weight loss also occurred at about this temperature. This shows that the

Table 5.1 Physical and chemical properties of the feed (lard)

Physical properties	
Density @40ºC (kg/m^3)	940
Heat of combustion (MJ/kg)	39.6
Viscosity @40ºC (mPa.s)	36.4
CHNS/O analysis, wt% (wppm)	
C	77.3
H	12.2
N	0.0008 (8)
S	0.0032 (32)
O*	10.5
Composition, wt% of total fatty acids**	
C10:0 (Capric)	0.1
C12:0 (Lauric)	0.1
C14:0 (Myristic)	1.4
C15:0 (Pentadecanoic)	0.1
C16:0 (Palmitic)	24.1
C16:1 (Palmitoleic)	2.4
C17:0 (Magaric)	0.4
C18:0 (Stearic)	14.0
C18:1 (Oleic)	39.4
C18:2 (Linoleic)	14.2
C18:3 (alpha-Linolenic)	0.8
C18:4 (Octadecatetraenoic)	0.1
C20:0 (Arachidic)	0.2
C20:1 (Eicosenoic)	0.7
C20:2 (Eicosadienoic)	0.5
Others	1.4

*obtained by difference **xx:y: xx number of carbon atoms; y number of double bonds

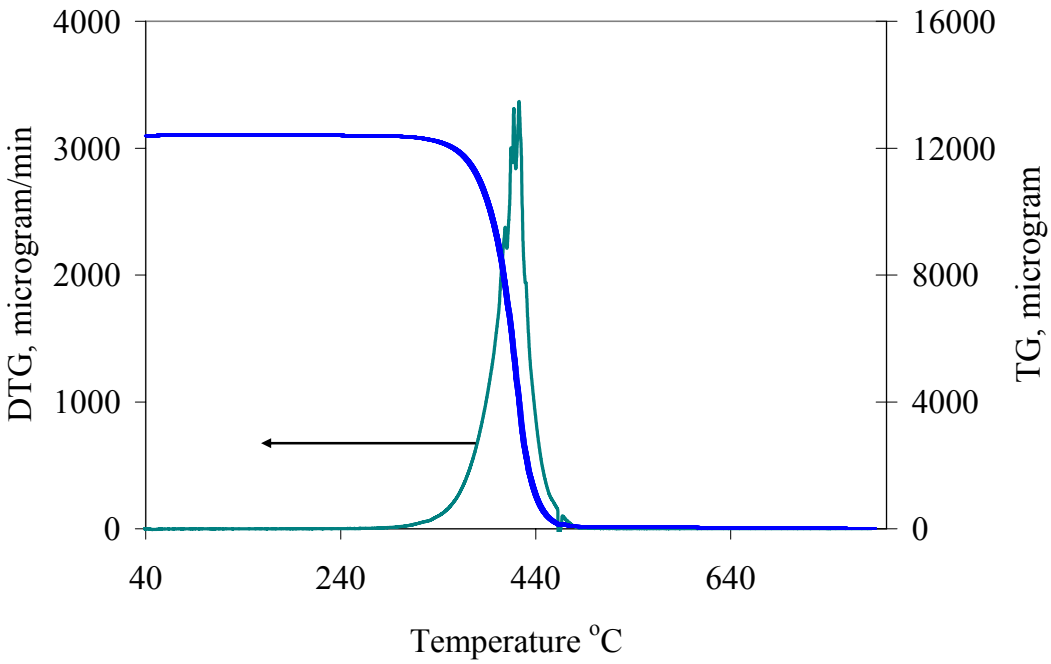

Figure 5.1 Thermo-Gravimetric/Differential Thermo-Gravimetric plots for lard

boiling point of the lard lies somewhere between 400 and 500^{o}C. It is therefore reasonable to start varying the pyrolysis temperature from 500^{o}C.

In this study, pyrolysis and steam reforming of lard were conducted in a fixed bed reactor. Generally, three products were recovered after each run. They were liquid condensate, char and gas. The liquids appeared brownish with a strong acrid smell. The effects of temperature, carrier gas flow rate and quartz packing particle size on gas and liquid yields, composition and calorific value of the product gas on steam reforming of lard were studied. The physical and chemical characteristics of the liquid product such as density, viscosity, cetane index and calorific value and how they compare to that of a conventional #2 diesel fuel were also discussed.

The material balances together with the gas composition and liquid product characterizations for all the experimental runs are given in Appendix C. The overall material balance was in the range of 90 to 98 wt%. The results for some of the runs at one set of conditions are given in Table 5.2. The results presented in the table include the mean value and the standard errors of the mean (SEM). The t-statistics of the data shows that there is no variation in the data at 95% confidence level. The statistical analysis was done by SAS V8 program.

5.2 Pyrolysis of Lard

Pyrolysis refers to a chemical change caused by the application of thermal energy in the absence of oxygen (Scott and Piskorz, 1982). The pyrolysis products of lard were gas, liquid and char. It was possible to determine CO, CO_2, and most of the C_1-C_4 hydrocarbon components (such as methane, ethylene, propane, propylene, isobutane, isobutylene, and 1-butene) in the gas product from GC analysis alone.

Table 5.2 Reproducibility of results during pyrolysis of lard (N_2: 50 cm^3/min, quartz particle size: 0.7-1.4 mm, lard: 5g/h, temperature: 550^oC)

	1	2	4	Mean ± SEM
Product gas composition, mol%				
H_2	0	0	0	0.00±0.0
CO	9.4	9.8	10.6	9.9±0.3
CO_2	4.6	4.5	5.1	4.7±0.2
CH_4	8.4	9.5	9.5	9.1±0.2
C_2H_4	21.6	24.6	24.6	23.6±0.6
C_2H_6	7.3	7.8	8	7.7±0.1
C_3H_6	10	15.6	15.6	13.7±1.1
C_3H_8	1.1	1	1.1	1.1±0.0
Gas heating value MJ/m^3	147.6	135.8	131.6	138.3±2.7
Liquid product characterization				
Diesel-like liquid product g/100g lard	28.1	30.7	31.4	30.1±2.0
Cetane Index	50.3	52.3	49.3	50.6±1.0
Density kg/m^3 @25^oC	880	875	880	878.3±4.0
Viscosity mPa.s @40^oC	10.6	9.5	11.1	10.4±0.5
Liquid heating value MJ/kg	40	39.5	39.9	39.8±0.1

GC/MS analysis was, however, required for identification of the compounds in the liquid product.

5.2.1 GC/MS study

The distribution of components in the liquid product as obtained by GC/MS is given in Table 5.3. The main components were alkanes and alkenes, which accounted for approximately 60% of the total weight. Carboxylic acids accounted for another 13–25%. Figure 5.2 shows, as an example, the GC/MS chromatogram for the liquid product obtained at a pyrolysis temperature of 550^{o}C with a carrier gas flow rate of 10 cm^{3}/min. Peaks identification was made by NIST search of the spectra. Those identification results of match quality higher than 90% were considered valid, once confirmed that the assignments were in agreement with published GC/MS data of similar products (Idem et al., 1996, Chan and Wan, 1947, Alencer et al., 1983). A detailed list of the compositions is presented in Appendix F. The liquid product contained a wide range of products (polar and non-polar) which made its analysis by gas chromatography difficult. Over 240 peaks were obtained when the liquid product was injected into a GC. Therefore detailed quantification of the components was not done.

5.2.2 Effects of residence time on pyrolysis of lard

The effects of residence time (RT) were studied at 600 and 800^{o}C, with packing particle size of 1.7-2.4 mm by varying the carrier gas (N_2) flow rate from 30 to 70 cm^{3}/min (RT, 1.5 to 3.4 s) for the runs at 600^{o}C and from 10 to 70 cm^{3}/min (RT, 1.2 to 8.4 s) for the runs at 800^{o}C. The packing particle size was chosen from the studies on BDO. The effects of residence time on the volume of product gas and its calorific value

Table 5.3 Distribution of groups (wt%) in the liquid product obtained during lard (~5g/h) pyrolysis

Components wt%	Conditions				
	Carrier gas cm^3/min	30	30	10	10
	Temperature ^oC	500	600	550	650
	Pump type	Eldex	Eldex	Syringe	Eldex
	Packing particle size, mm	1.7-2.4	1.7-2.4	1.7-2.4	1.7-2.4
Alkane		4.4	2.7	7.1	1.9
Cycloalkanes		2.8	10.9	7.3	2.4
Alkenes		21.2	27.3	35.0	23.6
Cycloalkenes		6.8	6.3	7.8	7.8
Alkynes		0.4	1.5	0	1.1
Dienes		4.7	7.5	6.2	3.9
Furan		0	0.9	0	0
Aromatics		1.6	10.4	4.0	32.3
Aldehyde		3.5	2.5	4.2	1.4
Ketones		4.1	2.8	2.4	1.4
Alcohol		6.7	5.9	3.7	7.0
Acids		25.8	17.5	13.1	13.2
Esters		18.2	3.9	9.1	4.1
Total		100	100	100	100
Hydrocarbons, HC		41.5	67.4	67.5	71.8
Oxygenated Hydrocarbons, OHC		58.2	32.6	32.5	27.1
HC/OHC		0.71	2.07	2.08	2.65

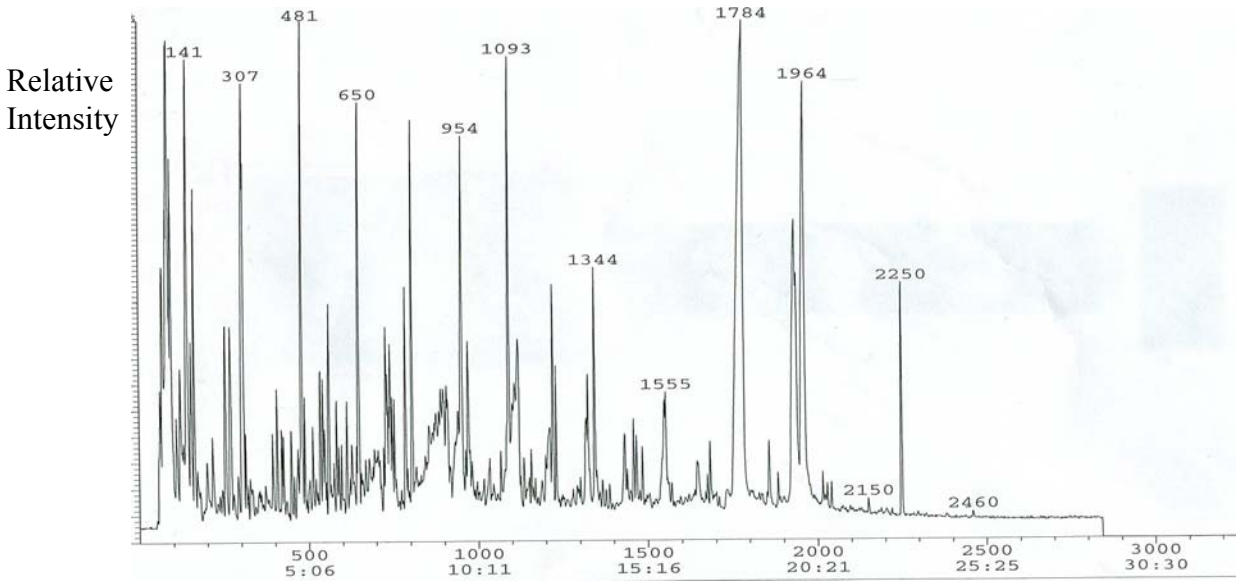

Figure 5.2 GC/MS Chromatogram for the pyrolysis liquid obtained at a temperature of 550^{o}C, carrier gas flow rate of 10 cm^{3}/min and quartz height of 70 mm and particle size of 1.7-2.4 mm

for the runs at 600^{o}C are shown in Figure 5.3. The volume of the product gas was observed to increase with an increase in residence time. This implies that reactions that are responsible for the bulk of the gas product are further down the reaction sequence and are thus favoured at high residence time. The calorific values of the product gas were high for all residence times. A maximum value of 133 MJ/m^3 was obtained at residence time of 2.1 s.

The effects of residence time on the total and diesel-like liquid yield are shown in Figure 5.4. The yields of both the total and the diesel-like liquid products decreased with increase in residence time. This implies that the reactions that are responsible for the formation of the liquid product such as C-C bond cleavage, decarboxylation, and decarbonylation (Idem *et al.*, 1996) are earlier in the sequence of reaction steps. Therefore, within the range of residence time used, an increase in residence time is detrimental to liquid production. However, Figure 5.5 shows that the CI of the liquid product is maximized at a residence time of 2.1 s. This implies that too low residence time can also be detrimental to the quality of the liquid product. Based on this observation, the residence time of 2.1 s was chosen as the optimum for high quality diesel yield. The viscosity of the liquid product increased from 1.8 to 3.8 mPa.s as the residence time increased from 1.5 to 3.4 s (Figure 5.5). The viscosity of a typical diesel fuel falls within this range. Figure 5.6 shows the effect of residence time on product gas composition. It is evident that there were no significant changes in the composition of most of the gases with residence time. For example, the concentration of $C_1 + C_2$ alkanes increased from 17 to 19 mol% with increase in residence time from 1.5 to 2.1 s but drops to 16 mol% at a residence time of 3.4 s. The concentrations of $C_2 + C_3$ olefins were high and varied between 41 and 46 mol percent.

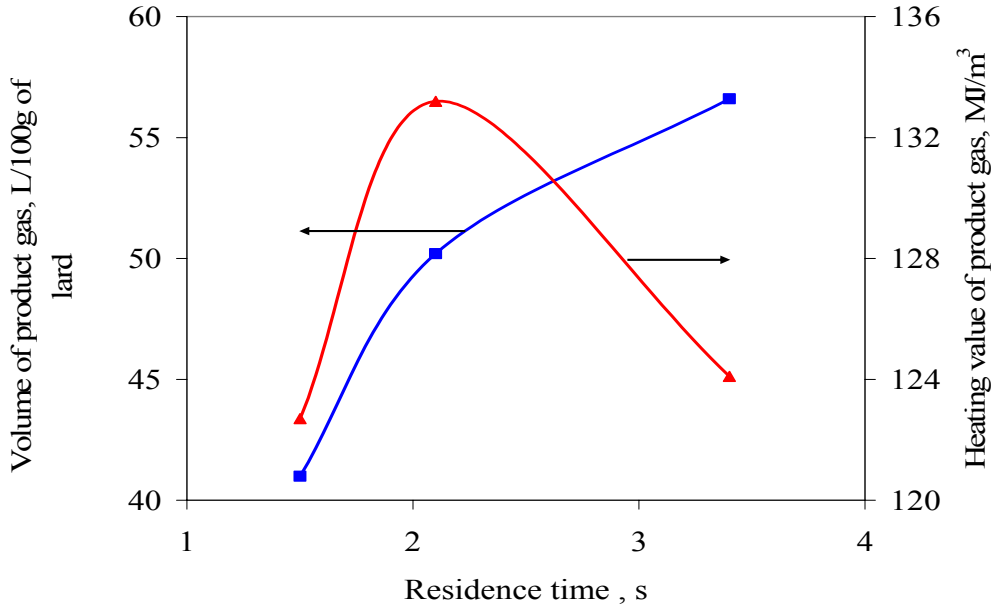

Figure 5.3 **Effects of residence time on volume and heating value of product gas (process: pyrolysis, temperature: 600°C, quartz packing height: 70 mm, size: 1.7-2.4 mm, reaction time: 30 min)**

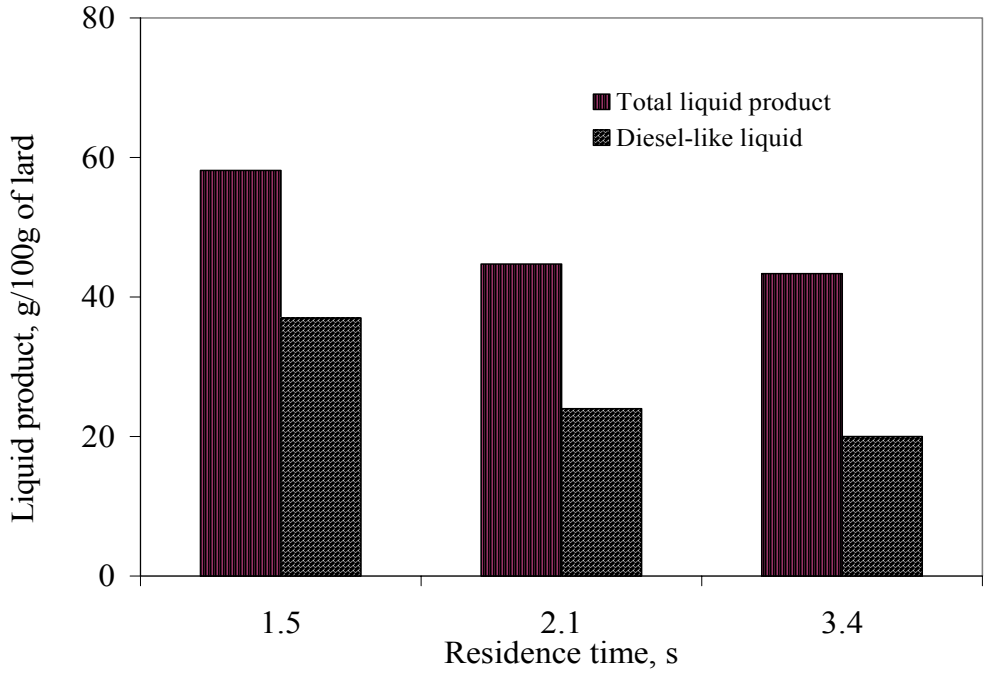

Figure 5.4 **Effects of residence time on total and diesel-like yields (process: pyrolysis, temperature: 600°C, quartz packing height: 70mm, size: 1.7-2.4 mm, reaction time: 30 min)**

Figure 5.5 **Effects of residence time on cetane index and viscosity of the total liquid product (process: pyrolysis, temperature 600°C, quartz packing height 70 mm, size 1.7-2.4 mm, duration 30 min)**

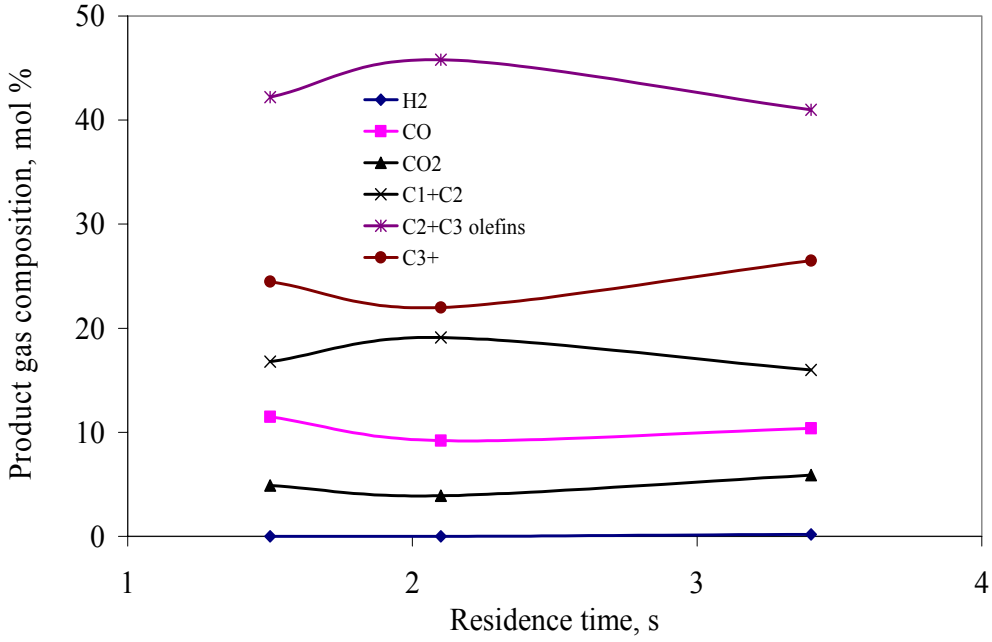

Figure 5.6 **Effects of residence time on products gas composition (Process: pyrolysis, temperature 600°C, quartz packing height 70mm, Size 1.7-2.4 mm, duration 30 min)**

At 800°C, the liquid production was quite small and could not be characterized. The effects of residence time on the gas composition are given in Figure 5.7. Similar to the observation at 600°C, there were no significant changes in the composition of most of the gases with residence time. However, contrary to what was observed at 600°C, there seems to be a reverse trend between the concentration of $C_1 + C_2$ alkanes and that of $C_2 + C_3$ olefins between the residence time of 1.2 to 2.8 s. The concentration of the alkanes increased from 25.9 to 31 mol% with increase in residence time from 1.2 to 2.8 s but drops to 29.6 mol% at a residence time of 8.4 s. On the other hand, the concentration of the olefins decreased from 45.3 to 42 mol% with increase in residence time from 1.2 to 1.4 s and remained almost constant as the residence time increased to 8.4 s.

Both at 600 and 800°C, olefin (ethylene and propylene) production were high. A maximum of 46 mol% was obtained at 600°C and a residence time of 2.1 s. Ethylene and propylene are important starting materials for the production of various chemicals in the petrochemical industry such as MTBE, polyethylene, and maleic anhydride. The C_{3+} concentration was low (~ 5 mol%).

5.2.3 Effects of quartz packing particle size

Idem et al. (1996) found out that the conversion of triglycerides was completely independent of the morphology of the cracking surface. Therefore no study was done on the effects of packing material. However, in order to know the effect, if any, of size of the packing material on pyrolysis, a study at 600°C was done on two different packing particle size ranges (0.7-1.4 mm and 1.7-2.4 mm) at a carrier gas flow rate of 50 cm^3/min, corresponding to a residence time of 2.1 s. The residence time of 2.1 s was chosen for further optimization based on the study on residence time in section 5.2.2.

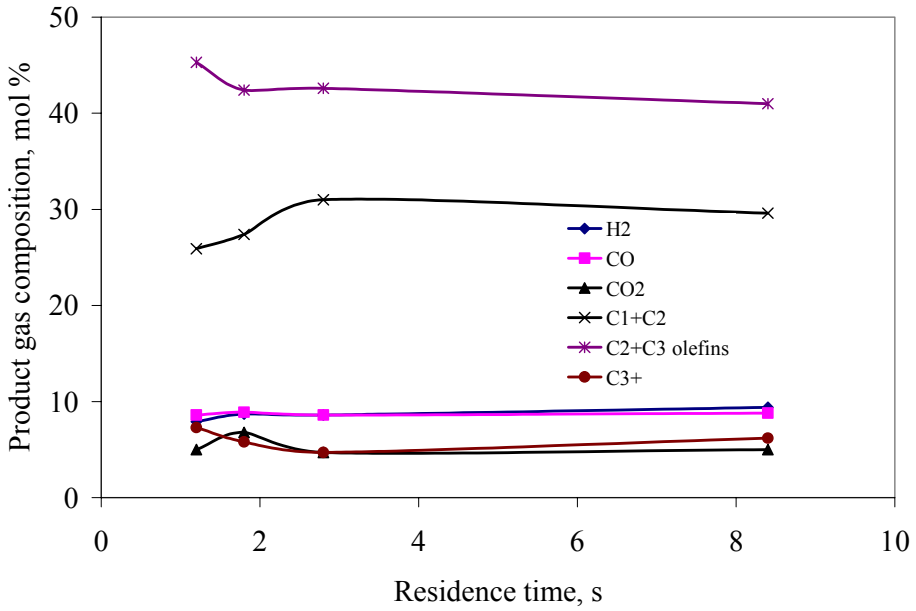

Figure 5.7 Effects of residence time on products gas composition (process: pyrolysis, temperature 800^{o}C, quartz packing height 70mm, size 1.7-2.4 mm, reaction time 30 min)

Table 5.4 shows the effects of packing particle size on gas composition and heating value, total and diesel-like liquid yields as well as on the CI and viscosity of the liquid product during pyrolysis of lard at 600^{o}C and carrier gas flow rate of 50 cm^{3}/min. The total liquid product increased from 45 to 53 g/100g lard with decrease in particle size. The residence time calculation in Appendix D was based on an empty reactor. The effect of the packing material was not considered in its calculation. The increase in total liquid product may be due to the fact that a higher residence time was achieved in the reactor with smaller particles. The smaller particles can also enhance better heat transfer. This probably reduced the residue retained in the reactor and increased the liquid product. Comparing the diesel-like liquid yield results with the error level observed in the reproducibility test (Table 5.2), it can be stated that there is no significant difference in the diesel like liquid yields from the two particle size ranges. It is interesting to observe a drastic drop (~ 50%) in viscosity with increase in packing particle size. However, the CI was also observed to decrease (~ 10%) with increase in packing particle size. This is because more lower molecular weight compounds are formed with the higher particle size packing. Mleczko *et al*. (1997) have stated that reactions in which H_2/CO are low (< 0.5) are mostly gas phase rather than surface reactions. Therefore, a large void volume (achieved by large particles) is necessary to enhance the reaction.

Based on the reproducibility of the experiment, there is a significant difference in the gas composition. The carbon oxides production increased while that of the hydrocarbons dropped. As explained above, the reactions are gas phase reactions, so a large void volume is required for effective cracking. This indirectly implies that the

Table 5.4 Effects of quartz packing particle size on pyrolysis of lard (N_2 flow rate 50 cm^3/min (STP), packing particle height 70 mm, lard 5g/h, and temperature 600^oC)

	Quartz packing particle size, mm	
	0.7-1.4	1.7-2.4
Product gas composition mol%		
H_2	0	0
CO	9	10.4
CO_2	3.6	5.9
CH_4	11	9.7
C_2H_4	27	25.2
C_2H_6	7.6	6.3
C_3H_6	17.1	15.8
C_3H_8	0.8	0.6
C_{4+}	24	26.1
Gas heating value MJ/m^3	130.0	133.2
Liquid product characterization		
Total liquid product, g/100glard	53	45
Diesel-like liquid, g/100g lard	24.40	25.04
Cetane Index	45.81	40.72
Density kg/m^3	860	860
Viscosity, mPa.s	4.53	2.32

liquid product at the higher particle size range is more deoxygenated and also explains why the cetane index is lower (Zhenyi et al., 2004).

5.2.4 Effects of temperature on pyrolysis of lard

The effects of temperature on the pyrolysis of lard to gas and liquid were studied by keeping the carrier gas flow rate (N_2-50 cm^3/min), packing bed height (70 mm of quartz, 0.7-1.4 mm particle size) and lard flow rate (≈ 5.0 g/h) constant and varying the temperature from 500 to 700^{o}C. The smaller particle size range was used for this study because of the higher liquid yield and higher cetane index obtained from the studies in section 5.2.3.

Figure 5.8 shows that the volume of the gas produced increased from 4.7 L/100g of lard at 500^{o}C to 102.3 L/ 100g of lard at 700^{o}C. The reactions such as decarboxylation, decarbonylation, C-C bond cleavage, and ethylene elimination that resulted in the formation of the bulk of the gas phase products are strongly endothermic (Idem et al., 1996). Thus the rate of reaction increased with temperature. The effects of temperature on the calorific value of the gas produced are also shown in Figure 5.8. The results indicated that the calorific value of the product gas was high (about three times that of natural gas). The calorific value of the gas decreased from 165 to 109 MJ/m^3 with an increase in temperature from 500 to 700 ^{o}C. This is due to an increase in hydrogen and carbon-dioxide concentration at higher temperature.

The amount of total liquid product decreased from 74 to 11g/100g of lard as the temperature increased from 500 to 700^{o}C (Figure 5.9). Low-temperature cracking results in the formation of relatively long-chain compounds. This led to increase in the yield of the total liquid product at the expense of gas phase product with decrease in temperature.

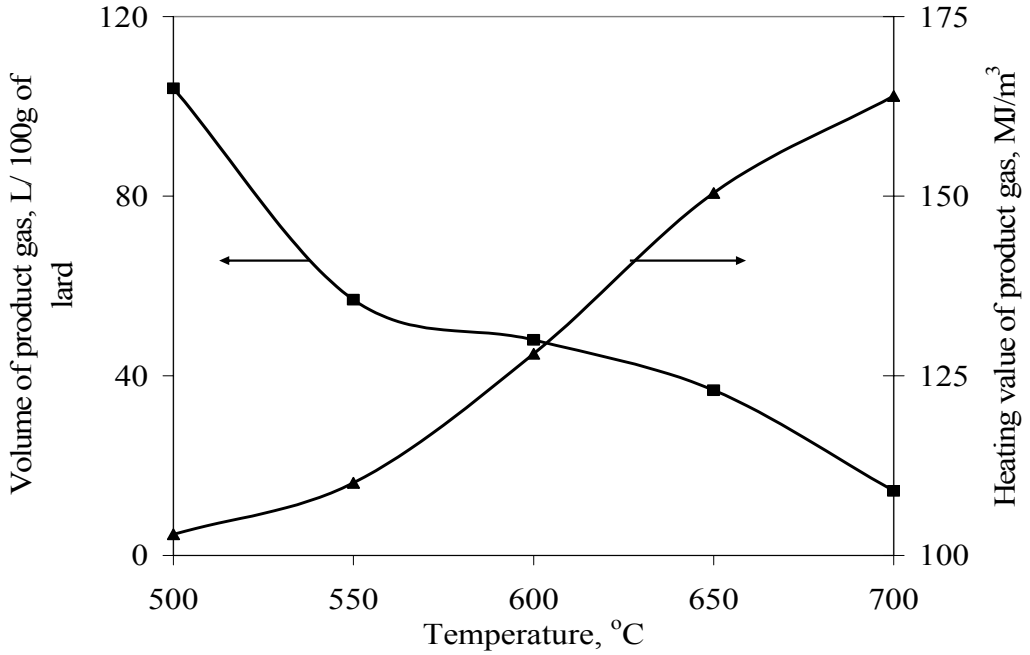

Figure 5.8 **Effects of temperature on volume and heating value of products gas (process: pyrolysis, carrier gas N_2: 50 cm^3/min, quartz packing height 70mm, size 0.7-1.4 mm, reaction time 30 min)**

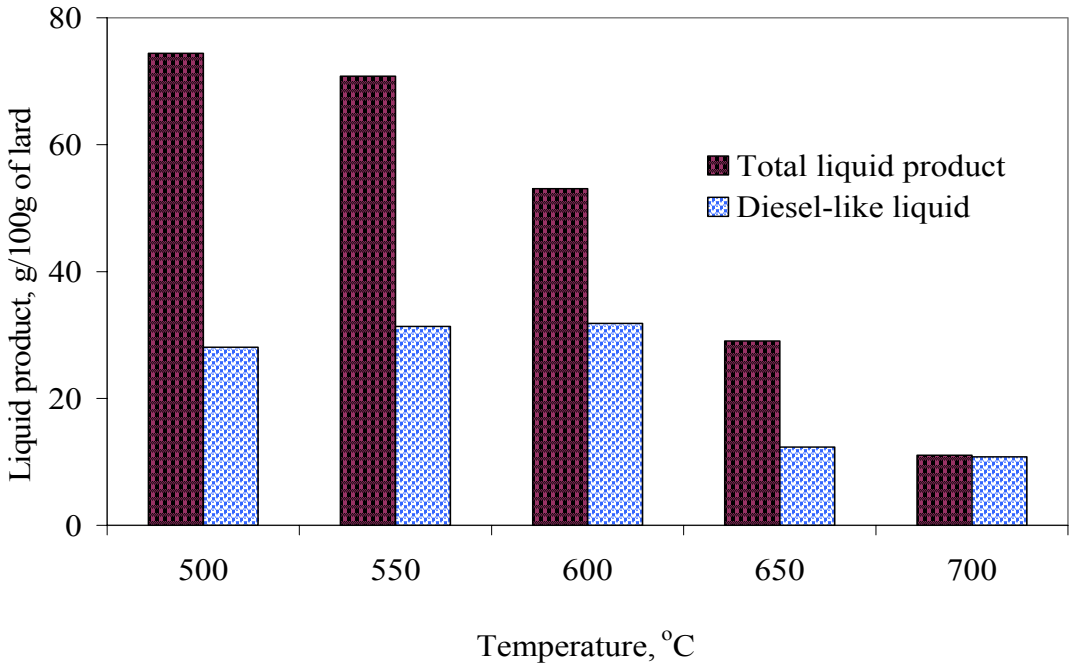

Figure 5.9 **Effects of temperature on total and diesel-like liquid yields (process: pyrolysis, carrier gas N_2: 50 cm^3/min, quartz packing height: 70mm, size: 0.7-1.4 mm, reaction time: 30 min)**

The diesel-like fraction of the liquid product is defined as the amount of liquid product boiling off in the #2 diesel range (171-350^{o}C). This is however seen to be maximized at reaction temperature of 550^{o}C and remained constant also at 600^{o}C (Figure 5.9). This can be explained thus: cracking at a low temperature implies that the lard undergoes only limited decomposition and consequently yields a small amount of low boiling components in the diesel range. Thus, there is a minimum temperature below which thermal cracking becomes unfavourable for diesel-like liquid production. Also, at the higher cracking temperatures, lower molecular weight products are formed. At higher temperature more of very low boiling components are formed which also reduces the quantity in the diesel boiling range.

The change in gas product composition as a function of temperature during pyrolysis of lard is shown in Figure 5.10. It is seen that with increase in temperature, the concentrations of H_2, paraffins and olefins increased whereas CO and CO_2 seems not to be affected by temperature. Also, the concentration of C_{3+} dropped significantly with temperature. As explained earlier, the higher the cracking temperature, the lower the molecular weights of the products formed. Therefore at high temperature more of the smaller molecular weight compounds such as methane, ethane, ethylene and ethane are formed at the expense of the C_{3+} hydrocarbons. In addition, dehydrogenation reaction for ethylene formation from ethyl radical is favoured at high temperatures, which explains why hydrogen formation at 700^{o}C, caused a further decrease in C_{3+} and an increase in olefin production. A similar trend was observed by Idem et al. (1996) from their study on canola oil pyrolysis. The effects of temperature (500-650 ^{o}C) on cetane index (CI) and viscosity of the liquid product are given in Figure 5.11. The CI decreased from 54 at 500^{o}C to 9.6 at 650^{o}C. The viscosity (at 40^{o}C) also decreased from 22.1 to

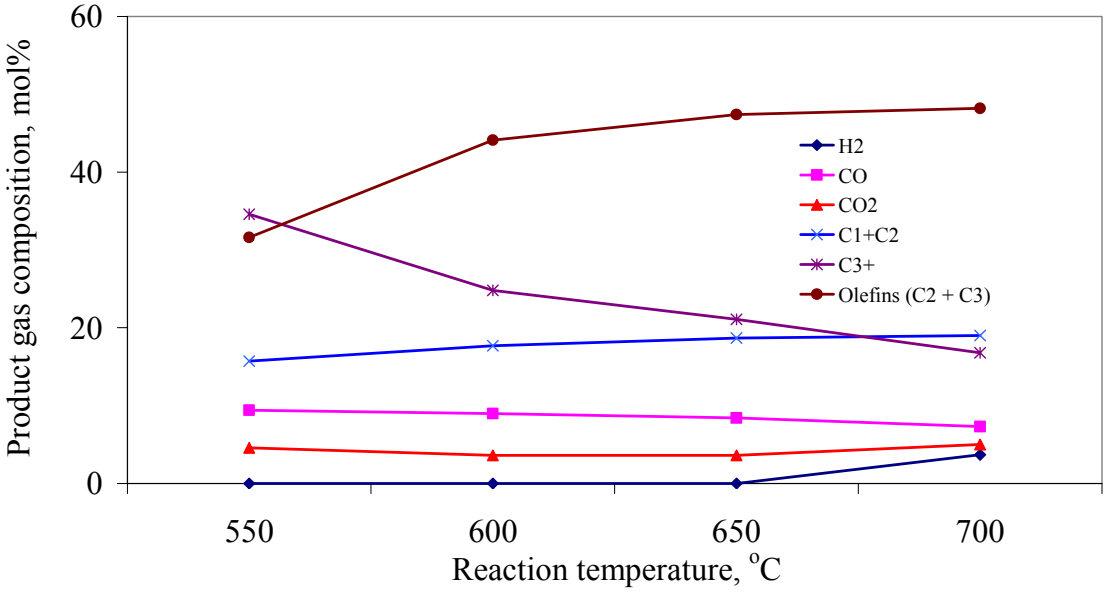

Figure 5.10 **Effects of temperature on products gas composition (process: pyrolysis, carrier gas N_2: 50 cm^3/min, quartz packing height 70 mm, Size 0.7-1.4 mm, reaction time 30 min)**

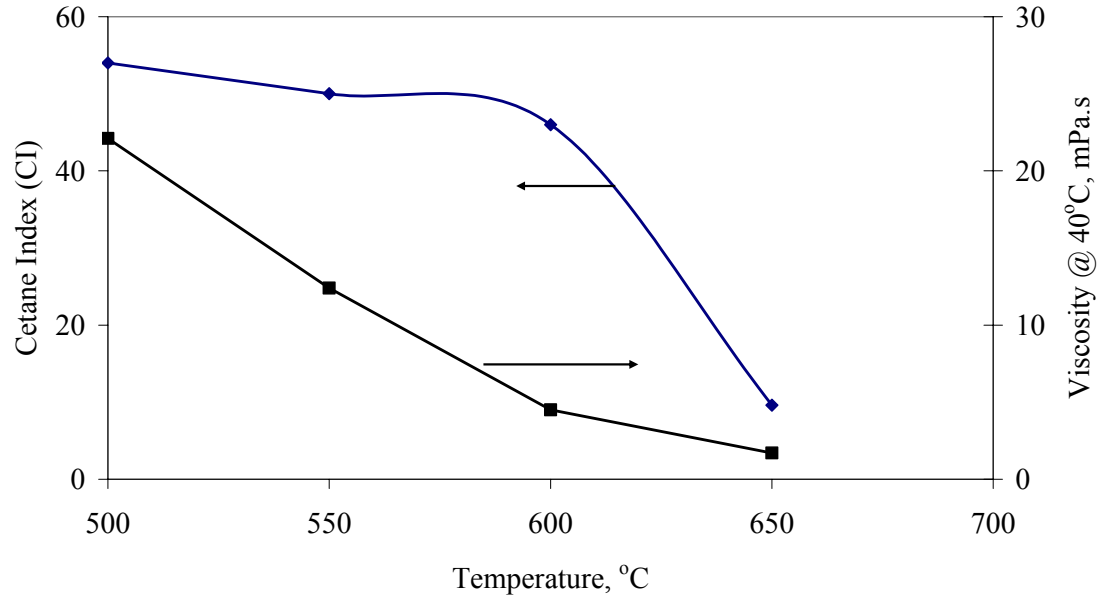

Figure 5.11 **Effects of temperature on cetane index and viscosity of the total liquid product (Process: Pyrolysis, Carrier gas N_2: 50 cm^3/min, Quartz packing height 70mm, Size 0.7-1.4 mm, Time 30 min)**

1.7 mPa.s. The decrease in the CI with temperature is due to the fact that more aromatics (having lower CI) are produced at higher temperature (Schwab *et al.,* 1987, Dandik and Aksoy, 1998). Also, the observed trend in viscosity is expected as the percent of the high molecular weight compounds in the liquid product decreased with temperature.

5.2.5 Effects of duration of experiment on product distribution

In order to collect enough samples for pour and cloud points determination, a run was conducted for a period of 225 minute. Table 5.5 shows a comparison among the products obtained for a run time of 30 minutes and 225 minutes. It was interesting to observe that the duration of the experiment has no significant effect on the gas phase composition, diesel-like liquid yield and the cetane index. However, the density and viscosity of the liquid product were significantly improved by the longer time experiment. This is probably due to the fact that the char formed over the longer time experiment had some catalytic effect on the reaction. It is worth noting also that the gas yield was increased and the char yield decreased significantly. A longer experiment time implies a longer period for the formed char to be gasified to gas.

5.3 Steam Reforming of Lard

All the steam reforming experiments were conducted with the smaller particle size quartz (0.7-1.4 mm). The liquid product in the steam reforming experiment refers to the organic portion of the total condensate. The aqueous layer was removed by decantation and analyzed for its water content. The organic layer was also analyzed for its water content. The mass of the aqueous portion was between 93.8 and 99.2 wt% of

Table 5.5 Effects of duration of experiment on pyrolysis of lard (N_2 flow rate 50 cm^3/min (STP), packing particle height 70 mm and size 0.7-1.4 mm, Lard 5g/h, and Temperature 600^oC)

	Duration of experiment, minutes	
	30	225
Product gas composition mol%		
H_2	0	0
CO	9	10.9
CO_2	3.6	4.7
CH_4	11	12.0
C_2H_4	27	27.2
C_2H_6	7.6	8.0
C_3H_6	17.1	17.2
C_3H_8	0.8	0.9
C_{4+}	24	19.1
Products yield (wt% of total product)		
Gas	39.8	51.7
Liquid	55.6	47.8
Char	4.5	0.45
Liquid product characterization		
Diesel-like liquid, g/100g lard	24.4	25.0
Cetane Index	45.8	45.9
Density kg/m^3	860	845
Viscosity, mPa.s	4.5	2.4

the water pumped during the experiment. The water content of the aqueous portion ranged between 97.5 and 99.8 wt% while that of the organic portion ranged between 0.85 and 1.12 wt% (Appendix C). For the runs conducted at 800^{o}C, the organic and the aqueous phases could not be separated because the organic portion was quite small. The quantity of the organic portion was therefore estimated by deducting the quantity of the water pumped from the total condensate (this evaluation assumes that water did not react which might not be the case). The determinations of the water content of the condensates obtained at 800^{o}C gave inconsistent results and were therefore not reported.

5.3.1 Effects of temperature on steam reforming of lard

The effects of temperature (500-600^{o}C) on steam reforming of lard to gas and liquid were studied while keeping the bed height (70 mm of quartz, 0.7-1.4), steam to lard ratio (S/L 1:1) and lard flow rate (≈ 5.0 g/h) constant. No carrier gas was used. Figure 5.12 shows the mass of the gas product increased from 1.2 wt% at 500^{o}C to 31.8 wt% at 600^{o}C. For comparison purpose, the results from pyrolysis experiment at a carrier gas flow rate of 50 cm^{3}/min were plotted along side with that of steam reforming (Figure 5.12). It is seen that the mass of the gas product increased from 4.7 wt% at 500^{o}C to 39.8 wt% at 600^{o}C during pyrolysis. The amount of liquid product during pyrolysis decreased linearly from 78.3 to 55.6 wt% as the temperature increased from 500 to 600^{o}C. The same trend was observed when steam was co-fed (88.7 to 63.2 wt%). The effect of co-feeding steam was to increase the liquid product. For example at 500^{o}C, 78.3 wt% of liquid was obtained during pyrolysis whereas 88.7 wt% was obtained when steam was co-fed. This same trend was observed by Idem et al. (1996) during their study

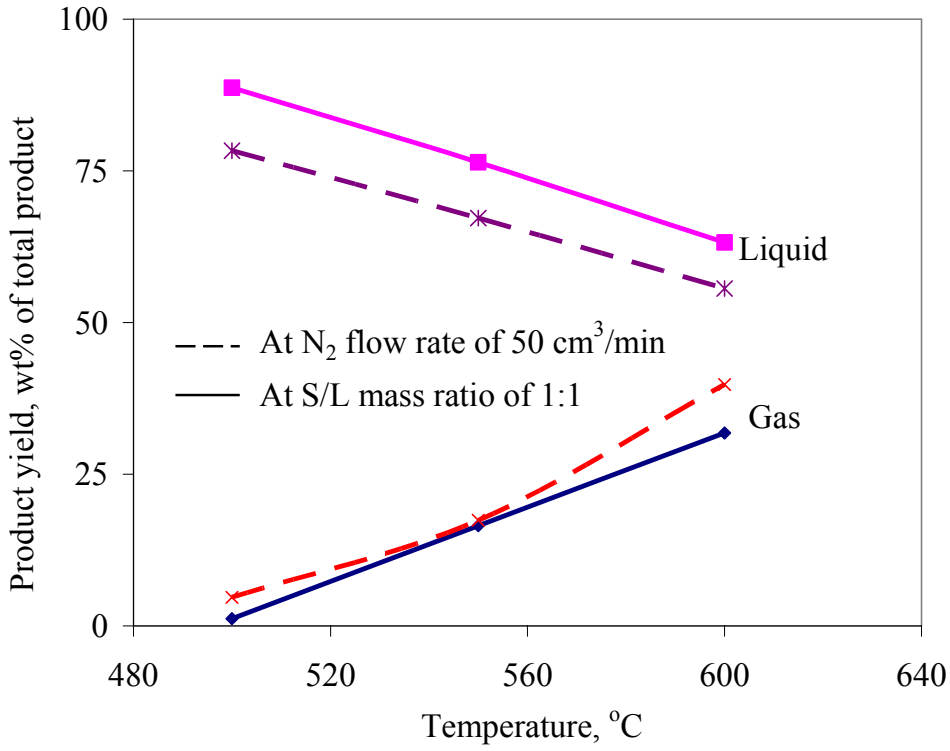

Figure 5.12 Comparison of the effects of temperature on gas and liquid yields of pyrolysis (Carrier gas N_2: 50 cm^3/min) and steam reforming (S/L :1, Quartz packing height 70mm, Size 0.7-1.4 mm, Time 30 min)

on canola oil where the organic liquid product increased from 14.8 to 21.1wt% when steam was introduced. On the other hand, the diesel-like liquid product was maximized at 550^{o}C (Figure 5.13). Similar observation was made for the pyrolysis reaction (cf Figure 5.10) but contrary to the case of pyrolysis, the same yield was not maintained at 600^{o}C.

The cetane index was high and found to remain almost constant (52 to 54) with increase in reaction temperature (Figure 5.14). The viscosity was observed to decrease with increase in temperature. The same trend was observed during pyrolysis but the viscosity was generally lower during steam reforming. It is shown from Figure 5.14 as compared to Figure 5.11 that the addition of steam helps to lower the viscosity. This is probably due to the higher water content of the liquid (see Appendix C).

5.3.2 Effects of steam to lard ratio on steam reforming of lard

The effects of steam to lard mass ratio (S/L) on product yield and product gas composition at a reaction temperature of 600^{o}C are shown in Figures 5.15 and 5.16 respectively. It should be noted that the term “liquid product” or “total liquid product” refers to the organic phase of the total condensate. The aqueous phase was removed and treated as unreacted water. Increasing the S/L from 0.5 to 1.5 increased the liquid product from 49.1 to 75.9 wt% and correspondingly decreased the gas product from 46 to 18.6 wt%. The char and residue yields were not affected by increase in S/L. A similar trend was observed by Idem et al. (1996). They explained that the effect of increasing S/L is similar to that of decreasing the residence time in the reactor. Therefore, the decrease in gas production with increase in S/L can be explained thus: the reactions

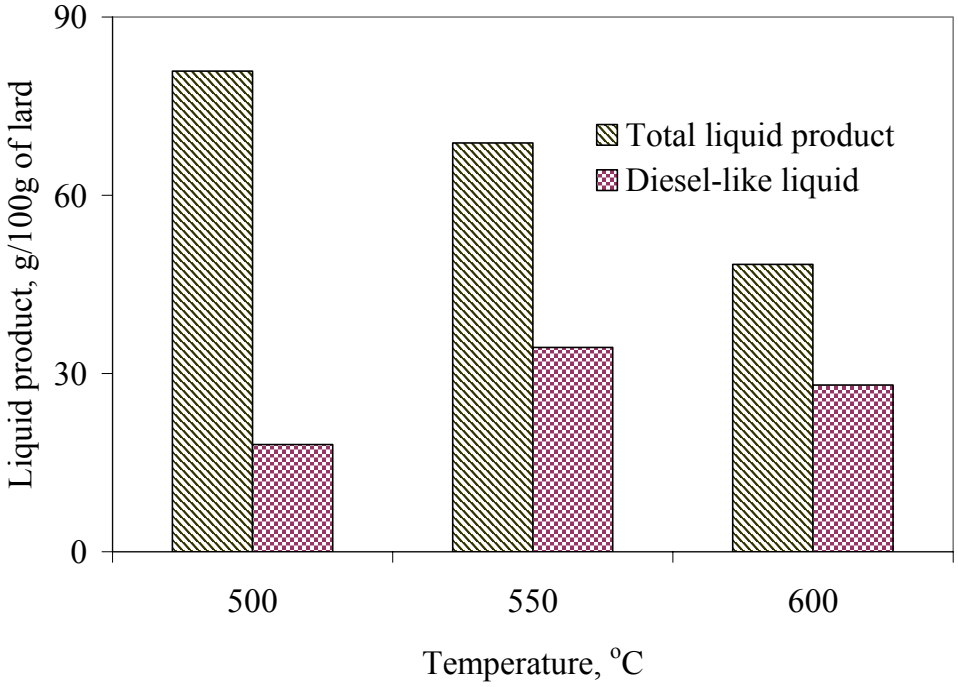

Figure 5.13 **Effects of temperature on total and diesel-like liquid yields (Process: steam reforming, S/L: 1, quartz packing height: 70mm, size: 0.7-1.4 mm, reaction time: 30 min)**

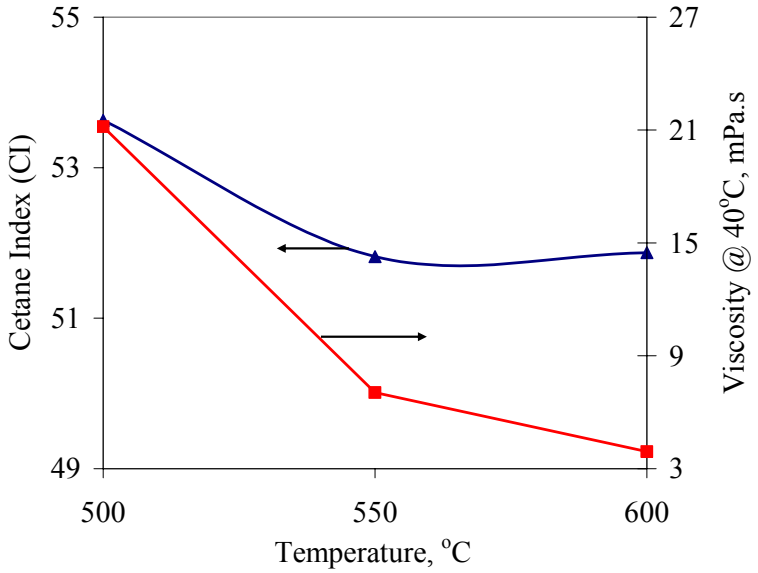

Figure 5.14 **Effects of temperature on cetane index and viscosity of the total liquid product (process: steam reforming, S/L: 1, quartz packing height: 70mm, size: 0.7-1.4 mm, reaction time: 30 min)**

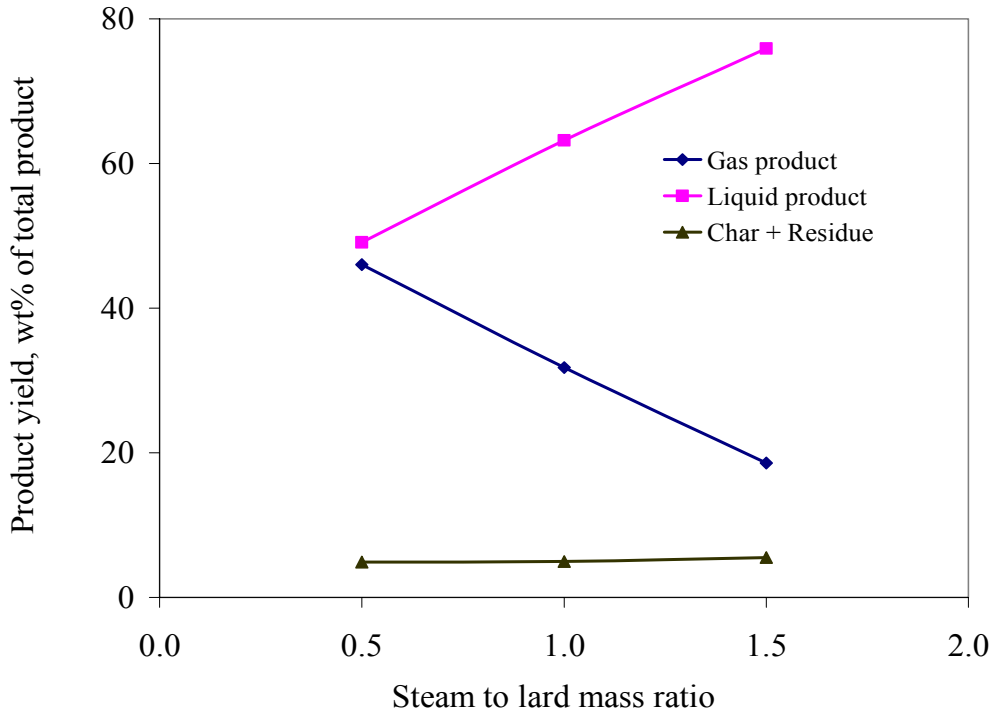

Figure 5.15 **Effects of steam to lard mass ratio (S/L) on products yield (process: steam reforming, temperature 600°C, quartz packing height 70mm, size: 0.7-1.4 mm, reaction time: 30 min)**

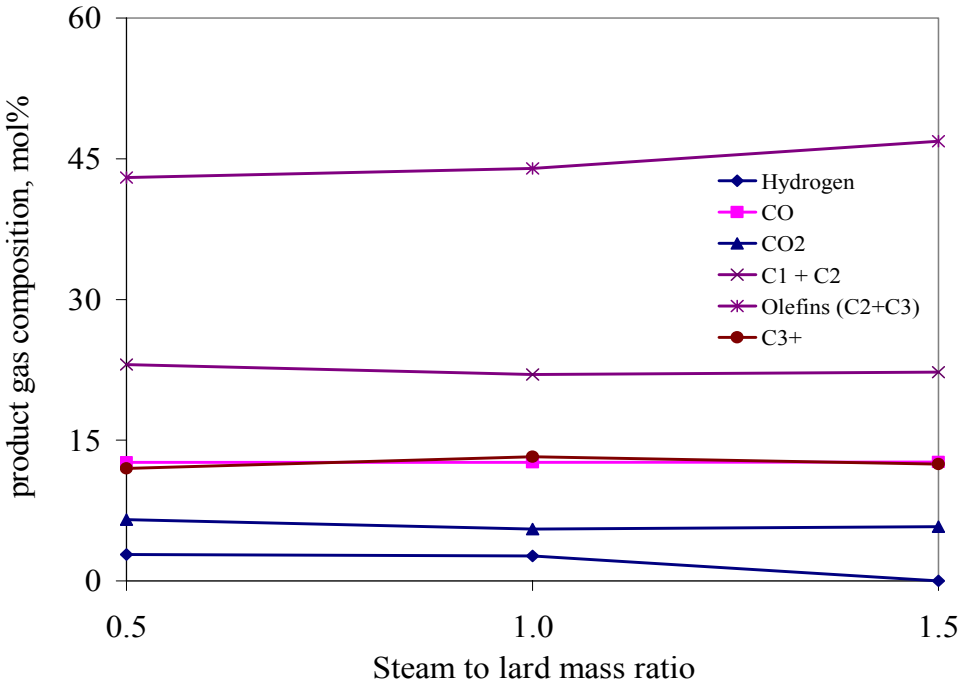

Figure 5.16 **Effects of steam to lard mass ratio (S/L) on product gas composition (process: steam reforming, temperature 600oC, quartz packing height: 70 mm, size: 0.7-1.4 mm, reaction time: 30 min)**

responsible for the formation of most of the compounds in the gas phase are further down in the reaction sequence and so a low residence time is detrimental to gas formation. The composition of the gas (Figure 5.16) is seen to almost be independent of S/L which might be due to equilibrium being reached in the gas phase. The yield of the diesel-like liquid was not affected by an increase in S/L even though the total liquid product increased with temperature (Figure 5.17). The effects of S/L on cetane index and viscosity are shown in Figure 5.18. Both viscosity and cetane index were found to increase with increase in S/L.

Steam reforming of lard was also conducted at 800^{o}C with the intent of totally gasifying the lard. However, it is interesting to observe that the trends followed by the liquid, gas and char yields were different from those observed at 600^{o}C as the S/L was increased (Figure 5.19). The gas yield increased with an increase in S/L while the liquid yield followed the reverse trend. An initial increase in S/L from 1 to 1.5 reduced the char formation from 11.8 to 7.8 wt% but a further increase in S/L caused an increase in char formation to 17 wt%. High temperature promotes cracking of feed to char (Czernik et al., 2004), as the S/L ratio was increased more steam was available to gasify the char. At higher S/L ratio, the residence time of the steam in the reactor was reduced so that there was not sufficient time to gasify the char. The variation observed in the composition of the gas is shown in Figure 5.20. Just as for the case at 600^{o}C, the composition of the gas was independent of S/L.

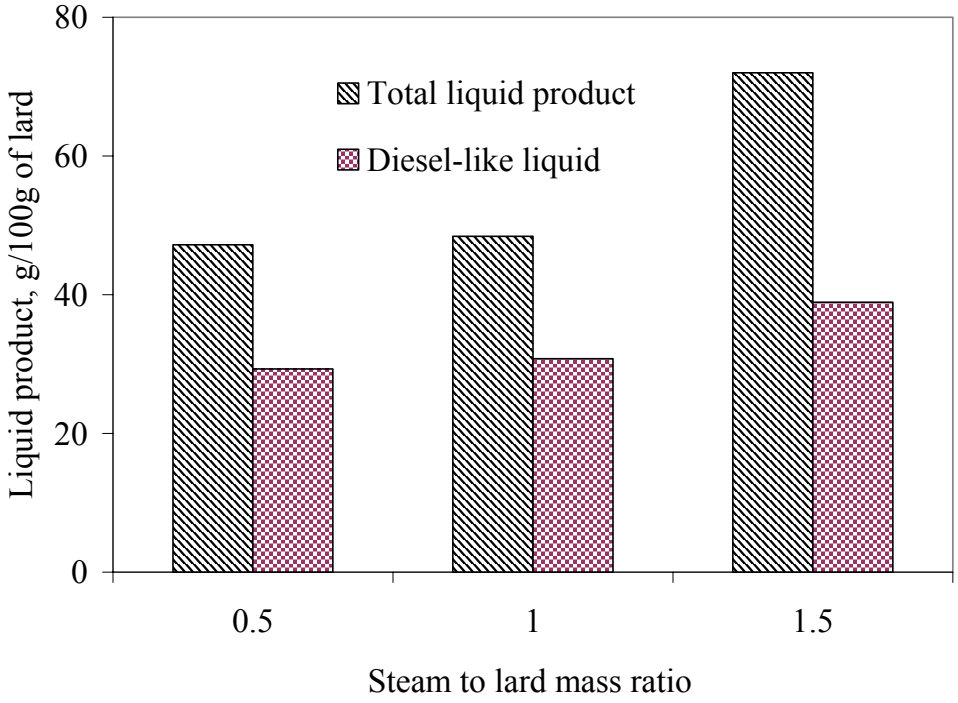

Figure 5.17 **Effects of steam to lard mass ratio (S/L) on total and diesel-like liquid yields (process: steam reforming, temperature 600°C, quartz packing height: 70mm, size: 0.7-1.4 mm, reaction time: 30 min)**

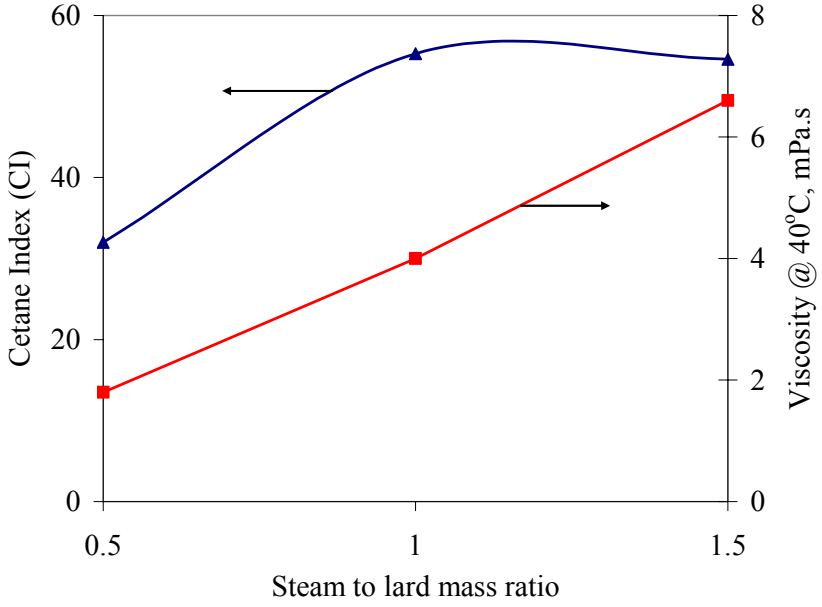

Figure 5.18 **Effects of steam to lard mass ratio (S/L) on cetane index and viscosity of the total liquid product (process: steam reforming, temperature 600°C, quartz packing height: 70mm, size: 0.7-1.4 mm, reaction time: 30 min)**

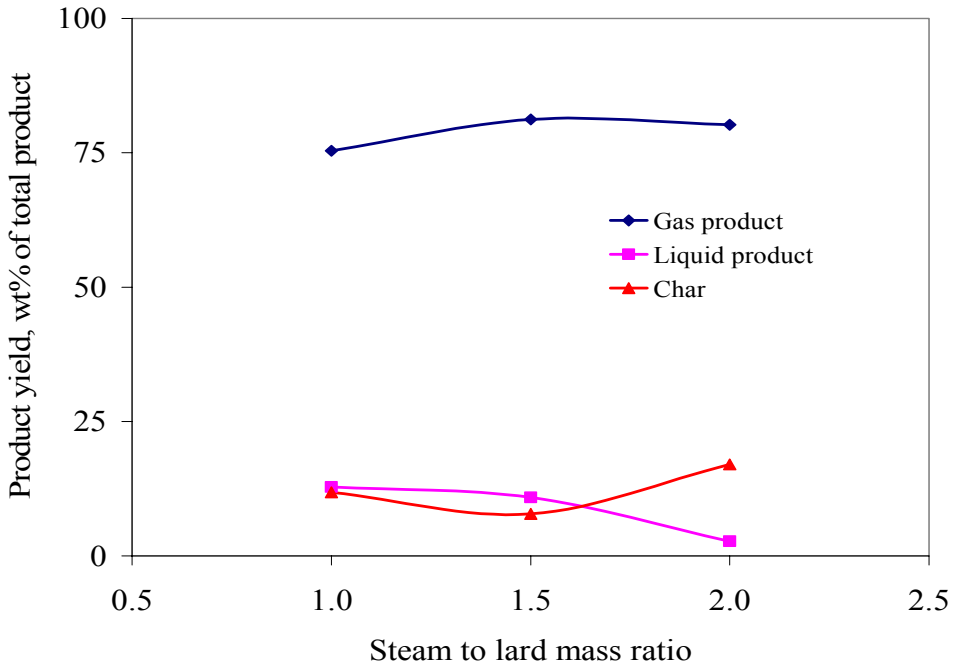

Figure 5.19 **Effects of steam to lard mass ratio (S/L) on products yield (process: steam reforming, temperature 800°C, quartz packing height: 70 mm, size: 0.7-1.4 mm, reaction time: 30 min)**

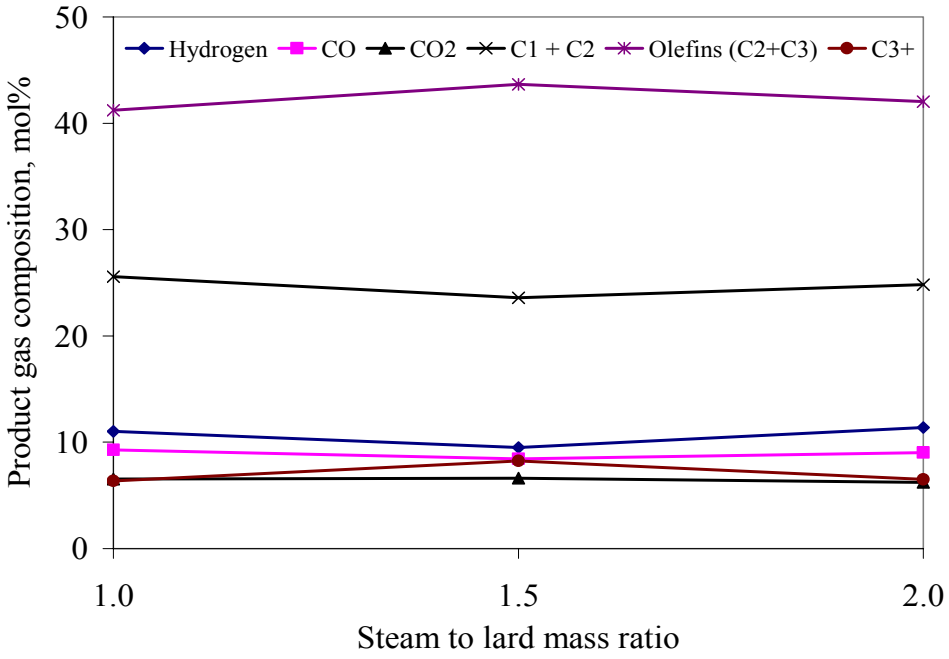

Figure 5.20 **Effects of steam to lard mass ratio (S/L) on product gas composition (process: steam reforming, temperature 800°C, quartz packing height: 70 mm, size: 0.7-1.4 mm, reaction time: 30 min)**

5.4 Fuel Properties of the Pyrolysis and Steam Reforming Liquid Products

The data collected from the characterization studies of the liquid product allowed for the comparison of the properties of this product with those of conventional diesel fuels. A comparison is shown in Table 5.6. The liquid product obtained through pyrolysis at 600^{o}C and 50 cm^{3}/min carrier gas (N_2) flow rate has a cetane index of 46 and density of 860 kg/m^{3} at 25^{o}C, which are in agreement with the specification for #2 diesel fuel. However, the viscosity (4.5 mPa.s at 40^{o}C) exceeds the specified value of 3.5 mPa.s for #2 diesel fuel. Also, the higher heating value of this liquid (~40 MJ/kg) is approximately 11% less than that of diesel fuel indicating a considerable amount of oxygenated compounds in the fuel (Schwab et al., 1988). The cloud point is high and well above that of #2 diesel whereas the pour point is comparable to that of #2 diesel. This is because the oxygenated compounds present interfere with the cloud point determination but did not interfere with that of pour point. A small amount of water (~ 0.5 wt%) was found in the liquid product. The water could easily be removed or retained as the case may be. There are some beneficial consequences of the presence of water. It causes a decrease in viscosity (as observed in this study), lowers the combustion temperature and, as a consequence, lowers the NO_x emission (Diebold, 1997). The liquid obtained during steam reforming has better fuel properties than that of the pyrolysis liquid (Table 5.6). No GC/MS studies were done on the liquid products from steam reforming experiments. These studies are necessary to elucidate the reason for the marked difference in the characteristics of the liquid products.

The simulated distillation curves for these liquids are compared to that of #2 diesel in Figure 5.21. These curves can be used to relate the volatilities of the three fuels

Table 5.6 Comparison of the properties of the optimum liquid obtained to automotive diesel fuel specifications for #2 diesel according to ASTM D975

Fuel property	#2 Diesel	Liquid product from pyrolysis	Liquid product from steam reforming
Cetane Index	45	46	52
Density @ 25°C, kg/m^3	860	860	860
Viscosity @ 40°C, mPa.s	3.5	4.5	4.0
Water content, %w/w	<0.05	0.53	0.89
Gross heat of combustion, MJ/kg	45	39.9	40.1
Cloud point, °C*	-8	10	nd
Pour point, °C*	-15	-18	nd

nd: not determined * cloud and pour points were determined for the run conducted over a period of 225 minutes

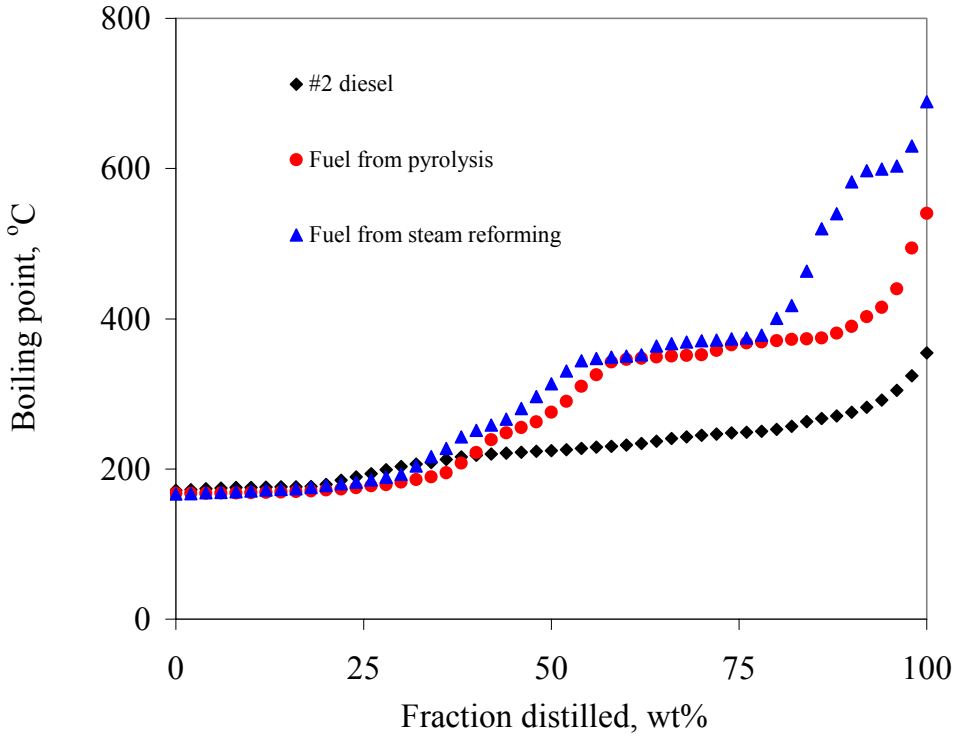

Figure 5.21 Comparison of the simulated distillation curves of the optimum liquid products obtained to that of #2 diesel

(Song, 2000). The distillation behaviour of the pyrolysis fuels is comparable to that of diesel at temperatures between 170 and 220^{o}C. Beyond 220^{o}C, #2 diesel is more volatile. It rapidly distilled and lost about 95 % of its initial weight when heated up to 300^{o}C. At about 350^{o}C, the diesel fuel was totally distilled off whereas only 70 wt% of the pyrolysis liquid product was distilled off at this temperature. Some residue still remained up to about 500^{o}C. The distillation curve of the fuel obtained through steam reforming is similar to that of the pyrolysis fuel. A discrepancy is however observed at about 400^{o}C. Only 60 wt% of the fuel obtained from steam reforming was distilled off at 350^{o}C. Some residue still remained until about 600^{o}C. The oxygenated compounds present in the liquid products contributed to their poor volatility as compared to #2 diesel. The liquid products can be improved by deoxygenation in order to obtain an enriched hydrocarbon diesel-like fuel (Lema et al., 2004). This might also improve the viscosity. The simulated distillation data for the other experimental runs are given in Appendix G.

5.5 Energy Balance

Due to the complex composition of lard (Neff et al, 2002), the energy balance study of this work was based on tristearin, a typical component of lard, whose thermodynamics data are readily available. Also, it was assumed that 1 mole tristearin cracked to produce 3 moles n-hexadecane, 2 moles ethylene, 4 moles CO and 1 mole CO_2. The energy balance was done for the experimental run conducted at a lard flow rate of 5g/h, temperature of 600^{o}C and carrier gas flow rate of 50 cm^{3}/min and also for the steam reforming experiment conducted at an S/L of 1:1 and 600^{o}C. The detailed energy balance is given in Appendix H. A summary table is shown in Table 5.7. The

Table 5.7 Summary of the energy balance during pyrolysis and steam reforming of lard

Process	Pyrolysis	Steam Reforming
Heat input kJ/g lard	2.4	6.3
Heat output kJ/g lard	24.2	28.2
Net energy gain kJ/g lard	21.8	21.9

heat required to preheat the feed to the reaction temperature and that required for the endothermic cracking (pyrolysis) reaction at 600^{o}C, taking 15% heat loss into consideration, sum up to 2.4 kJ/g of lard fed. The energy content of the liquid and gaseous fuels produced sum up to 24.2 kJ/g lard fed. Therefore, the net energy gain was 21.7 kJ/g of lard.

For the case of the steam reforming experiment, it was assumed that steam did not take part in the reaction. The total energy required for preheating lard and water and for the reaction, accounting for 15% heat loss, was 6.3 kJ/g of lard. The total energy recoverable from the liquid and gaseous fuel produced was 28.1 kJ/g of lard. Therefore, the net energy gain from the steam reforming process was 21.9 kJ/g of lard.

It should be noted that substantial amount of heat can be recovered by cooling the products to room temperature from the reaction temperature. This heat has not been considered in the energy balance calculation. Inclusion of this heat will give the energy balance a better picture.

5.6 Comparison of Products from Pyrolysis of BDO and Lard

A comparison between the products yields, gas composition and properties obtained during pyrolysis of BDO and lard is given in Table 5.8. The data is based on the runs conducted at 800^{o}C, carrier gas (N_2) flow rate of 30 cm^3/min and quartz packing particles of 1.7-2.4 mm using Eldex A-10-S pump.

It is interesting to note from Table 5.8 that under similar operating conditions, hydrogen yield from lard is over 56% more than that obtainable from BDO. This can be explained based on their respective CHN analysis. The percentage of hydrogen in BDO is 8.3 wt% whereas it is 12.2 wt% in lard (Tables 4.2 and 5.1). The higher percentage of carbon oxides (CO and CO_2) observed in BDO (45.8 mol%) than lard (20.7 mol%) is also due to the marked difference (56.0 wt% for BDO and 10.5 wt% for lard) in the oxygen wt% obtained by difference from CHN analysis. The synthesis gas yield from BDO (73.0 mol%) was higher than from lard (62.2 mol%) because the CO yield from BDO was very large. However, very high H_2/CO (~5) was obtained from lard as against ~1 from BDO. In addition, the hydrocarbon yield from lard (28.3 mol%) was slightly higher than that from BDO (21.2 mol%).

Thus, higher heating value gas was obtained from lard. This is probably also due to the marked difference in their (BDO and lard) carbon content. The volume of gas produced per 100 g of feed was quite high for lard (~ 160 L) whereas about 38 L of gas per 100g of feed was obtained for BDO. The lard was completely converted to gas and char. About 42 wt% of condensate was obtained from BDO which explains why the gas yield was low.

Table 5.8 Comparison of products obtained from BDO and lard pyrolysis (temperature: 800°C, quartz packing height: 70mm, size: 1.7-2.4 mm, reaction time: 30 min)

Feed stock	Biomass-derived oil	Lard
Temperature °C	800	800
Q. particle size mm	1.7-2.4	1.7-2.4
Carrier gas (N_2) cm^3/min	30	30
Feed pumped	2.0	2.2
Condensate wt%	41.9	0
Char wt%	23.4	31.8
Gas wt%	34.8	67.2
Gas composition mol%		
H_2	33.1	51.8
CO	39.9	10.4
CO_2	5.9	10.3
CH_4	14.4	11.4
C_2H_4	5.5	10.1
C_2H_6	0.6	2.5
C_3H_6	0.4	2.7
C_3H_8	0.03	0.1
C_{4+}	0.3	1.5
H_2+CO	73.0	62.2
H_2/CO	0.83	4.98
Heating Value MJ/m^3	22.1	30.5
Volume of gas L/100g feed	37.7	160.0

On the basis the results in Table 5.8, it can be inferred that lard is a better feedstock for the production of hydrogen, char, high heating value gas and high H_2/CO ratio than BDO. On the other hand, BDO is the preferred feedstock for the production of synthesis gas with H_2/CO in the vicinity of 1. With possible steam reforming reaction, this feedstock can be further improved to H_2/CO ratio of 2 which is a good ratio for Fischer-Tropsch synthesis.

6. CONCLUSIONS AND RECOMMENDATIONS

6.1 Conclusions

This research focused on two main feed stocks (BDO and lard) and their conversion to value added products. The main objective of the study on BDO was to use CO_2 for its reforming thereby finding a sink for the greenhouse gas (CO_2). A list of the conclusions drawn from the observations on this study is presented in Section 6.1.1. The objective on the study on lard was based on converting animal fats, a waste product of the livestock industry, to gaseous and liquid fuels. The conclusions drawn from results obtained on this study are listed in Section 6.1.2.

6.1.1 CO_2 reforming of biomass derived oil

The following conclusions were drawn from the studies on CO_2 reforming of BDO.

1. BDO has been converted to synthesis gas and medium heating value gaseous fuel by CO_2 reforming. The product gas consisted mostly of H_2, CO, CO_2, CH_4 and C_2H_4. Composition of product gas ranged between synthesis gas 61-76 mol%, CH_4 3-18 mol%, and C_2H_4 1-6.5 mol%.
2. The synthesis gas production was high (> 60 mol%) in all cases, with or without addition of CO_2. The maximum production of synthesis gas (~76 mol%) was observed at a total carrier gas flow rate of 60 cm^3/min and a mole fraction of CO_2 in carrier gas of 0.1. The maximum gas production (51 wt%) was observed at a total carrier gas flow rate of 30 cm^3/min containing 20 mol% of CO_2.

3. Maximum hydrogen (42 mol%) and H_2 to CO molar ratio (1.44) were obtained while using only N_2 as the carrier gas at a flow rate of 50 cm^3/min.
4. The addition of CO_2 to N_2 in the carrier gas led to less char formation and more gas production. The char formation decreased with an increase in mole fraction of CO_2 in the carrier gas (50 cm^3/min) from 0 to 0.5 but increased as the mole fraction of CO_2 increased to one. The minimum char formation (18 wt%) for all the experiments conducted was observed at a total carrier gas (N_2 + CO_2) flow rate of 50 cm^3/min containing 50 mol% CO_2.
5. The maximum product gas heating value (25 MJ/m^3) and alkanes production (18 mol%) were obtained at a total carrier gas flow rate of 30 cm^3/min containing 40 mol% CO_2.
6. The study shows that in the range of residence time considered, CO_2 is not consumed in BDO gasification at 800^oC.

6.1.2 Pyrolysis and steam reforming of lard

The following conclusions were drawn from the studies on pyrolysis and steam reforming of lard in a fixed bed reactor.

1. A diesel-like liquid has been produced from pyrolysis and steam reforming of lard in the absence of a catalyst. This study also identifies animal fats as a source of high calorific value (68 - 165 MJ/m^3) gaseous fuel. Lard was converted to liquid product containing diesel boiling range hydrocarbons and gas product which consists mostly of C_1-C_3 hydrocarbons, CO, CO_2 and H_2 by pyrolysis and steam reforming.

2. Pyrolysis of lard is strongly influenced by temperature, residence time and packing particle size in the reactor. The total liquid product increased with decrease in temperature. The diesel-like liquid yield decreased with increase in residence time but was not affected with increase in packing particle size. The maximum yield for diesel-like liquid product (37g/100g lard) was obtained at 600^{o}C, residence time of 1.5 s and packing particle size of 1.7- 2.4 mm.

3. The liquid product essentially consists of linear and cyclic alkanes and alkenes, aromatics, ketones, aldehydes and carboxylic acids. The liquid product having fuel properties closest to that of conventional #2 diesels was obtained at a pyrolysis temperature of 600^{o}C and carrier gas flow rate of 50 cm^{3}/min (residence time 1.8 s) while using quartz chips particle size of 0.7-1.4 mm as reactor packing material. The liquid has a CI of 46, specific gravity of 0.86, viscosity of 4.5 mPa.s at 40^{o}C, a heating value of ~ 40MJ/kg, and cloud and pour points of 10 and -18 respectively.

4. The total liquid product from steam reforming of lard increased with increase in the steam to lard ratio. The maximum diesel-like liquid yield from the steam reforming process (39 g/100g of lard) was obtained at a steam to lard mass ratio of 1.5 and a temperature of 600^{o}C. This value is not significantly different from that obtained from pyrolysis. Higher cetane index (52) and lower viscosity (4.0 at 40^{o}C) were obtained by adding steam.

5. The net energy recovered from pyrolysis and steam reforming processes was approximately 21.9 kJ/g of lard. Thus, the processes are energy efficient.

In comparison, lard is a better feedstock for the production of hydrogen, char, high heating value gas and high H_2/CO ratio than BDO. On the other hand, BDO is the preferred feedstock for the production of synthesis gas with H_2/CO in the vicinity of 1.

6.2 Recommendations

6.2.1 CO_2 reforming of biomass-derived oil

From the experimental work and the results obtained from CO_2 reforming of BDO, the following recommendations are made:

1. CO_2 reforming of BDO could be carried out at a higher pressure and/or temperature to enhance char gasification to CO.
2. Analysis of the liquid products obtained of CO_2 reforming of BDO is necessary to thoroughly understand the role of CO_2 in the process

6.2.2 Pyrolysis and steam reforming of lard

The following recommendations are made based on the experiments and the results obtained from pyrolysis and steam reforming of lard to fuels and chemicals.

1. A detailed analysis of the liquid product is required; this could be done by first converting the carboxylic acids in the product into water soluble salts by neutralization with KOH. The water insoluble hydrocarbon phase can then be separated and analyzed by GC. The resultant solution of salts of carboxylic acids can then be converted to esters by acidification. The esters can then be analyzed by gas chromatography (Dandik and Aksoy, 1998).
2. For the heat source, microwave assisted heating rather than the conventional heating can be considered. It has been shown that microwave assisted heating

during pyrolysis leads to less aromatics and polyaromatics formation (Dominguez *et al*, 2003)

3. Although there is an advantage of using oxygenated fuel (e.g. biodiesel) in terms of reduction in the release of CO into the atmosphere, if needed, the produced fuel can be deoxygenated further by distillation to remove the heavy oxygenated compounds.
4. The experimental design in this study was based on the study of a single factor such as temperature at a time. A further study is needed to examine the interactive effects of the factors affecting the process so as to obtain a "true" optimum.

6. REFERENCES

Adjaye, J. D., R. K. Sharma. and N. N. Bakhshi, "Characterization and Stability Analysis of Wood-Derived Bio-oil", Fuel Processing Technology, **31,** 241-256 (1992).

Alencer, J.W., P. B. Alves and A. A. Craveiro, "Pyrolysis of Tropical Vegetable Oils", J. Agric. Food Chem., **31,** 1268-1270 (1983).

Ali, Y. and M. A. Hanna, "Physical Properties of Tallow Ester and Diesel Fuel Blends", Bioresource Technology, **47**, 131-134 (1994).

AOCS Ca 5a-40: Free fatty acids. In: Official Methods and Recommended Practices of the AOCS, 5th ed. American Oil Chemists' Society Press, Champaign, IL (1997).

ASTM D97-96: Standard test method for pour point of petroleum products. In: Annual Book of ASTM Standards, vol. 05.01. ASTM, Philadelphia, PA, 76–79 (1998).

ASTM D240-92: Standard test method for heat of combustion of liquid hydrocarbon fuels by bomb calorimeter. In: Annual Book of ASTM Standards, vol. 05.01. ASTM, Philadelphia, PA,133–140 (1998).

ASTM D2500-91: Standard test method for cloud point of petroleum products. In: Annual Book of ASTM Standards, vol. 05.01. ASTM, Philadelphia, PA, 845–847 (1998).

ASTM D5002-94: Standard test method for calculated cetane index of distillate fuels. In: Annual Book of ASTM Standards, vol. 05.03. ASTM, Philadelphia, PA, 263–266 (1998).

ASTM D976-91: Standard test method for cloud point of petroleum products. In: Annual Book of ASTM Standards, vol. 05.01. ASTM, Philadelphia, PA, 340-342) (1998).

ASTM D2887-97: Standard test method for boiling range distribution of petroleum fractions by gas chromatography. In: Annual Book of ASTM Standards, vol. 05.03. ASTM, Philadelphia, PA, 195–204 (1998).

Bharadwaj, S.S. and L.D. Schmidt, "Catalytic Partial Oxidation of Natural Gas to Syngas", Fuel Processing Technology, **42**, 109-127 (1995).

Billaud, F., V. Dominguez, P. Broitin and C. Busson, "Production of Hydrocarbons by Pyrolysis of Methyl Esters from Rapeseed Oil", J. Am. Oil Chem. Soc., **72,** 1149–1154 (1995).

Caballero, M. A., M. P. Aznar, J. Gil, J.A. Martin, E. Frances and J. Corella, "Commercial Steam Reforming Catalysts To Improve Biomass Gasification with Steam-Oxygen Mixtures: 1. Hot Gas Upgrading by the Catalytic Reactor", Ind. Eng. Chem. Res., **36**, 5227-5239 (1997).

Chaala A. and C. Roy, "Recycling of Meat and Bone Meal Animal Feed by Vacuum Pyrolysis", Environ. Sci. Technol., **37,** 4517-4522 (2003).

Chang, C.C. and S.W. Wan, "China's Motor Fuels from Tung Oil", Ind. Eng. Chem., **39,** 1543-548 (1947).

Chaudhari, S.T. and N.N. Bakhshi "Steam Gasification of Chars and Bio-oil" Report to Bioenergy Development Program Renewable Energy Branch, Energy, Mines and Resources, Ottawa Canada, 219-242 (2002).

Chaudhari, S.T., S.K. Bej, N. N. Bakhshi, and A.K. Dalai, "Steam Gasification of Biomass-Derived Char for the Production of Carbon Monoxide-Rich Synthesis Gas", Energy & Fuels, **15**, 736-742 (2001).

Corella, J., A. Orio, and P. Aznar, "Biomass Gasification with Air in Fluidized Bed: Reforming of the Gas Composition with Commercial Steam Reforming Catalysts" Ind. Eng. Chem. Res, **37,** 4617- 4624 (1998).

Czernik, S., R. French, C. Feik and E. Chornet, "Production of Hydrogen from Biomass Derived Liquids", Proceeding of the 2001 DOE Hydrogen Program Review NREL/CP-570-30535 (2001).

Dandik, L. and H.A. Aksoy, "Pyrolysis of Used Sunflower Oil in the Presence of Sodium Carbonate by Using Fractionating Pyrolysis Reactor", Fuel Processing Technology, **57**, 81- 92 (1998).

Demirbas, A "Biodiesel Fuels from Vegetable Oils via Catalytic and Non-catalytic Supercritical Alcohol Transesterifications and Other Methods: a Survey", Energy Conversion and Management, **44**, 2093-2109 (2003).

Diebold, J.P., T.A. Milne, S. Czernik, A. Oasmaa, A.V. Bridgwater, A. Cuevas, S. Gust, D. Huffman and J. Piskorz, "Proposed Specifications for Various Grades of Pyrolysis Oils" In: A.V. Bridgwater and D.G.B. Boocock (Eds.), Developments in Thermochemical Biomass Conversion, Blackie Academic and Professionals, London, 433–447 (1997).

Dominguez, A., J.A. Menendez, M. Inguanzo, P.L. Bernad, and J.J. Pis, "Gas Chromatographic-Mass Spectrometric Study of the Oil Fractions Produced by Microwave-Assisted Pyrolysis of Different Sewage Sludges", Journal of Chromatography A, **1012**, 193-206 (2003)

Diebold, J. and J. Scahill, "Production of Primary Pyrolysis Oil in a Vortex Reactor" In: E.J. Soltes, T.A. Milne (Eds.), Pyrolysis Oils from Biomass: Producing, Analyzing and Upgrading, ACS Symposium Series 376, American Chemical Society, 31- 40 (1988).

Diebold, J. P. and A.V. Bridgwater, "Overview of Fast Pyrolysis of Biomass for the Production of Liquid Fuels" In: A.V. Bridgwater, D.G.B. Boocock (Eds.), Developments in Thermochemical Biomass Conversion, Blackie, London, **1**, 5-26 (1997).

DynaMotive Energy Systems Corporation,"Fast Pyrolysis of Bagasse to Produce Bio-oil Fuel for Power Generation" 2001 Sugar Conference, (2001).

Ferdous, D., A.K. Dalai, S.K. Bej, R.W. Thring, and N.N. Bakhshi, "Production of H_2 and Medium Btu Gas via Pyrolysis of Lignins in a Fixed-Bed Reactor**",** Fuel Process. Technol., **70**, 9-26 (2001).

Graham, R.G., B.A. Freel and M.A. Bergougnou, "The Production of Pyrolysis Liquids, Gas, and Char from Wood and Cellulose by Fast Pyrolysis" In: A.V. Bridgwater, J.L. Kuester (Eds.), Research in Thermochemical Biomass Conversion, Elsevier, London, 629-641 (1988).

Green Oasis EnviroEconomics™, http://www.greenoasis.com/product/overview.html, accessed on March 10, 2004

Gunstone, F.D. http://www.britanniafood.com/german/invite_05.htm#three, accessed on Sept 4, 2004

Hoogwijk, M., A. Faaij, R. Broek, G. Berndes, D. Gielen and W. Turkenburg "Exploration of the Ranges of the Global Potential of Biomass for Energy", Biomass and Bioenergy, **25,** 119-133 (2003).

Idem, R.O., S.P.R. Katikaneni, and N. N. Bakhshi, "Thermal Cracking of Canola Oil: Reaction Products in the Presence and Absence of Steam", Energy and Fuels **10**, 1150-1162 (1996).

Ikura, M, M. Stanciulescu, and E. Hogan, "Emulsification of Pyrolysis Derived Bio-oil in Diesel Fuel" Biomass and Bioenergy, **24**, 221-232 (2003).

Islam, M. N., M. N. Islam and M. R. A. Beg, "The Fuel Properties of Pyrolysis Liquid Derived from Urban Solid Wastes in Bangladesh" Bioresource Technology, **92,** 181-186 (2004).

Janse, A.M.C., W. Prins and W.P.M. van Swaaij, "Development of a Small Integrated Pilot Plant for Flash Pyrolysis of Biomass" In: A.V. Bridgwater, D.G.B. Boocock (Eds.), Developments in Thermochemical Biomass Conversion, **1**, 368-377 (1997).

Katikaneni, S. P. R., J. D. Adjaye, R.O. Idem and N. N. Bakhshi. " Performance Studies of Various Cracking Catalysts in the Conversion of Canola Oil to Fuels and Chemicals in a Fluidized-Bed Reactor" J. Am. Oil Chem. Soc., **75,** 381-391 (1998).

Karaosmonoglu, F. "Vegetable Oil Fuels: a Review" Energy Sources, **21,** 221–231 (1999).

Krawczyk, T., "Biodiesel – Alternative Fuel Makes Inroads but Hurdles Remain". INFORM **7**, 801–829 (1996)

Lima, D. G., V. C. D. Soares, E. B. Ribeiro, D. A. Carvalho, E.C.V. Cardoso, F.C. Rassi, K.C. Mundim, J.C. Rubim and P. A. Z. Suarez, "Diesel-like Fuel Obtained by Pyrolysis of Vegetable Oils" Journal of Analytical and Applied Pyrolysis, **71**, 987-996 (2004).

Ma, F. and M.A. Hanna, "Biodiesel Production: a Review" Bioresource Technology, **70**,1-15 (1999).

Ma, F., L. D.Clements, and M.A. Hanna, "The Effects of Catalyst, Free Fatty Acids and Water on Transesterification of Beef Tallow" Trans. ASAE, **41**, 1261–1264 (1998).

Marquevich, M., R. Coll and D. Montane, "Steam Reforming of Sunflower Oil for Hydrogen Production", Ind. Eng. Chem. Res., **39,** 2140–2147 (2000).

Meier, D., A. Oasmaa and G.V.C. Peacocke, "Properties of Fast Pyrolysis Liquids: Status of Test Methods" In: A.V. Bridgwater, D.G.B. Boocock (Eds.), Developments in Thermochemical Biomass Conversion, Blackie, London, **1**, 391- 408 (1997).

Milne, T., F. Agblevor and M. Davis., "A Review of the Chemical Composition of Fast Pyrolysis Oils from Biomass" In: A.V. Bridgwater, D.G.B. Boocock (Eds.), Developments in Thermochemical Biomass Conversion, Blackie, London, **1**, 409-424 (1997).

Mleczko, L., S. Malcus, and T. Wurzel "Catalytic Reformer-Combustor: A Novel Reactor Concept for Synthesis Gas Production", Ind. Eng. Chem. Res., **36**, 4459 – 4465 (1997).

Neff, W. E., K. R. Steidley, G. R. List, G. Snowder and W.C. Byrdwell, **"**Triacylglycerol Structure of Animal Tallows, Potential Food Formulation Fats, by High Performance Liquid Chromatography Coupled with Mass Spectrometry", Journal of Liquid Chromatography and Related Technologies, **25,** 985-998 (2002).

Panigrahi, S., A.K. Dalai and N.N. Bakhshi, "Production of Syngas/High Btu Gaseous

Fuel from the Pyrolysis of Biomass Derived Oil", Paper # 508572. ACS Division of Fuel Chemistry Symposium, Orlando, FL, April 7-11, 6 pages, (2002).

Panigrahi, S., A.K. Dalai, S. T. Chaudhari, and N.N. Bakhshi, "Synthesis Gas Production from Steam Gasification of Biomass-Derived Oil", Energy and Fuels, **17,** 637-642 (2003).

Panigrahi, S, "Pyrolysis and Steam Gasification of Bio-oil to Produce High Calorific Value and Synthesis Gases", M.Sc. thesis, University of Saskatchewan, (2003).

Parr® Operating Instructions Manual for the 1108 Oxygen Combustion Bomb, 2 (1997).

Pioch, P., P. Lozano, M.C. Rasoanatoandro, J. Grailla, P. Geneste and A. Guida, "Biofuels from Catalytic Cracking of Tropical Vegetable Oils", Oleagineux, **48,** 289–291 (1993).

Piskorz, J., D.S. Scott, and D. Radlein, "Composition of Oils Obtained by Fast Pyrolysis of Different Woods" In: E.J. Soltes, T.A. Milne (Eds.), "Pyrolysis Oils From Biomass: Producing, Analyzing and Upgrading", ACS Symposium Series 376, American Chemical Society, Washington, D.C., 167-178, (1988).

Prasad, Y.S., N. N. Bakhshi, J. F. Mathews and R. L. Eager. "Catalytic Conversion of Canola Oil to Fuels and Chemical Feedstocks. Part I. Effect of Process Conditions on the Performance of HZSM-5 Catalyst", Can. J. Chem. Eng., **64,** 278-284 (1986).

Quick, G.R. "Developments in Use of Vegetable Oil as Fuel for Diesel Engines" In: *ASAE paper No. 80-1525*, ASAE, St Joseph, MI (1980).

Radovanovic, M., R. H. Venderbosch, W. Prins and W. P. M. van Swaaij, "Some Remarks on the Viscosity Measurement of Pyrolysis Liquids", Biomass and Bioenergy, **18,** 209-222 (2000).

Rathi, A. K. A., "Environmental Control, Energy Conservation and Utilization of Carbon-dioxide", Chemical Engineering World, Industrial Publications, Bombay, India, 33-39, (1994).

Robertson, Ernest E. "Biomass" Solar Energy Conversion 2: Selected Lectures from the 1980 International Symposium on Solar Energy Utilization, London, Ontario, Canada Pergamon Press 355-357 (1981).

Russell, S. and M. Cannon, "Cattle market update", Saskatchewan Agricultural, Food and Rural Revitalization, August 16-20, 2004 accessed on Jan 4, 2005 http://www.agr.gov.sk.ca/docs/reports/catt_market/CM040820.pdf

Sanford S. and J. Allshouse, "Have we turned the corner on fats consumptions?" Food Review (http://www.findarticles.com/p/articles/mi_m3765/is_3_21/ai_56013999) Sept-Dec (1998) assessed on Jan 4, 2005

Schwab, A.W., M.O. Bagby and B. Freedman, “Preparation and Properties of Diesel Fuels from Vegetable Oils”, Fuel, **66**, 1372–1378 (1987).

Schwab, A.W., G.J. Dykstra, E. Selke, S.C. Sorenson and E.H. Pryde, “Diesel Fuel from Thermal Decomposition of Soybean Oil” J. Am. Oil Chem. Soc., **65**, 1781–1785 (1988).

Scott, D.S., J. Piskorz and D. Radlein, “Liquid Products from Continuous Flash Pyrolysis of Biomass”, Ind. Eng. Chem. Process Des. Dev., **24,** 581-588 (1985).

Sipila, K., E. Kuoppala, L. Fagernas, and A. Oasmaa, “Characterization of Biomass-Based Flash Pyrolysis Oils", Biomass and Bioenergy, **14**, 103-113 (1998).

Snoeck, J.W. and G.F. Froment, “Steam/CO_2 Reforming of Methane. Carbon Filament Formation by the Boudouard Reaction and Gasification by CO_2, by H_2, and by Steam: Kinetic Study”, Ind.Eng.Chem.Res, **41**, 4252-4265 (2002).

Song, C. “Introduction to Chemistry of Diesel Fuels” In: C. Song, C.S. Hsu and I. Moshida (Eds.), Chemistry of Diesel Fuels, Taylor and Francis, London, 13 (2000).

Sonntag, N.O.V, “Structure and Composition of Fats and Oils. Bailey's Industrial Oil and Fat Products”, vol. 1, 4th edition, Swern, D. (Ed.) John Wiley and Sons, New York, 1(1979).

Srivastava, A and R. Prasad, “Triglycerides-Based Diesel Fuels”, Renewable and Sustainable Energy Reviews, **4**, 111-133 (2000)

Supple, B., R. Howard-Hildige, E. Gonzalez-Gomez, and J.J. Leahy, “The Effect of Steam Treating Waste Cooking Oil on the Yield of Methyl Ester”, J. Am. Oil Chem. Soc., **79**, 175–178 (1999).

Vonghia, E., D.G. B. Boocock, S. K. Konar and A. Leung. “Pathways for the Deoxygenation of Triglycerides to Aliphatic Hydrocarbons over Activated Alumina” Energy and Fuel, **9**, 1090- 1096 (1995).

Watson, R.T. and the Core Writing Team (Eds.) “Climate Change 2001 Synthesis Report- Summary for Policy Makers” Intergovernmental Panel on Climate Change (IPCC), Geneva, Switzerland, (2001).

Wiltsee, G., “Waste Grease Resource in 30 US Metropolitan Areas” In: Proceedings of Bioenergy Conference, 4-8 October Wisconsin Madison USA, 956–963 (1998).

Zhenyi, C. J. Xing, L. Shuyuan and L. Li, “Thermodynamics Calculation of the Pyrolysis of Vegetable Oils” Energy Sources, **26**, 849 – 856 (2004)

APPENDICES

Appendix A: Calibration Curves

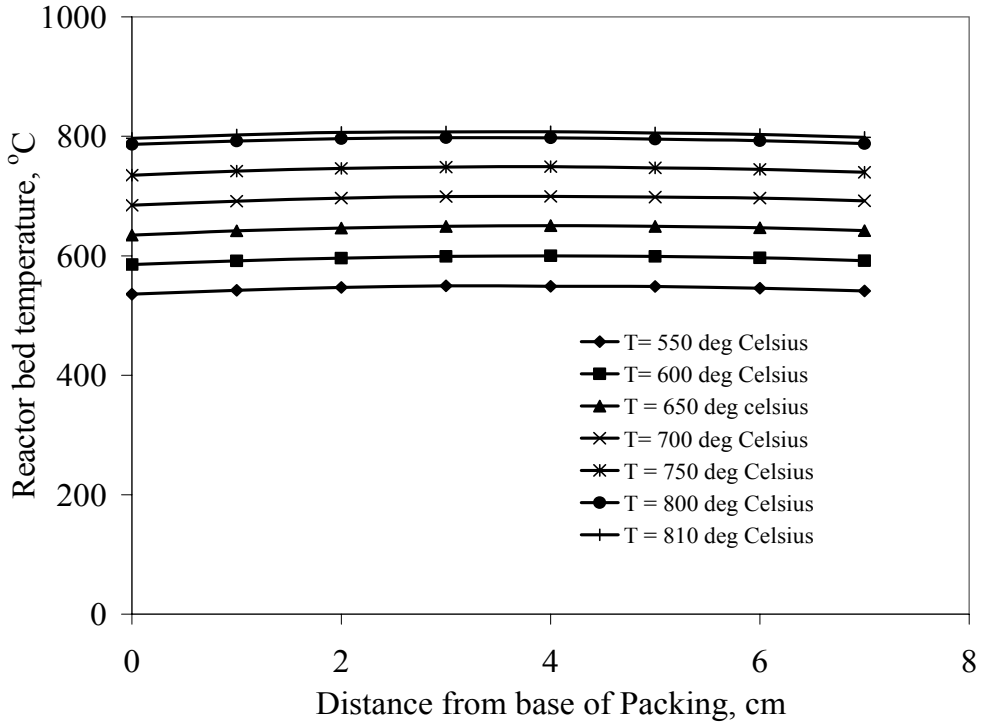

Figure A-1 Temperature profile in the reactor

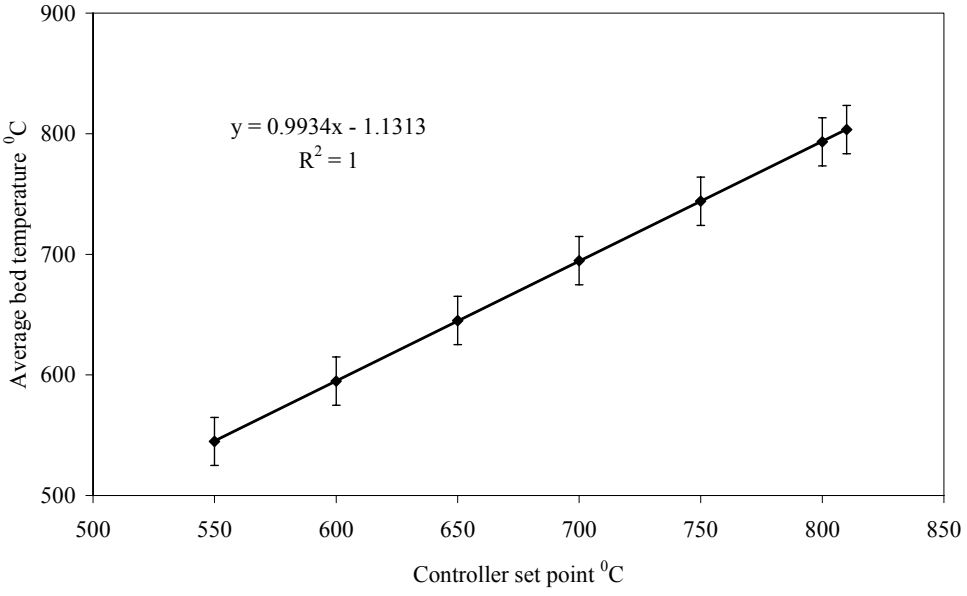

Figure A-2 Temperature Controller Calibration

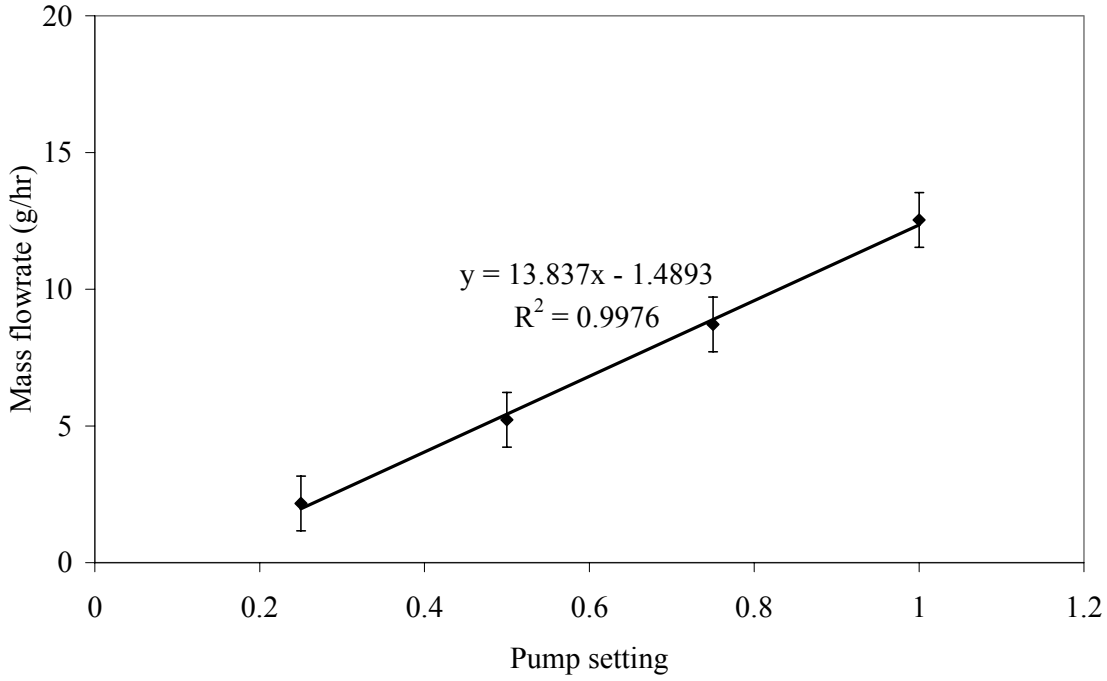

Figure A-3 Calibration of Eldex A-10-S pump for BDO

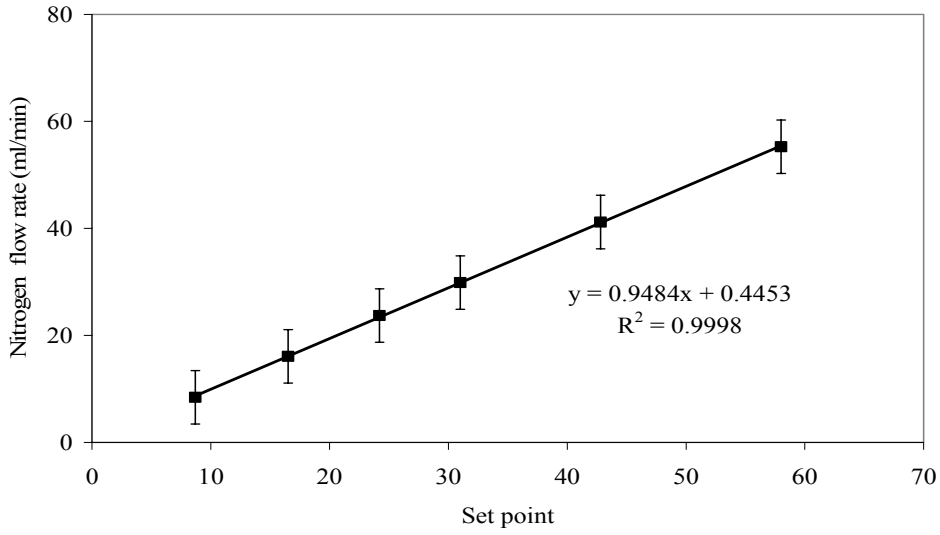

Figure A-4 Calibration of mass flow meter (SN 70327) for N_2 at STP

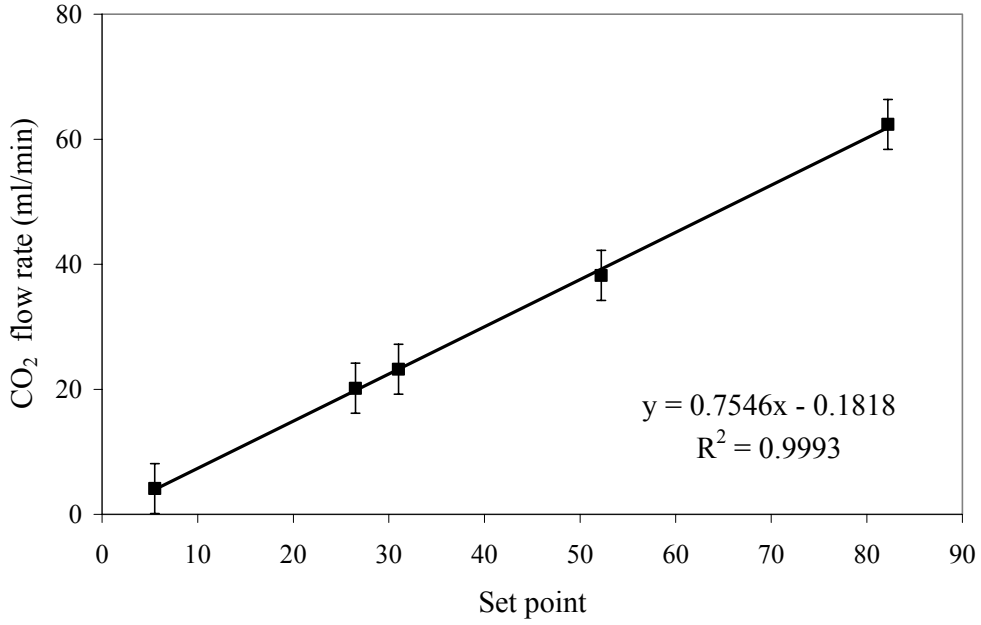

Figure A-5 Calibration of mass flow meter (SN 70328) for CO_2 at STP

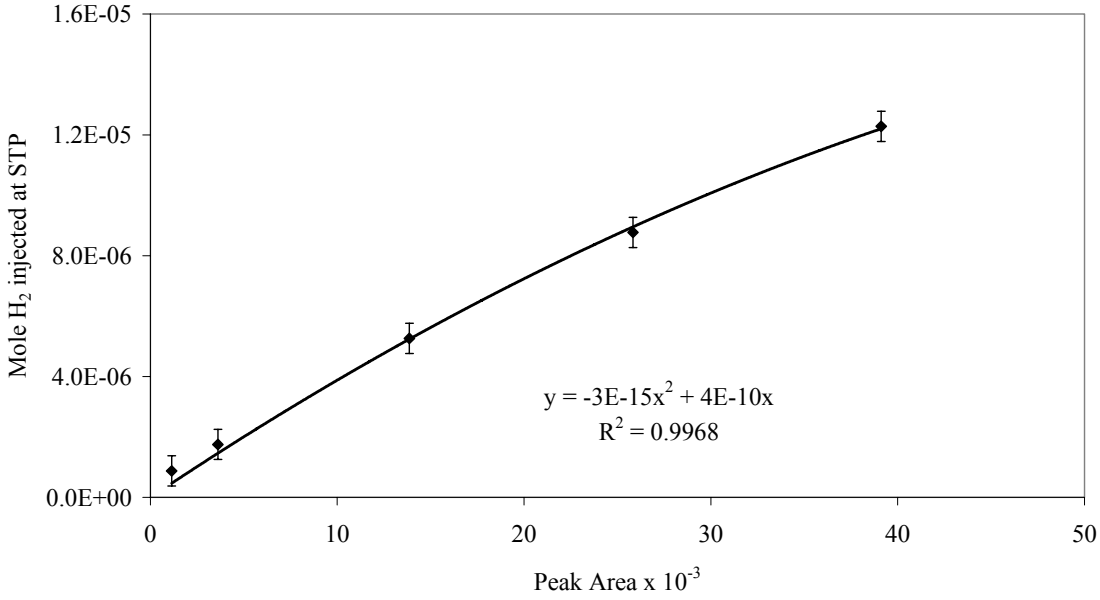

Figure A-6 Calibration of GC 5890 for Hydrogen

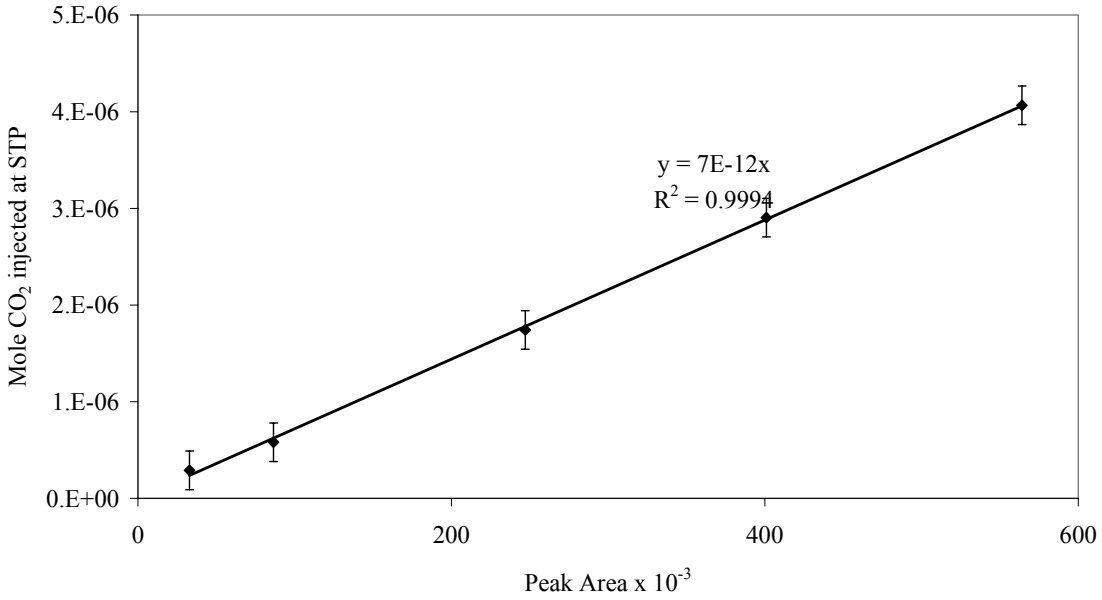

Figure A-7 Calibration of GC 5890 for Carbon dioxide

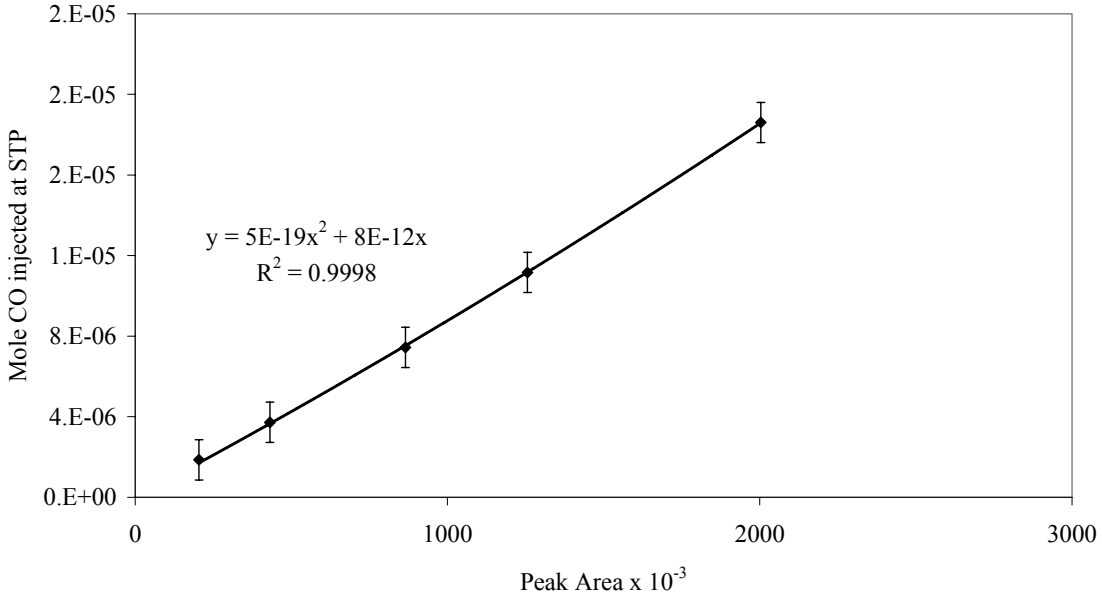

Figure A-8 Calibration of GC 5890 for Carbon monoxide

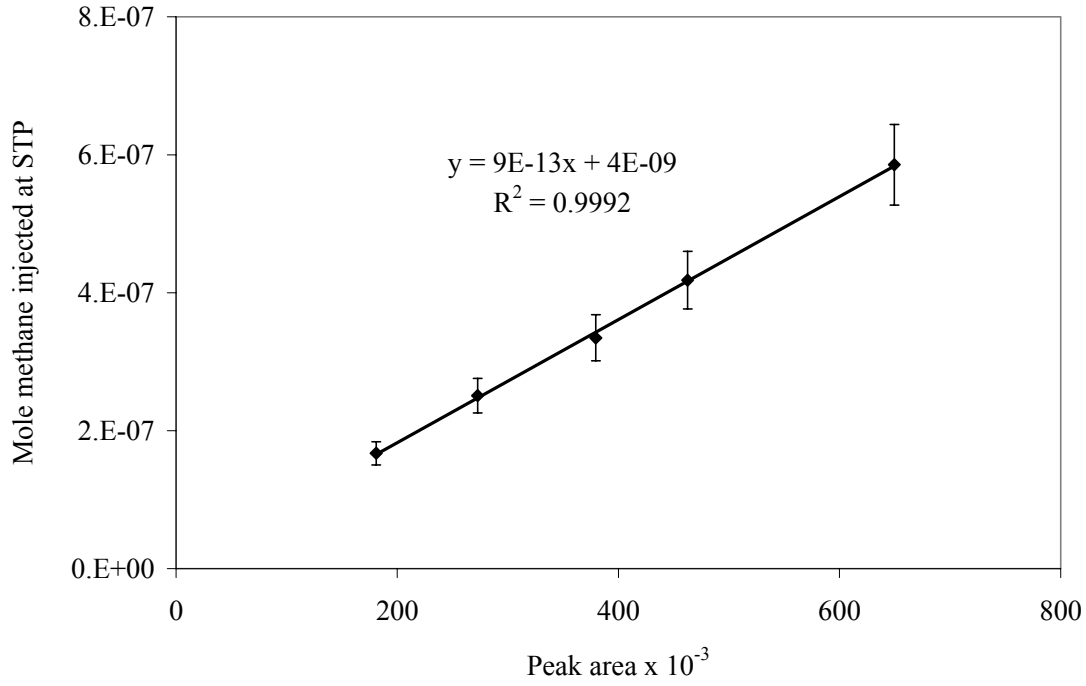

Figure A-9 Calibration of Carle GC for methane

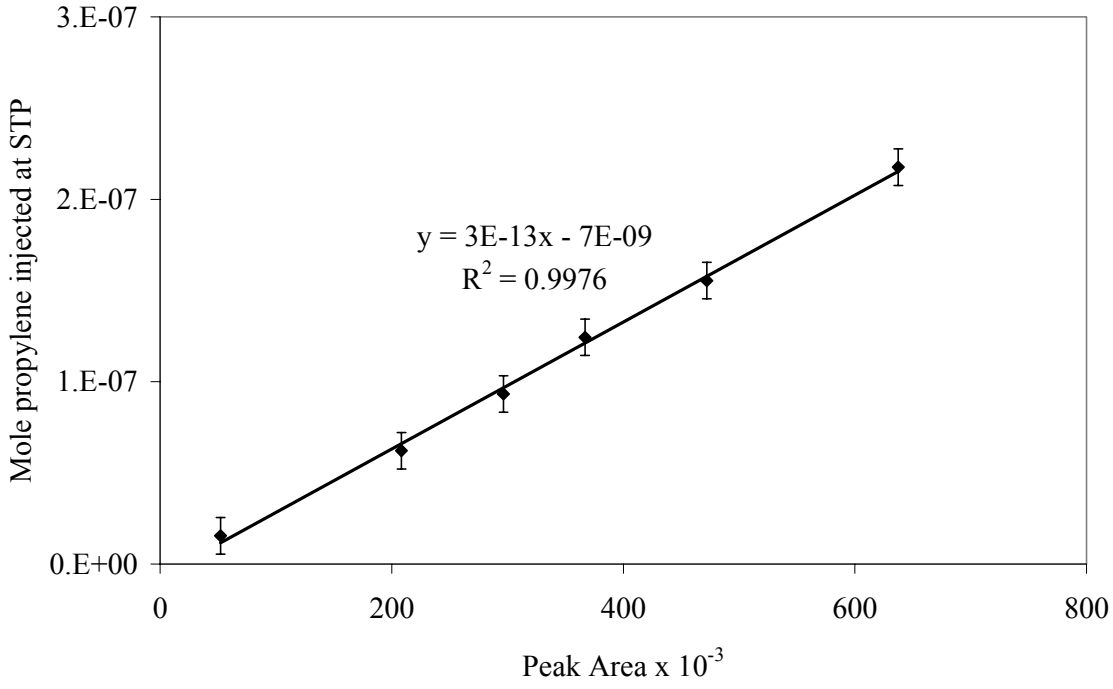

Figure A-10 Calibration of Carle GC for propylene

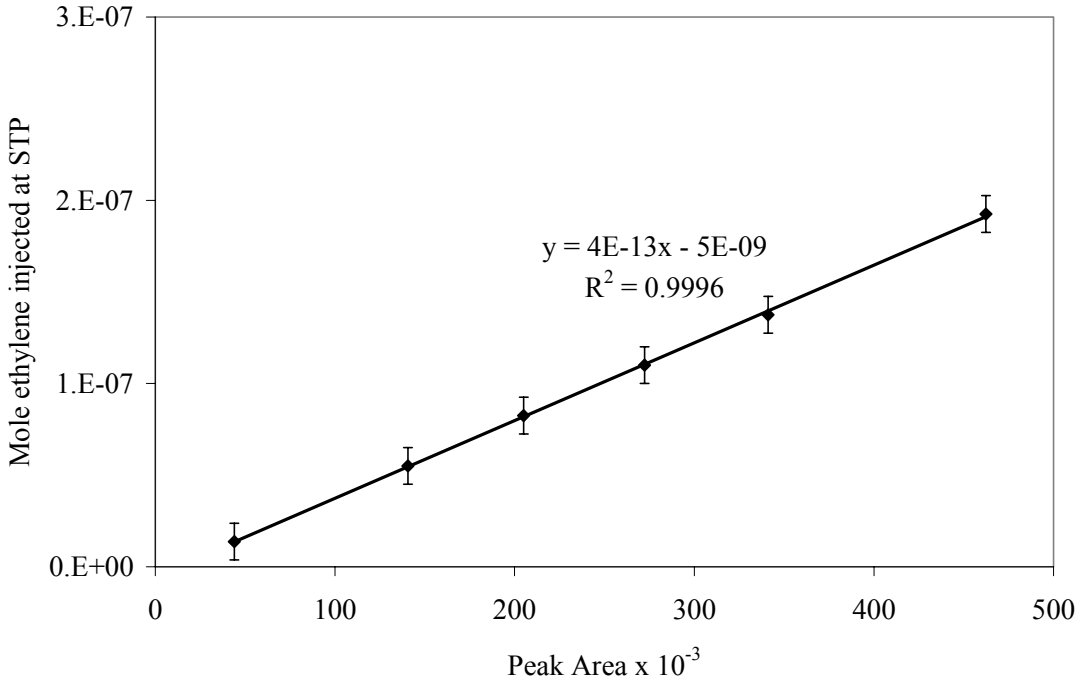

Figure A-11 Calibration of Carle GC for ethylene

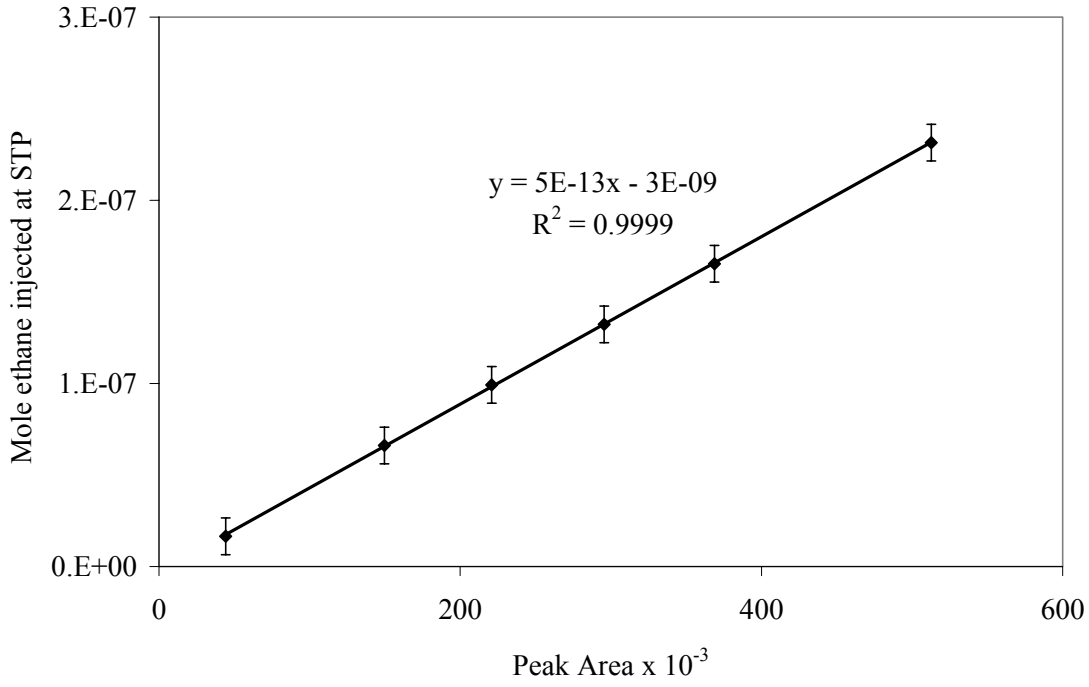

Figure A-12 Calibration of Carle GC for ethane

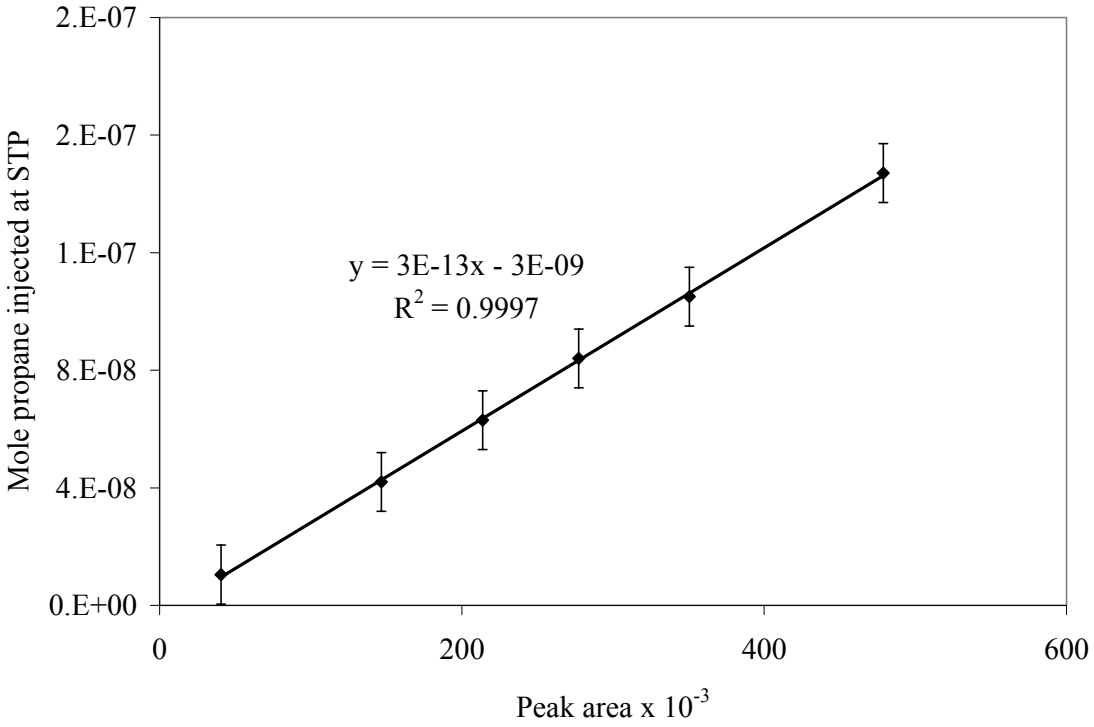

Figure A-13 Calibration of Carle GC for propane

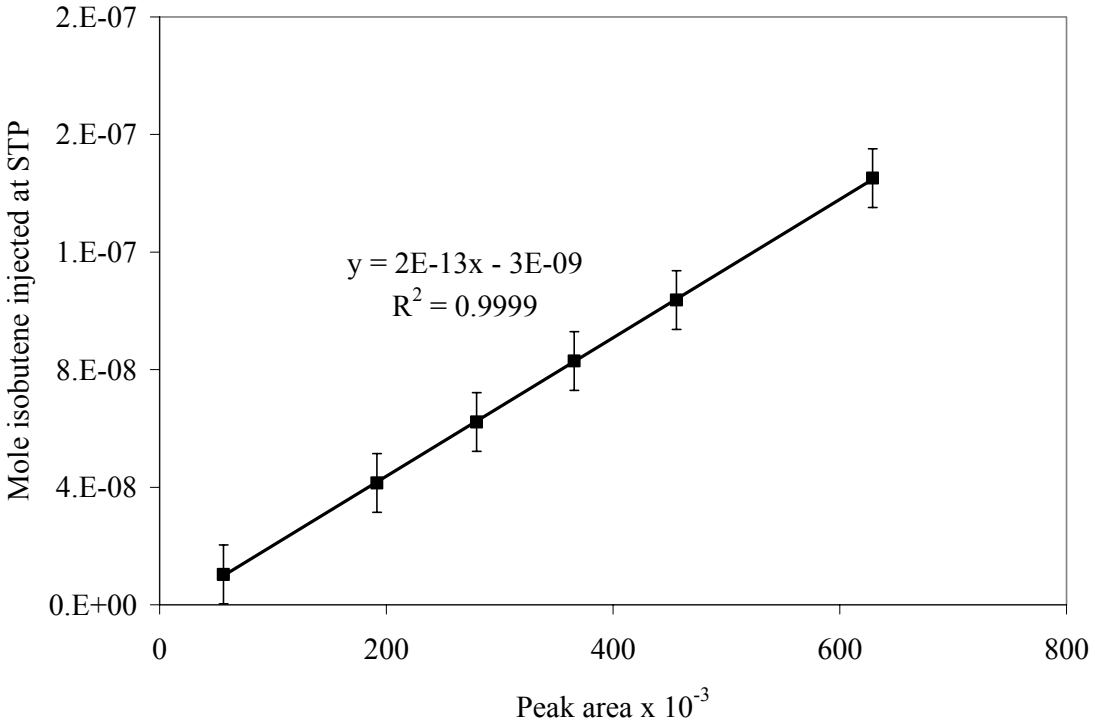

Figure A-14 Calibration of Carle GC for isobutene

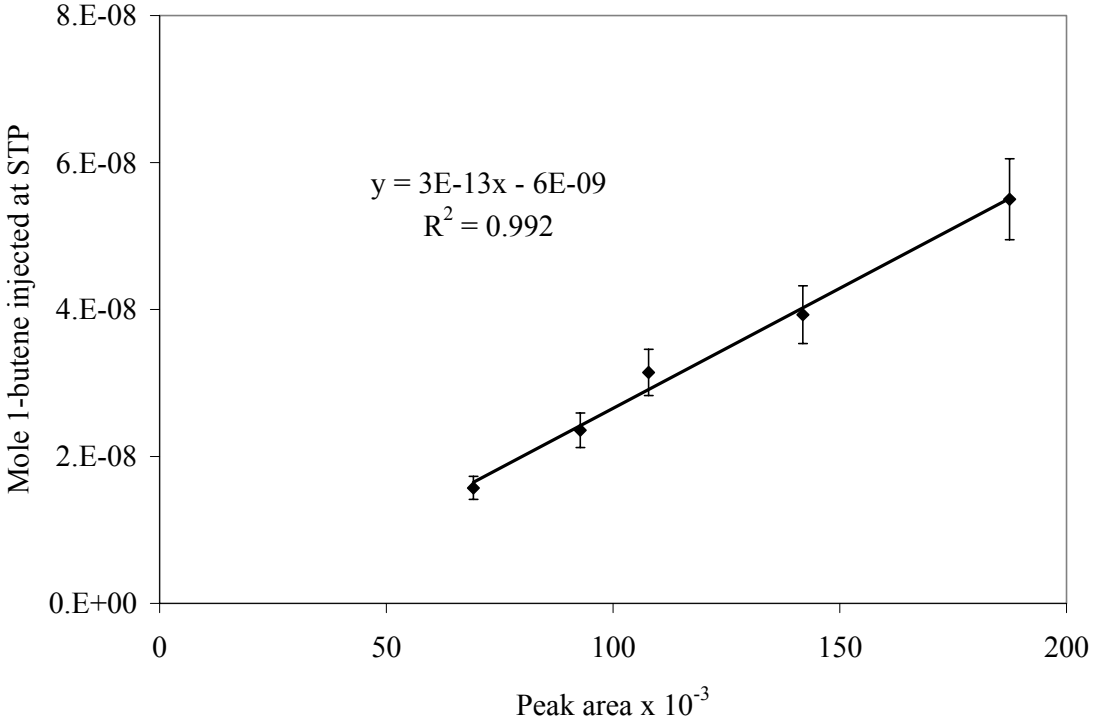

Figure A-15 Calibration of Carle GC for 1-butene

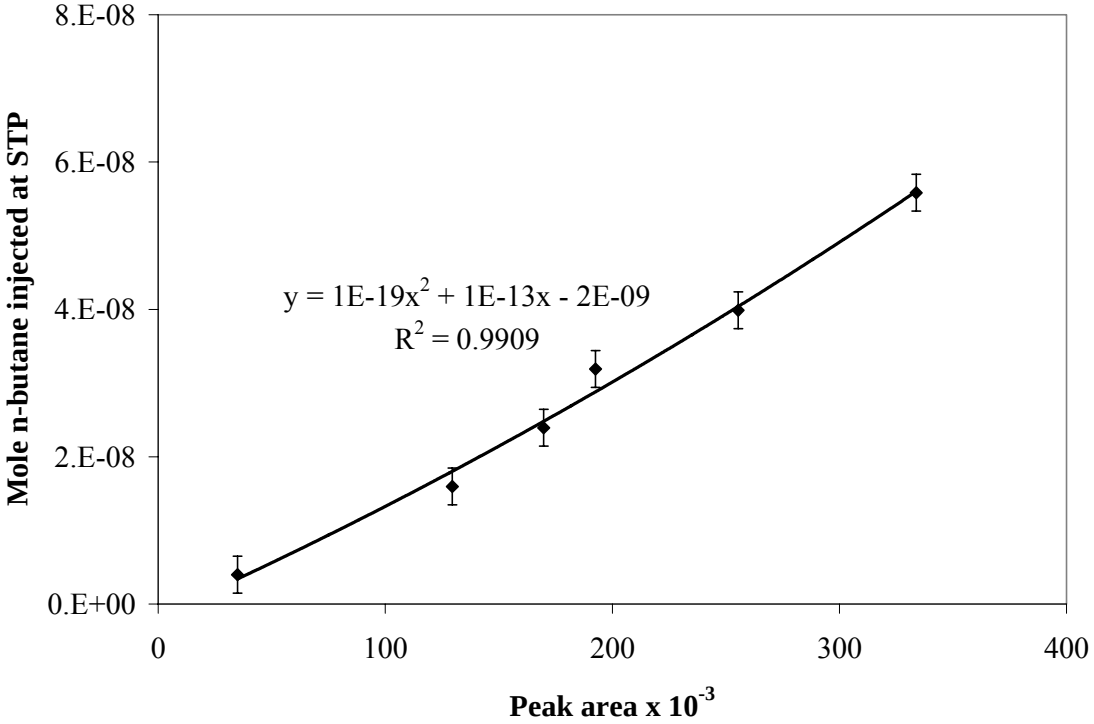

Figure A-16 Calibration of Carle GC for n-butane

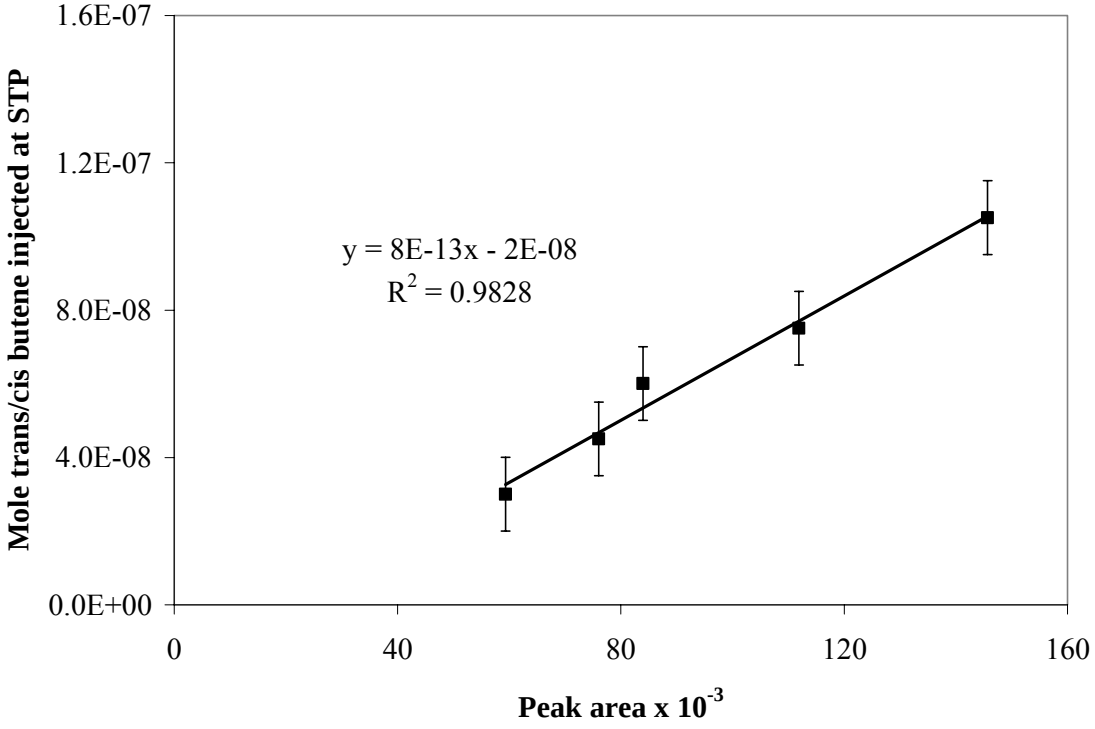

Figure A-17 Calibration of Carle GC for cis/trans-butene

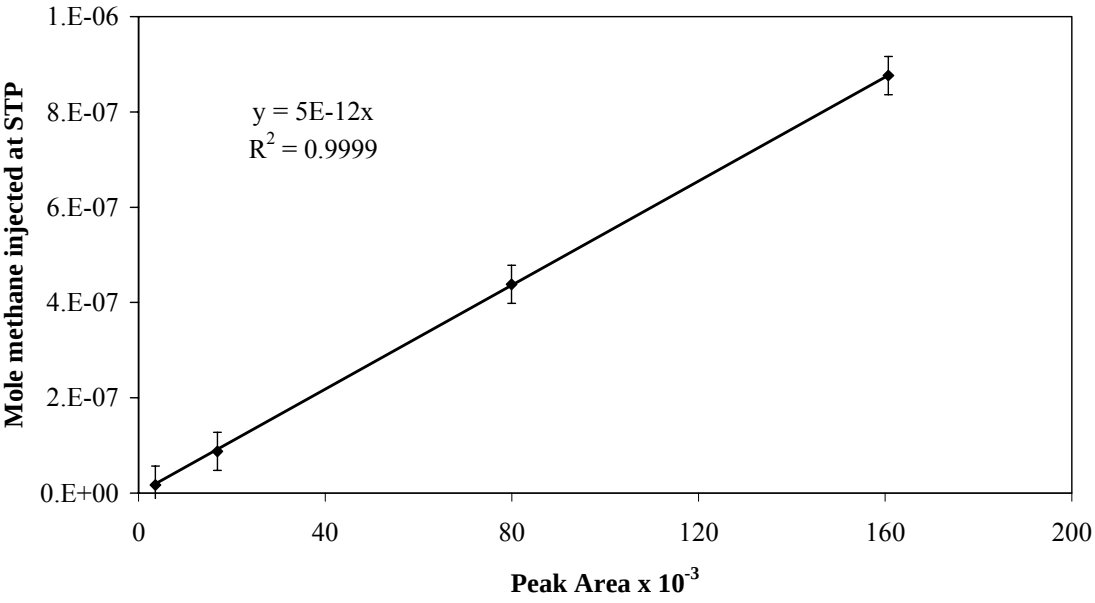

Figure A-18 Calibration of GC 5880 for methane

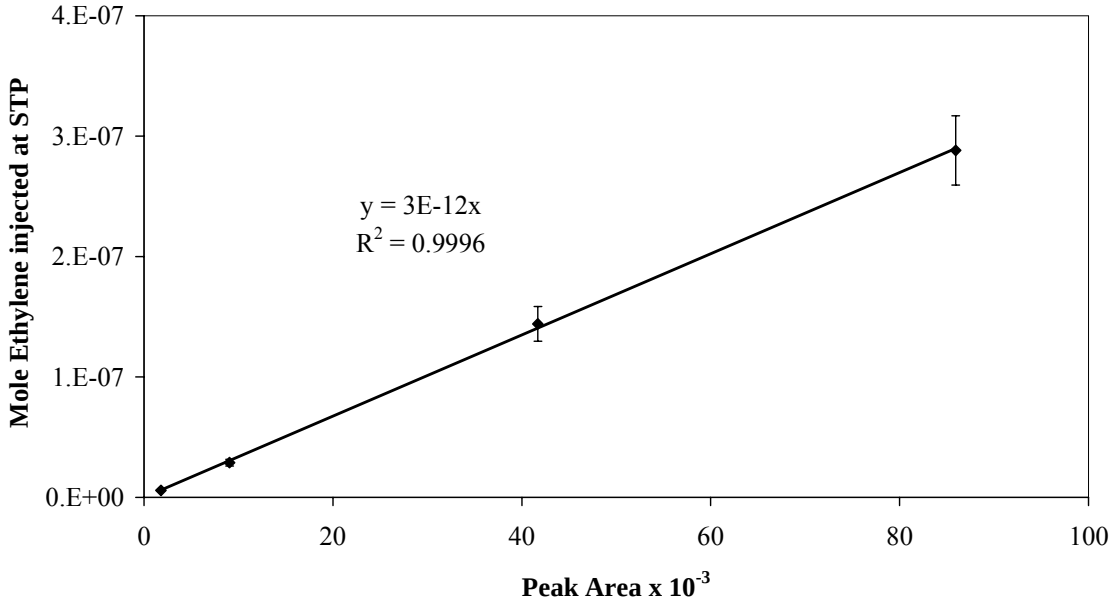

Figure A-19 Calibration of GC 5880 for ethylene

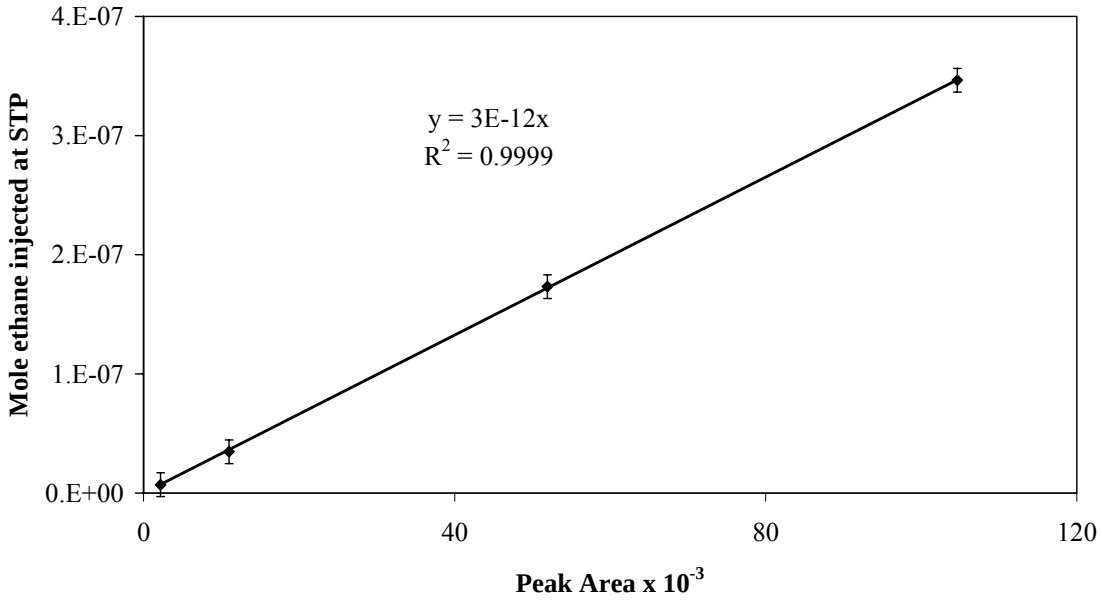

Figure A-20 Calibration of GC 5880 for ethane

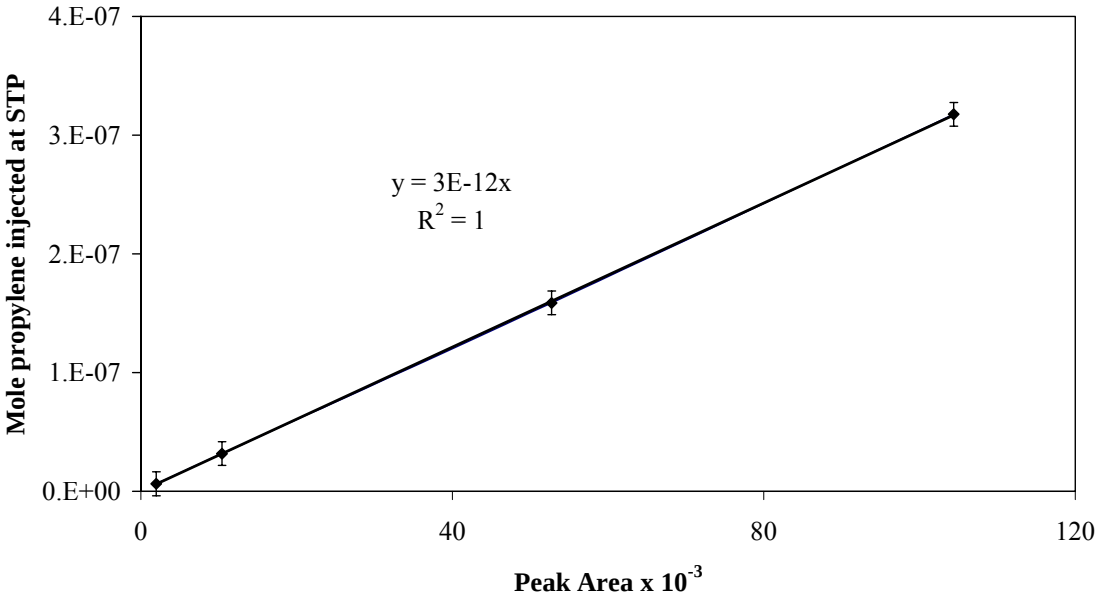

Figure A-21 Calibration of GC 5880 for propylene

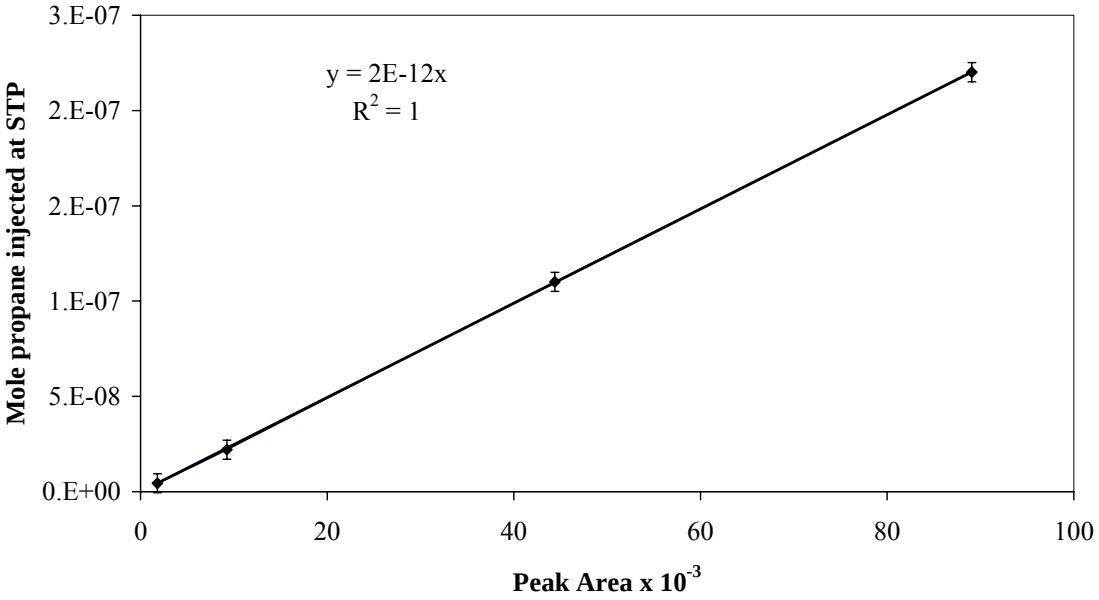

Figure A-22 Calibration of GC 5880 for propane

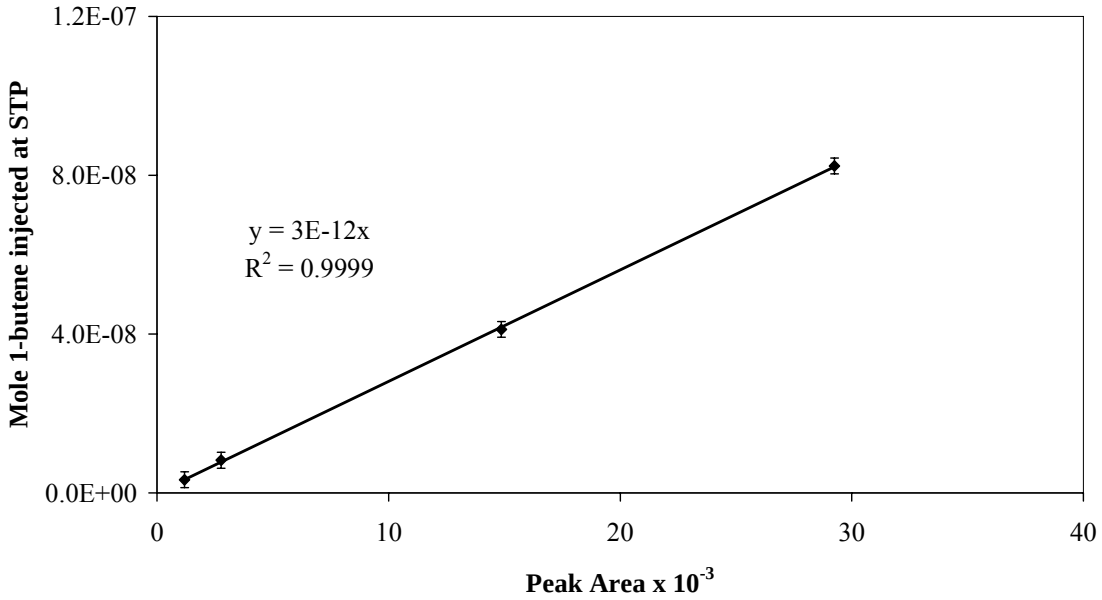

Figure A-23 Calibration of GC 5880 for 1-butene

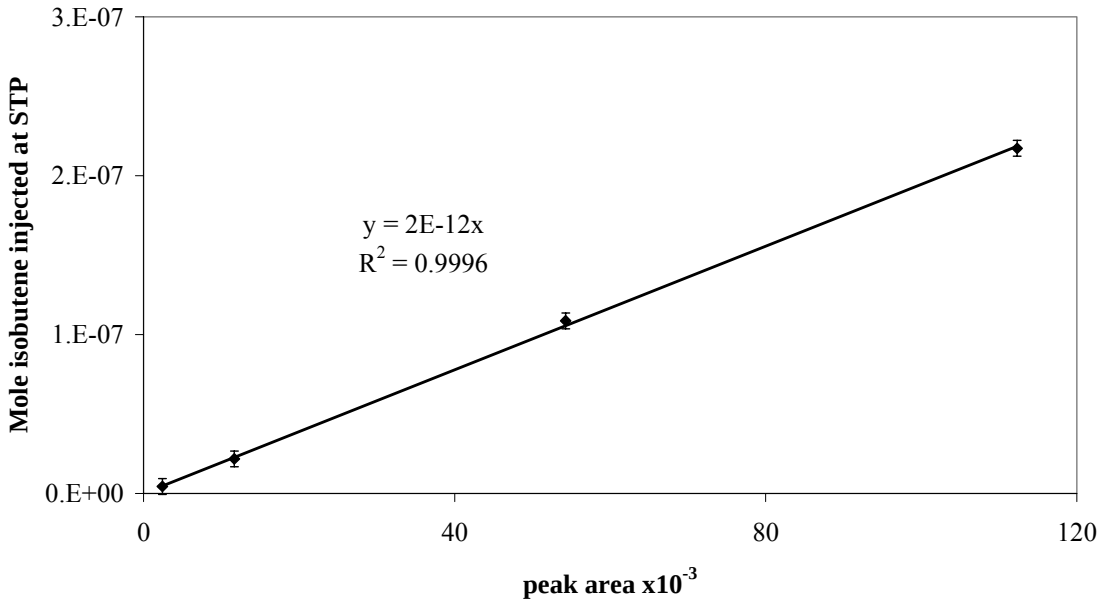

Figure A-24 Calibration of GC 5880 for isobutene

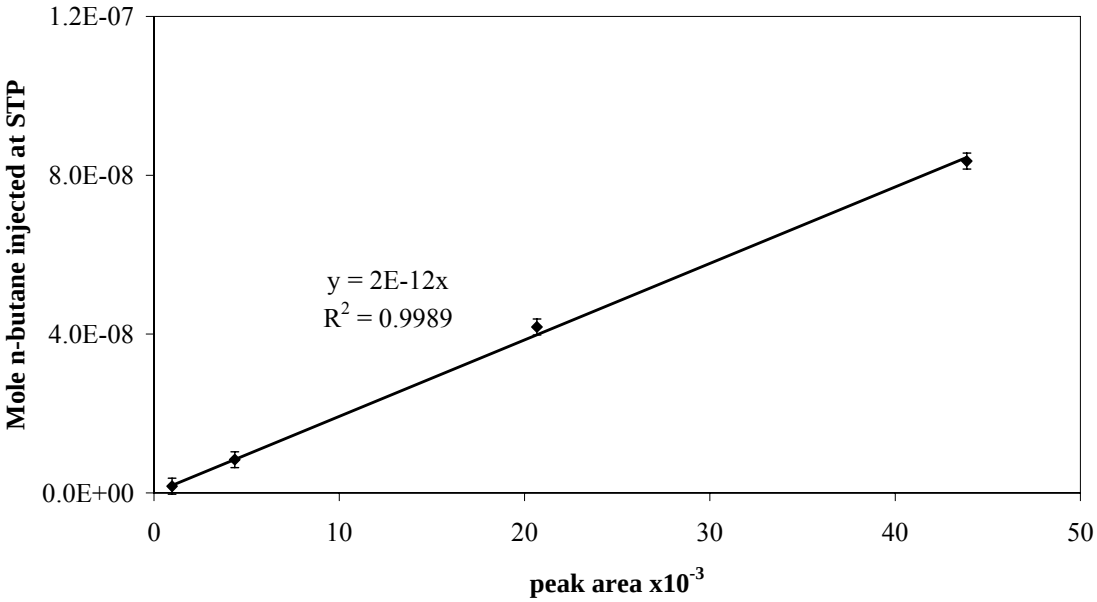

Figure A-25 Calibration of GC 5880 for n-butane

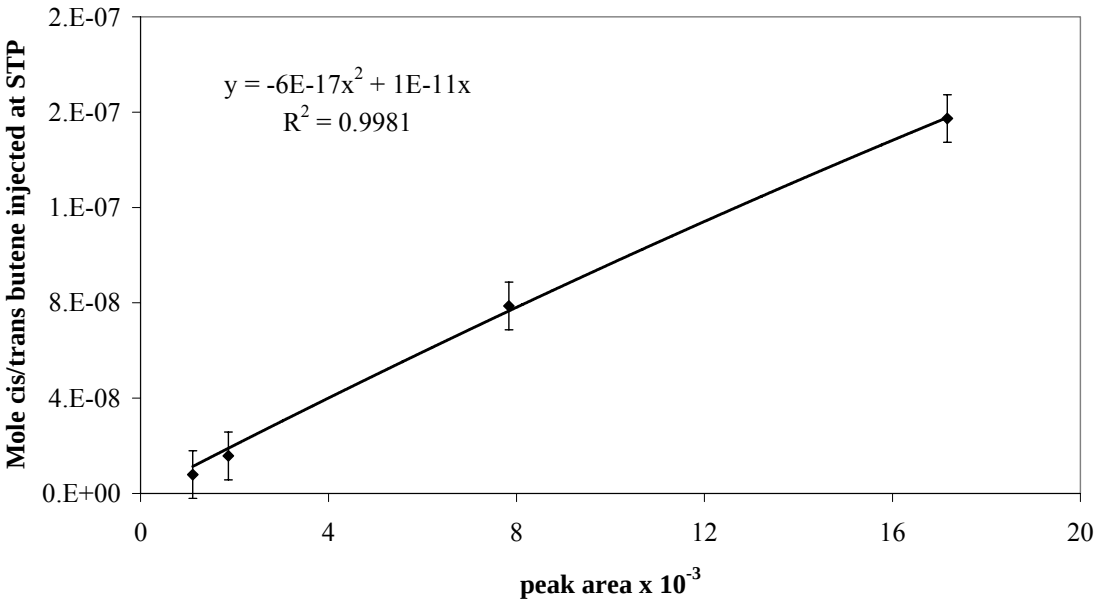

Figure A-26 Calibration of GC 5880 for cis/trans butene

Appendix B: Sample Calculations of Mass Balance

Appendix B-1 Pyrolysis of Lard

The calculations are based on the data collected for experimental Run # 23 (Appendix C-2)
Feed
Lard = 2.79g Duration of experiment 30 minutes

Mass Balance calculation:

Total volume of gas collected excluding nitrogen at room temperature and pressure
= 3107 cm^3 = 2713 cm^3 at STP
Gas analysis from GC:
Volume of gas injected into GCs was 0.5 cm^3 at room temperature and pressure which is 0.44 cm^3 at STP. Table B-1 shows the calculations of gas composition and mass of the product gas.
Weight of the liquid product collected in the condenser = 1.48g
Weight of the char and residue retained in the reactor = 0.12 g
Weight of the product gas (calculated above) = 1.06g
Total product = 1.48 +0.12+ 1.06 =2.66 g
Mass balance = [(mass of feed - mass of total product)/Mass of feed]*100
= (2.79-2.66)/2.79 *100 = 95.3 %

Appendix B-2 Steam Reforming of Lard

The calculations are based on the data collected for experimental Run # 39 (Appendix C-2)
Feed
Lard = 2.68 g Duration of experiment 30 minutes
Water pumped = 2.58 g

Mass Balance Calculation:

Total volume of gas collected excluding nitrogen at room temperature and pressure
= 1102 cm^3 = 962 cm^3 at STP
Gas analysis from GC:
Volume of gas injected into GCs was 0.5 cm^3 at room temperature and pressure which is 0.44 cm^3 at STP. Table B-2 shows the calculations of gas composition and mass of the product gas.
Weight of the liquid collected in the condenser = 4.19 g
Weight of water obtained from total liquid = 2.54 g
Weight of liquid product = 1.65

Table B-1 Calculation of gas composition and mass during pyrolysis of lard at 600°C and carrier gas flow rate of 50 cm^3/min

Components	Volume (cm^3)	Sample (g mole)	Total (g mole)	Total (ml)	Composition mol%	Total (g)
Hydrogen	0.0000	0.00E+00	0.00E+00	0.0000	0.00E+00	0.0000
Nitrogen	0.3353	1.50E-05	9.30E-02	2083.8365		2.6043
CO	0.0116	5.19E-07	3.23E-03	72.3655	1.15E+01	0.0904
CO_2	0.0049	2.17E-07	1.35E-03	30.1784	4.79E+00	0.0593
Methane	0.0107	4.75E-07	2.95E-03	66.1979	1.05E+01	0.0474
Ethylene	0.0262	1.17E-06	7.26E-03	162.7733	2.59E+01	0.2037
Ethane	0.0073	3.27E-07	2.03E-03	45.5161	7.23E+00	0.0611
propylene	0.0166	7.40E-07	4.60E-03	103.0281	1.64E+01	0.1934
propane	0.0008	3.52E-08	2.19E-04	4.9004	7.78E-01	0.0096
1-butene	0.0132	5.90E-07	3.67E-03	82.2345	1.31E+01	0.2058
isobutene	0.0001	3.12E-09	1.94E-05	0.4342	6.90E-02	0.0011
n-butane	0.0005	2.15E-08	1.34E-04	2.9993	4.76E-01	0.0078
cis/trans	0.0013	5.95E-08	3.70E-04	8.2908	1.32E+00	0.0208
C5+	0.0081	3.63E-07	2.26E-03	50.6356	8.04E+00	0.1584
Product Gas	0.1013		0.0281	629.5543	100.00	1.0588
Total Gas	0.44		0.1211			3.6631

Weight of the char and residue retained in the reactor = 0.13 g
Weight of the product gas (calculated above) = 0.83g
Total product = 1.65 + 0.13 + 0.83 =2.61 g
Mass balance = [(mass of feed - mass of total product)/Mass of feed]*100
= (2.68-2.61)/2.68 *100 = 97 %

Table B-2 Calculation of gas composition and mass during steam reforming at 600^{o}C and S/L ratio of 1

Component	Volume (cm^3)	sample (g mole)	Total (g mole)	Total (ml)	Composition (mol%)	Total (g)
Hydrogen	0.0068	3.01E-07	6.64E-04	14.8940	2.65E+00	0.0013
Nitrogen	0.1815	8.10E-06	1.79E-02	400.2652		0.5002
CO	0.0323	1.44E-06	3.17E-03	71.1438	1.26E+01	0.0889
CO_2	0.0141	6.29E-07	1.39E-03	31.0874	5.53E+00	0.0610
Methane	0.0337	1.50E-06	3.32E-03	74.3698	1.32E+01	0.0532
Ethylene	0.0689	3.07E-06	6.77E-03	151.8335	2.70E+01	0.1900
Ethane	0.0224	9.99E-07	2.20E-03	49.3602	8.77E+00	0.0662
propylene	0.0433	1.93E-06	4.26E-03	95.4582	1.70E+01	0.1792
propane	0.0028	1.27E-07	2.80E-04	6.2706	1.11E+00	0.0123
1-butene	0.0209	9.32E-07	2.06E-03	46.0698	8.19E+00	0.1153
isobutene	0.0001	3.39E-09	7.48E-06	0.1677	2.98E-02	0.0004
n-butane	0.0014	6.36E-08	1.40E-04	3.1429	5.59E-01	0.0081
cis/trans	0.0034	1.50E-07	3.32E-04	7.4378	1.32E+00	0.0186
C5+	0.0051	2.28E-07	5.04E-04	11.2925	2.01E+00	0.0353
Product Gas	0.255		0.0251	562.5283	100.0000	0.8301
Total Gas	0.44		0.0430			1.3303

Appendix C: Experimental Data

Appendix C-1 Experimental Results for CO_2 Reforming of Biomass Derived Oil

Run #		**1**	**2**	**3**	**4**	**5**	**6**
Temperature	^oC	800	800	800	800	800	800
Q. chip size	mm	1.7-2.4	1.7-2.4	1.7-2.4	1.7-2.4	1.7-2.4	1.7-2.4
Total carrier gas ($N_2 + CO_2$)	cm^3/min	30	30	50	50	50	50
N_2 flow rate	cm^3/min	30	30	50	25	25	25
CO_2 flow rate	cm^3/min	0	0	0	25	25	25
Mole fraction of CO_2 in total carrier gas		0	0	0	0.5	0.5	0.5
Pump type		Eldex	Eldex	Eldex	Eldex	Eldex	Eldex
BDO fed	g	2.0	2.5	2.2	3.0	2.5	2.7
Duration	min	30	30	30	30	30	30
Condensate	g	0.8	0.8	0.7	1.1	0.5	1.0
Char	g	0.4	0.6	0.6	0.6	0.9	0.5
Gas	g	0.6	0.9	0.7	1.2	1.0	1.0
Material Balance	g	1.8	2.3	2.0	2.9	2.4	2.5
	wt%	90.8	92.0	90.5	95.0	96.0	91.6
Composition (mol%) , volume and heating value of gas							
H_2		33.1	30.2	41.8	29.0	36.4	33.2
CO		39.9	40.0	29.0	39.3	34.5	38.2
CO_2		5.9	6.6	14.5	6.19	2.7	5.6
CH_4		14.4	16.9	10.7	16.3	16.9	15.6
C_2H_4		5.5	5.3	3.6	7.4	7.1	6.1
C_2H_6		0.6	0.6	0.3	0.6	0.7	0.5
C_3H_6		0.4	0.3	0.1	0.6	0.7	0.4
C_3H_8		0.03	0.01	0.00	0.1	0.1	0.04
C_{4+}		0.3	0.2	0.03	0.6	1.0	0.4
H_2+CO		73.0	70.2	70.8	68.3	70.9	71.4
H_2/CO		0.83	0.75	1.44	0.74	1.06	0.87
Heating Value	MJ/m^3	22.1	22.8	19.2	24.7	24.0	22.0
Volume of gas	L/100g BDO	37.7	42.2	37.7	90.2	105.2	92.1

Run #		**7**	**8**	**9**	**10**	**11**	**12**
Temperature	^{o}C	800	800	800	800	800	800
Q. chip size	mm	1.7-2.4	1.7-2.4	1.7-2.4	1.7-2.4	1.7-2.4	1.7-2.4
Total carrier gas ($N_2 + CO_2$)	cm^3/min	30	30	60	60	60	30
N_2 flow rate	cm^3/min	18	24	48	60	54	24
CO_2 flow rate	cm^3/min	12	6	12	0	6	6
Mole fraction of CO_2 in total carrier gas		0.4	0.2	0.2	0	0.1	0.2
Pump type		Eldex	Eldex	Eldex	Eldex	Eldex	Eldex
BDO fed	g	2.7	2.5	2.5	3.0	3.1	2.2
Duration	min	30	30	30	30	30	30
Condensate	g	0.7	0.5	0.9	1.0	1.1	0.7
Char	g	0.6	0.6	0.8	0.9	0.5	0.7
Gas	g	1.3	1.2	0.7	0.8	1.1	0.7
Material Balance	g	2.6	2.4	2.4	2.7	2.7	2.1
	wt%	94.0	94.2	95.8	90.2	90.0	98.4
Composition (mol%) and volume and heating value of gas							
H_2		27.0	28.4	25.9	23.7	24.5	22.6
CO		38.0	33.4	45.8	45.2	44.5	42.0
CO_2		9.9	15.0	12.5	13.7	11.9	24.7
CH_4		17.0	15.7	11.0	11.8	13.3	7.8
C_2H_4		6.5	6.0	4.2	4.4	4.8	2.6
C_2H_6		0.7	0.6	0.3	0.4	0.4	0.2
C_3H_6		0.6	0.5	0.1	0.3	0.2	0.1
C_3H_8		0.1	0.1	0.0	0.03	0.0	0.0
C_{4+}		0.4	0.4	0.3	0.5	0.5	0.1
H_2+CO		65.0	61.8	71.6	68.9	69.0	64.6
H_2/CO		0.71	0.85	0.56	0.52	0.55	0.54
Heating Value	MJ/m^3	24.9	24.5	20.6	19.2	22.2	18.8
Volume of gas	L/100g BDO	96.5	101.5	56.8	55.0	82.6	59.6

Run #		**13**	**14**	**15**	**16**	**17**	**18**
Temperature	^{o}C	800	800	800	800	800	800
Q. chip size	mm	1.7-2.4	1.7-2.4	1.7-2.4	1.7-2.4	1.7-2.4	1.7-2.4
Total carrier gas ($N_2 + CO_2$)	cm^3/min	60	60	50	50	50	30
N_2 flow rate	cm^3/min	0	54	45	40	0	0
CO_2 flow rate	cm^3/min	60	6	5	10	50	30
Mole fraction of CO_2 in total carrier gas		1	0.1	0.1	0.2	1	1
Pump type		Eldex	Eldex	Eldex	Eldex	Eldex	Eldex
BDO fed	g	2.5	2.7	2.8	3.0	2.9	2.1
Duration	min	30	30	30	30	30	30
Condensate	g	0.8	0.9	2.1	1.0	1.1	0.6
Char	g	0.7	0.9	1.1	0.6	0.8	0.7
Gas	g	0.8	0.7	2.4	1.1	0.8	0.6
Material Balance	g	2.3	2.6	5.6	2.7	2.7	1.9
	wt%	92.4	93.8	90.4	90.2	90.8	89.8
Composition (mol%) and volume and heating value of gas							
H_2		22.7	28.4	23.4	22.8	24.7	24.7
CO		43.5	47.2	46.6	45.9	48.8	47.7
CO_2		20.2	8.4	15.4	19.2	12.6	16.4
CH_4		9.8	11.4	10.2	8.6	9.8	8.1
C_2H_4		3.2	3.9	3.6	3.1	3.3	2.7
C_2H_6		0.2	0.3	0.3	0.2	0.2	0.2
C_3H_6		0.1	0.1	0.2	0.1	0.1	0.1
C_3H_8		0.02	0.0	0.0	0.01	0.01	0.01
C_{4+}		0.2	0.2	0.3	0.3	0.3	0.1
H_2+CO		66.2	75.6	70.0	68.6	73.5	72.4
H_2/CO		0.52	0.60	0.50	0.50	0.51	0.52
Heating Value	MJ/m^3	20.1	18.7	20.4	19.4	19.8	18.5
Volume of gas	L/100g BDO	58.8	117.2	83.0	66.4	56.5	53.9

Appendix C-2 Experimental Results for Studies on Lard

Run #		**1**	**2**	**3**	**4**	**5**	**6**
Temperature	^{o}C	500	600	700	800	700	600
Q. chip size	mm	1.7-2.4	1.7-2.4	1.7-2.4	1.7-2.4	1.7-2.4	1.7-2.4
Carrier gas (N_2)	cm^3/min	30	30	30	30	10	10
Pump type		Eldex	Eldex	Eldex	Eldex	Eldex	Eldex
Lard fed	g	2.9	2.5	2.7	2.2	2.5	2.6
S/L mass ratio		0	0	0	0	0	0
Duration	min	30	30	30	30	30	30
Gas	g	0.2	1.6	2.0	1.3	1.9	1.0
Liquid	g	2.6	1.2	0.1	0.0	0.3	1.4
Char + Residue	g	0.1	0.1	0.4	0.6	0.1	0.04
Material Balance	g	2.8	2.3	2.5	2.0	2.3	2.4
	wt%	97.5	92.5	94.3	90.2	93.3	94.1
Gas composition and heating value							
H_2		0	0	7	51.8	6.9	1.8
CO		11.3	25.4	9.6	10.4	9.1	10.2
CO_2		18.5	9.1	11.2	10.3	16.7	14.2
CH_4		5.6	8.2	13.4	11.4	15.3	10
C_2H_4		12.7	20.3	26.4	10.1	24.4	23.7
C_2H_6		5.5	5.5	4.9	2.5	5.5	6.9
C_3H_6		9	12.9	15	2.7	16.7	15.6
C_3H_8		13.1	0.6	0.4	0.1	13.9	0.9
C_{4+}		35.9	18	12.2	1.5	7.8	16.7
H_2+CO		11.3	25.4	16.6	62.2	16	12
H_2/CO		0.00	0.00	0.73	4.98	0.76	0.18
Heating Value	MJ/m^3	190.1	98.8	93.2	30.5	83.7	112.6
Liquid product characterization							
Diesel-like liq	g/100g lard	12.5	24.1	2.8	nd	11.4	42.4
Cetane Index		45.5	47.1	nd	nd	nd	23.5
Density	kg/m^3	880	860	nd	nd	nd	860
Viscosity	mPa.s	22.3	4.0	nd	nd	nd	5.1
Water content	%w/w	0.5	0.5	nd	nd	nd	0.5
Heating Value	MJ/kg	40.1	39.9	nd	nd	nd	39.5

Run #		**7**	**8**	**9**	**10**	**11**	**12**
Temperature	^{o}C	650	450	600	550	750	600
Q. chip size	mm	1.7-2.4	1.7-2.4	1.7-2.4	1.7-2.4	1.7-2.4	1.7-2.4
Carrier gas (N_2)	cm^3/min	10	10	50	10	10	70
Pump type		Eldex	Syinge	Syinge	Syinge	Syinge	Syinge
Lard fed	g	2.5	2.5	2.1	2.7	2.5	2.5
S/L mass ratio		0	0	0	0	0	0
Duration	min	30	30	30	30	30	30
Gas	g	1.6	0.2	0.9	0.5	1.8	0.9
Liquid	g	0.7	2.2	0.9	2.1	0.4	1.4
Char + Residue	g	0.04	0.2	0.2	0.01	0.01	0.2
Material Balance	g	2.3	2.5	2.0	2.6	2.2	2.4
	wt%	93.7	98.3	97.2	95.1	90.5	96.2
Gas composition and heating value							
H_2		2.5	0	0	0	6.2	0
CO		8.4	19.1	10.4	12.4	9.1	11.5
CO_2		11.2	34.5	5.9	9.9	5.4	4.9
CH_4		12.4	3.6	9.7	9.8	22	10.2
C_2H_4		25.6	5.3	25.2	23.8	32.8	25.9
C_2H_6		6.6	4	6.3	8.1	5.7	6.7
C_3H_6		17.2	8.3	15.8	15.6	12	16.3
C_3H_8		0.6	2.4	0.6	1.4	0.3	1.7
C_{4+}		15.5	22.8	26.1	19	6.5	22.8
H_2+CO		10.9	19.1	10.4	12.4	15.3	11.5
H_2/CO		0.30	0.00	0.00	0.00	0.68	0.00
Heating Value	MJ/m^3	109.4	121.5	133.2	116.7	78.1	122.7
Liquid product characterization							
Diesel-like liq	g/100g lard	26.6	25.8	25.0	36.7	13.0	34.2
Cetane Index		20.2	45.4	40.7	52.2	nd	34.5
Density	kg/m^3	860	900	860	870	nd	860
Viscosity	mPa.s	2.0	21.7	2.3	6.4	nd	2.0
Water content	%w/w	0.5	0.5	0.5	0.5	nd	0.5
Heating Value	MJ/kg	39.9	39.2	40.0	40.1	nd	39.5

Run #		**13**	**14**	**15**	**16**	**17**	**18**
Temperature	^{o}C	600	800	800	800	800	500
Q. chip size	mm	1.7-2.4	1.7-2.4	1.7-2.4	1.7-2.4	1.7-2.4	1.7-2.4
Carrier gas (N_2)	cm^3/min	70	10	50	70	30	30
Pump type		Syinge	Syinge	Syinge	Syinge	Syinge	Syinge
Lard fed	g	2.2	2.5	2.6	2.5	2.5	2.5
S/L mass ratio		0	0	0	0	0	0
Duration	min	30	30	30	30	30	30
Gas	g	0.7	1.6	1.9	2.0	2.0	0.1
Liquid	g	1.3	0.6	0.3	0.2	0.1	2.1
Char + Residue	g	0.1	0.2	0.2	0.2	0.1	0.1
Material Balance	g	2.0	2.3	2.4	2.4	2.3	2.3
	wt%	93.1	93.8	91	94.7	90.7	92.2
Gas composition and heating value							
H_2		0	9.4	8.7	7.9	8.6	0
CO		10.2	8.8	8.9	8.6	8.6	12.2
CO_2		14.7	5	6.8	5	4.7	8.6
CH_4		10.3	25.3	23.9	22.7	27.1	8.8
C_2H_4		23.4	33.8	35.9	37.7	36.7	22.5
C_2H_6		6.9	4.3	3.5	3.2	3.9	8.3
C_3H_6		15.1	7.2	6.5	7.6	5.9	14.1
C_3H_8		0.8	0.2	0.1	0.1	0.1	1.9
C_{4+}		10.6	6	5.7	7.2	4.6	23.6
H_2+CO		10.2	18.2	17.6	16.5	17.2	12.2
H_2/CO		0.00	1.07	0.98	0.92	1.00	0.00
Heating Value	MJ/m^3	119.4	70.5	70.2	74.9	67.6	126.5
Liquid product characterization							
Diesel-like liq	g/100g lard	38.4	16.9	10.7	6.1	1.9	19.7
Cetane Index		38.7	nd	nd	nd	nd	47.8
Density	kg/m^3	860	nd	nd	nd	nd	880
Viscosity	mPa.s	1.8	nd	nd	nd	nd	18.3
Water content	%w/w	0.5	nd	nd	nd	nd	0.5
Heating Value	MJ/kg	39.6	nd	nd	nd	nd	40.1

Run #		**19**	**20**	**21**	**22**	**23**	**24**
Temperature	^{o}C	600	700	500	550	600	550
Q. chip size	mm	1.7-2.4	1.7-2.4	0.7-1.4	0.7-1.4	0.7-1.4	0.7-1.4
Carrier gas (N_2)	cm^3/min	30	30	50	50	50	50
Pump type		Syinge	Syinge	Syinge	Syinge	Syinge	Syinge
Lard fed	g	2.6	2.2	2.5	2.5	2.8	2.5
S/L mass ratio		0	0	0	0	0	0
Duration	min	30	30	30	30	30	30
Gas	g	1.2	1.7	0.1	0.4	1.1	0.4
Liquid	g	1.1	0.2	1.9	2.0	1.5	1.8
Char + Residue	g	0.1	0.1	0.4	0.2	0.1	0.3
Material Balance	g	2.5	2.1	2.4	2.5	2.7	2.5
	wt%	94.5	92.8	95.2	99.4	95.3	99.5
Gas composition and heating value							
H_2		0	3.4	0	0	0	0
CO		9.2	7.3	0	10.5	9	9.4
CO_2		3.9	3.4	13.9	5.1	3.6	4.6
CH_4		11.6	15.7	8.3	9.1	11	8.4
C_2H_4		28.1	31.5	22.3	24.1	27	21.6
C_2H_6		7.5	5.8	7.9	7.5	7.6	7.3
C_3H_6		17.7	18	15.4	15.2	17.1	10
C_3H_8		0.7	0.4	1.4	0.9	0.8	1.1
C_{4+}		21.3	14.5	30.9	27.5	24	33.5
H_2+CO		9.2	10.7	0	10.5	9	9.4
H_2/CO		0.00	0.47	0.00	0.00	0.00	0.00
Heating Value	MJ/m^3	124.1	104.0	165.2	135.6	130.0	147.6
Liquid product characterization							
Diesel-like liq	g/100g lard	31.2	6.9	16.4	28.1	31.8	30.7
Cetane Index		19.9	nd	53.6	50.4	45.8	50.3
Density	kg/m^3	870	nd	870	880	860	880
Viscosity	mPa.s	3.8	nd	22.1	12.4	4.5	10.6
Water content	%w/w	0.5	nd	0.5	0.5	0.5	0.5
Heating Value	MJ/kg	39.2	nd	39.5	39.5	38.4	40.0

Run #		**25**	**26**	**27**	**28**	**29**	**30**
Temperature	^{o}C	550	550	550	650	700	600
Q. chip size	mm	0.7-1.4	0.7-1.4	0.7-1.4	0.7-1.4	0.7-1.4	0.7-1.4
Carrier gas (N_2)	cm^3/min	50	50	50	50	50	50
Pump type		Syinge	Syinge	Syinge	Syinge	Syinge	Syinge
Lard fed	g	2.5	2.5	2.5	2.5	2.0	2.9
S/L mass ratio		0	0	0	0	0	0
Duration	min	30	30	30	30	30	30
Gas	g	0.4	0.4	0.4	1.6	1.6	1.5
Liquid	g	1.6	1.9	1.8	0.6	0.2	1.1
Char + Residue	g	0.4	0.2	0.2	0.2	0.2	0.1
Material Balance	g	2.4	2.5	2.3	2.3	1.9	2.6
	wt%	97.2	98.0	93.0	93.8	95.5	92.0
Gas composition and heating value							
H_2		0	0	0	0	3.7	0
CO		9.8	10.6	11.3	8.4	7.3	11.1
CO_2		4.5	5.1	5.4	3.6	5	7
CH_4		9.5	9.5	9	13	14.1	11
C_2H_4		24.6	24.6	23.5	28.7	30.7	25.9
C_2H_6		7.8	8	7.7	6.7	4.9	7.2
C_3H_6		15.6	15.6	15	18.7	17.5	16.8
C_3H_8		1	1.1	1	0.6	0.4	0.8
C_{4+}		27.1	25.4	27.2	20.5	16.4	20.1
H_2+CO		9.8	10.6	11.3	8.4	11	11.1
H_2/CO		0.00	0.00	0.00	0.00	0.51	0.00
Heating Value	MJ/m^3	135.8	131.6	134.6	122.8	108.7	119.8
Liquid product characterization							
Diesel-like liq	g/100g lard	31.4	37.2	38.2	12.3	10.8	24.3
Cetane Index		52.3	49.3	54.8	9.6	nd	34.4
Density	kg/m^3	870	880	860	860	nd	850
Viscosity	mPa.s	9.5	11.1	10.3	1.7	nd	2.9
Water content	%w/w	0.5	0.5	0.5	0.6	nd	0.5
Heating Value	MJ/kg	39.5	39.9	39.5	39.8	nd	39.8

Run #		**31**	**32**	**33**	**34**	**35**	**36**
Temperature	^{o}C	600	600	500	600	600	500
Q. chip size	mm	0.7-1.4	0.7-1.4	0.7-1.4	0.7-1.4	0.7-1.4	0.7-1.4
Carrier gas (N_2)	cm^3/min	0	0	0	0	0	0
Pump type		Syinge	Syinge	Syinge	Syinge	Syinge	Syinge
Lard fed	g	2.2	2.5	2.2	2.7	2.5	2.2
S/L mass ratio		0	4	1	1.5	1.5	1
Duration	min	30	30	30	30	30	30
Gas	g	1.1	0.5	0.3	0.5	0.7	0.2
Liquid	g	1.3	1.9	1.8	1.9	1.5	1.7
Char + Residue	g	0.1	0.1	0.03	0.1	0.1	0.2
Material Balance	g	2.0	2.5	2.1	2.5	2.3	2.1
	wt%	93.0	98.0	97.0	95.0	93.0	92.0
		Gas composition and heating value					
H_2		2.8	0	0	0	3.2	0
CO		11.9	11.1	0	12.7	14.5	0
CO_2		6.7	9.1	51.1	5.8	8.5	39.4
CH_4		13.1	10.0	1.0	13.3	12.9	2.0
C_2H_4		26	28.6	9.3	29.7	28.4	11.2
C_2H_6		8.9	5.5	1.3	9.0	8.0	3.1
C_3H_6		17	15.1	10	17.2	14.6	14.3
C_3H_8		1.2	0.5	0	1.1	0.8	0.7
C_{4+}		12.5	20.1	27.4	11.3	9.1	29.5
H_2+CO		14.7	11.1	0	12.7	17.7	0
H_2/CO		0.24	0.00	0.00	0.00	0.22	0.00
Heating Value	MJ/m^3	98.8	119.8	223.1	98.9	87.3	211.0
		Liquid product characterization					
Diesel-like liq	g/100g lard	40.9	24.5	32.4	38.9	35.7	19.8
Cetane Index		40.5	56.3	50.3	54.6	49.7	50.6
Density	kg/m^3	850	860	870	860	860	880
Viscosity	mPa.s	1.2	5.2	8.2	6.6	4.3	14.6
Water content	%w/w	0.5	1.0	1.1	0.9	0.9	1.0
Heating Value	MJ/kg	38.6	38.9	39.0	38.5	38.5	38.5

Run #		**37**	**38**	**39**	**40**	**41**	**42**
Temperature	^{o}C	600	600	600	800	550	500
Q. chip size	mm	0.7-1.4	0.7-1.4	0.7-1.4	0.7-1.4	0.7-1.4	0.7-1.4
Carrier gas (N_2)	cm^3/min	0	0	0	0	0	0
Pump type		Syinge	Syinge	Syinge	Syinge	Syinge	Syinge
Lard fed	g	2.4	2.5	2.7	2.5	2.5	2.5
S/L mass ratio		0.5	1	1	1	1	0.5
Duration	min	30	30	30	30	30	30
Gas	g	1.0	0.2	0.8	1.8	0.4	0.01
Liquid	g	1.1	1.2	1.7	0.3	1.7	2.0
Char + Residue	g	0.1	0.1	0.1	0.3	0.2	0.4
Material Balance	g	2.3	2.4	2.6	2.3	2.3	2.4
	wt%	96.0	94.0	97.0	97.0	90.0	96.0
Gas composition and heating value							
H_2		2.8	0	2.7	11	0	0
CO		12.6	9.1	12.6	9.3	17.1	0
CO_2		6.5	22.3	5.5	6.6	8.9	29.7
CH_4		14	9.9	13.2	21.4	30.2	6.5
C_2H_4		26.1	18.8	27	33.4	26.2	25.8
C_2H_6		9.1	5.2	8.8	4.2	5.4	4.6
C_3H_6		16.9	14.1	17.0	7.8	6.9	14.5
C_3H_8		1.2	0.7	1.1	0.3	0.6	1
C_{4+}		10.8	20	12.1	6.1	4.8	17.9
H_2+CO		15.4	9.1	15.3	20.3	17.1	0
H_2/CO		0.22	0.00	0.21	1.18	0.00	0.00
Heating Value	MJ/m^3	94.2	127.1	97.2	70.5	68.5	144.5
Liquid product characterization							
Diesel-like liq	g/100g lard	29.3	28.1	30.8	nd	34.4	25.7
Cetane Index		32.0	51.9	55.3	nd	51.8	53.3
Density	kg/m^3	850	860	860	nd	870	870
Viscosity	mPa.s	1.8	3.9	4.0	nd	7.0	15.8
Water content	%w/w	1.0	0.9	0.9	nd	0.9	1.0
Heating Value	MJ/kg	39.1	40.1	39.7	nd	39.8	39.2

Run #		**43**	**44**	**45**	**46**	**47**	**48**
Temperature	^oC	600	500	600	800	800	800
Q. chip size	mm	0.7-1.4	0.7-1.4	0.7-1.4	0.7-1.4	0.7-1.4	0.7-1.4
Carrier gas (N_2)	cm^3/min	50	0	0	0	0	0
Pump type		Syinge	Syinge	Syinge	Syinge	Syinge	Syinge
Lard fed	g	19.4	2.5	2.5	2.5	2.5	2.6
S/L mass ratio		0	1	3	1.5	1.5	2
Duration	min	225	30	30	30	30	30
Gas	g	9.2	0.03	0.1	1.9	2.0	2.1
Liquid	g	8.5	2.0	2.0	0.3	0.2	0.1
Char + Residue	g	0.1	0.2	0.4	0.1	0.2	0.4
Material Balance	g	17.8	2.3	2.4	2.4	2.4	2.6
	wt%	92.0	93.0	98.0	95.0	94.0	98.0
Gas composition and heating value							
H_2		0	0	0	8.8	10.2	11.4
CO		10.9	0	0	8.1	8.8	9
CO_2		4.7	50.2	68.3	6	7.2	6.2
CH_4		12.0	4.8	5.6	20	20.6	21.4
C_2H_4		27.2	21.7	13.8	36.4	35.1	34.9
C_2H_6		8.0	1.3	1.7	3.3	3.2	7.1
C_3H_6		17.2	7.8	4.4	8.5	7.4	7.1
C_3H_8		0.9	0	0	0.2	0.2	0.1
C_{4+}		19.1	14.2	6.1	8.7	7.4	6.4
H_2+CO		10.9	0	0	16.9	19	20.4
H_2/CO		0.0	0.00	0.00	1.09	1.16	1.27
Heating Value	MJ/m^3	116.4	142.0	115.9	78.9	73.8	70.3
Liquid product characterization							
Diesel-like liq	g/100g lard	25.0	18.1	36.1	8.1	5.6	2.2
Cetane Index		45.9	53.6	55.5	nd	nd	nd
Density	kg/m^3	845	870	860	nd	nd	nd
Viscosity	mPa.s	2.4	21.2	3.7	nd	nd	nd
Water content	%w/w	0.5	0.9	0.9	nd	nd	nd
Heating Value	MJ/kg	38.7	39.8	38.8	nd	nd	nd
Pour point	^oC	-18.0	nd	nd	nd	nd	nd
Cloud point	^oC	10.0	nd	nd	nd	nd	nd

Appendix D: Residence Time Calculation

Assumptions for calculating residence time of the reactant in the pyrolysis process

1. Residence time of the reactant was calculated based on the flow rate of carrier gas
2. Reactor bed volume was calculated on the basis of empty bed

Height of bed h = 7.0 cm
Radius of the reactor r = 0.5 cm
Volume of the reactor bed $V = \pi r^2 h$
$= 3.14 \times 0.5^2 \times 7.0 = 5.50\ cm^3$

For a volumetric flow rate of nitrogen of 50 cm^3/min (STP) and a reactor temperature T of 600°C

Actual volumetric flow rate in the reactor
$Q = 50\ cm^3/min \times 873.15/273.15 = 159.8\ cm^3/min$

Residence time $t = V / Q = 0.034$ min = 2.1 s

Table D-1 Residence time of reactant during pyrolysis at 600 and 800°C

Carrier gas flow rate at STP (mL/min)	Residence time (s)	
	600°C	800°C
10	10.3	8.4
30	3.4	2.8
50	2.1	1.7
60	1.7	1.4
70	1.5	1.2

Appendix E: Determination of the Heating Value of the Product Gas

Heating value of a fuel gas mixture can be calculated as the sum of the heating values of the components, each multiplied by the corresponding mole fraction, the sum so obtained being corrected for the compressibility of the mixture. The ideal gas mixture heating value is given by Wrobel and Wirght(1978) as

$CV_{ideal} = x_1 * CV_1 + x_2 * CV_2 + \ldots\ldots\ldots\ldots..$
where $x_1, x_2, \ldots$ are the mole fractions, CV_1, CV_2, ….. are the heating values.

The compressibility factor z_m for the mixture is calculated and the real gas heating value is given by:

$CV_{real} = CV_{ideal} / z_m$

The factor z_m is given by:
$z_m = 1-(x1*\sqrt{b1}+x2*\sqrt{b2}.....)^2 + 5 * 10^{-4} * (2*x_H - x_H^2)$
where b1,b2,……. are the gas law deviations of the components (except hydrogen)

b= 1-pV/RT
and x_H is the mol fraction of hydrogen present in the gas mixture.
Sample calculation of the heating value of the product gas is presented in Table E-1

Table E-1 Sample calculation of the product gas heating value for steam reforming experiment at 800°C and S/L of 2

Comp.	Total volume (cm^3)	Total moles	mol %	CV (MJ/m^3)	b	$x_i * b_i$	Total wt. (g)	CV (total) (MJ/m^3)
H_2	206.3	9.2E-03	11.4	12.1	0.00		0.02	1.6
CO	163.6	7.3E-03	9.0	12.0	0.02	0.014	0.20	1.2
CO_2	112.6	5.0E-03	6.2	0.0	0.06	0.016	0.22	0.0
Methane	387.8	1.7E-02	21.4	37.7	0.04	0.045	0.28	9.1
Ethylene	633.1	2.8E-02	34.9	59.7	0.08	0.097	0.79	23.6
Ethane	62.0	2.8E-03	3.4	66.1	0.09	0.010	0.08	2.6
propene	128.9	5.8E-03	7.1	87.1	0.13	0.025	0.24	7.0
propane	2.8	1.2E-04	0.2	93.9	0.13	0.001	0.01	0.2
1-butene	83.8	3.7E-03	4.6	115.0	0.17	0.019	0.21	6.0
i-butene	3.1	1.4E-04	0.2	114.3	0.18	0.001	0.01	0.2
n-butane	1.4	6.3E-05	0.1	121.8	0.18	0.000	0.00	0.1
cis/trans	6.2	2.7E-04	0.3	114.6	0.19	0.001	0.02	0.4
C_{5+}	20.9	9.3E-04	1.2	147.1	0.22	0.005	0.07	1.9
Product Gas	1812.4	0.0809	100		*z_m=	0.23 0.7654	2.15	70.3

Appendix F: Compounds Identified and Quantified by GC/MS

In order to determine the distribution of compounds in the liquid product, a semi-quantitative study was made by means of the percentage of area of the chromatographic peaks. It should be pointed out that these values do not represent the real concentration of the compounds. They serve to show the different composition of the pyrolysis fuel. Peaks with relatively weak intensity were not identified.

Table F-1 Compounds identified in GC/MS for the liquid product obtained during pyrolysis of lard at 500^{o}C, carrier gas flow rate of 30 cm^{3}/min, quartz particles packing height of 70 mm and size 1.7-2.4 mm

Components	scan no	peak area	area%
3-methyl-1-butanol	61	7.00E+06	0.69
cyclopentene	67	4.50E+06	0.44
1-hexene	71	1.10E+07	1.08
methyl-1,3 cyclopentadiene	83	4.40E+06	0.43
benzene	90	4.40E+06	0.43
1,5 hexadiene	94	5.30E+06	0.52
cyclohexene	93	5.30E+06	0.52
1-heptene	97	1.50E+07	1.47
ethylidenecyclopentane	115	4.00E+06	0.39
3-methyl-cyclohexene	124	3.90E+06	0.38
1-ethyl-3- methylene cyclobutane	133	3.30E+06	0.32
1,7-octadiene	156	5.30E+06	0.52
toulene	144	6.40E+06	0.63
1-octene	164	1.10E+07	1.08
octane	173	4.00E+06	0.39
cyclohexanone	181	3.80E+06	0.37
2-octene	190	3.10E+06	0.30
1,3 octadiene	207	4.00E+06	0.39
1-nonene	308	1.20E+07	1.18
cyclooctene	315	4.30E+07	4.21
1,3 nonadiene	366	4.00E+06	0.39
3,4 nonadiene	398	4.20E+06	0.41
1-decene	479	1.53E+07	1.50
decane	494	4.10E+06	0.40
cyclodecene	537	4.40E+06	0.43
11-octadecynoic acid	598	4.40E+06	0.43
1-undecene	648	1.70E+07	1.67
undecane	662	5.20E+06	0.51

2-undecene	682	4.80E+06	0.47
heptanoic acid	667	8.30E+06	0.81
1,4 undecadiene	703	8.40E+06	0.82
6-butyl-1,4-cycloheptadiene	733	4.00E+06	0.39
pentyl-benzene	748	5.20E+06	0.51
2,4 dodecadiene	758	4.20E+06	0.41
1,13 Tetradecadiene	799	3.80E+06	0.37
1-dodecene	806	1.70E+07	1.67
octanoic acid	813	5.00E+06	0.49
dodecane	818	4.80E+06	0.47
cyclododecyne	837	3.80E+06	0.37
cyclododecene	858	8.60E+06	0.84
2-methyl-bicyclo(2.2.1)-heptane	890	3.50E+06	0.34
1-tridecene	958	1.30E+07	1.27
tridecane	963	5.70E+06	0.56
1-pentadecene	1092	3.20E+07	3.14
decanoic acid	1103	1.50E+07	1.47
1- propenyl-cyclohexane	1170	4.80E+06	0.47
1-octadecene	1222	9.90E+06	0.97
hexadecane	1231	1.35E+07	1.32
9-octadecen-1-ol	1320	7.80E+06	0.76
1-hexadecene	1345	1.50E+07	1.47
1-octadecene	1442	9.70E+06	0.95
1-heptadecene	1462	6.00E+06	0.59
heptadecane	1470	8.00E+06	0.78
hexadecanal	1487	1.65E+07	1.62
tetradecanoic acid	1555	1.70E+07	1.67
9-octadecenal	1678	1.25E+07	1.23
2-nonadecanone	1685	7.50E+06	0.74
17-octadecenal	1705	6.80E+06	0.67
9-hexadecenoic acid	1736	8.00E+06	0.78
hexadecanoic acid	1796	1.00E+08	9.80
2-propenyl ester octadecanoic acid	1861	2.70E+07	2.65
2-hydroxycyclopentadecanone	1841	7.00E+06	0.69
2,3 -dihydroxypropyl ester-9-octadecenoic acid	1965	1.20E+08	11.76
octadecanoic acid	1983	1.05E+08	10.29
1-eicosanol	2022	4.30E+07	4.21
tricosane-2,4-dione	2046	2.30E+07	2.25
cyclotetracosane	2125	1.25E+07	1.23
octahydro-4,8a-dimethyl-4a(2H)-Naphthalenol	2154	1.00E+07	0.98
3-hydroxypropyl ester, oleic acid	2170	1.58E+07	1.55
2-hydroxy-1-(hydroxymethyl)ethyl ester, octadecanoic acid	2193	1.10E+07	1.08
1,2- benzenedicarboxylic acid, diisooctyl ester	2252	1.20E+07	1.18
11 haxacosyne	2267	1.55E+07	1.52
9-hexacosene	2287	9.00E+06	0.88
	sum	1.02E+09	100.00

Table F-2 Compounds identified in GC/MS for the liquid product obtained during pyrolysis of lard at 600^{o}C, carrier gas flow rate of 30 cm^{3}/min, quartz chips packing height of 70 mm and size 1.7-2.4 mm

Components	scan no	peak area	area %
cyclopentene	71	1.40E+07	0.44
2,4 dimethyl-1-heptene	66	1.25E+07	0.39
1-hexene	75	6.00E+07	1.87
2-methyl-1,3 pentadiene	80	2.50E+07	0.78
acetic acid	83	2.90E+07	0.90
trans-hexa-2,4-dienyl acetate	87	3.60E+07	1.12
1-methyl-cyclopentene	89	2.10E+07	0.65
benzene	92	4.30E+07	1.34
1,3-cyclohexadiene	95	2.90E+07	0.90
cycloheptane	102	8.10E+07	2.53
1-heptene	97	3.65E+07	1.14
3-methyl-cyclohexanol	106	1.00E+07	0.31
1,5-dimethylcyclopentene	112	8.10E+06	0.25
ethylidenecyclopentane	118	1.80E+07	0.56
3-methyl-cyclohexene	127	2.40E+07	0.75
methylene-cyclohexane	138	2.05E+07	0.64
toulene	146	5.10E+07	1.59
2-methyl-bicyclo(4.1.0)heptane	155	9.00E+06	0.28
cis-bicyclo(5.1.0)octane	162	6.20E+07	1.93
1-octene	171	7.50E+07	2.34
1-nonyne	179	1.30E+07	0.41
1,7-octadiene	187	9.00E+06	0.28
2-octene	196	7.00E+06	0.22
1,3-cycloheptadiene	201	7.50E+06	0.23
ethylidenecyclohexane	205	1.80E+07	0.56
1,3-octadiene	213	8.00E+06	0.25
3-methylfuran	223	1.50E+07	0.47
3-propylcyclopentene	239	7.50E+06	0.23
1-ethyl-cyclohexene	245	1.10E+07	0.34
2,4-octadiene	252	1.35E+07	0.42
ethylbenzene	260	2.20E+07	0.69
3-methyl-1,4-heptadiene	265	8.00E+06	0.25
p-xylene	276	1.60E+07	0.50
1-ethenyl-2-methyl-cyclohexane	285	9.00E+06	0.28
1-8-nonadiene	298	1.60E+07	0.50
benzenepropanoic acid	310	2.60E+07	0.81
1-nonene	315	7.00E+07	2.18
cyclooctene	321	5.90E+07	1.84
nonane	327	8.00E+06	0.25
3,6-nonadien-1-ol	335	9.00E+06	0.28
ethyl-cyclohexane	339	1.20E+07	0.37
1-propenyl-cyclohexane	358	1.10E+07	0.34

1,1'-dimethyl-1,1'-bicyclopropyl	365	9.00E+06	0.28
2-cyclohexen-1-one	376	1.30E+07	0.41
2-methyl-octyne	402	1.15E+07	0.36
propyl-benzene	412	1.85E+07	0.58
2-4-nonadiene	420	7.00E+06	0.22
1-ethyl-3-methyl-benzene	426	9.50E+06	0.30
1-methylethyl-benzene	432	1.00E+07	0.31
1,3-octadiene	437	6.00E+06	0.19
9-decen-1-ol	470	1.60E+07	0.50
phenyl propyl ester carbonic acid	472	1.20E+07	0.37
1-decene	486	8.30E+07	2.59
1-ethenyl-4-methyl-benzene	493	9.00E+06	0.28
tetradecane	499	8.00E+06	0.25
9,12,15-octadecatrienoic acid	509	9.00E+06	0.28
bicyclo(2.2.1)-5-heptene-2-carboxaldehyde	517	1.70E+07	0.53
1,3,5-trimethyl-benzene	526	9.00E+06	0.28
cyclohexanebutanol	533	9.20E+06	0.29
2-propenyl-benzene	540	1.30E+07	0.41
indane	547	1.00E+07	0.31
2,4-decadien-1-ol	551	1.00E+07	0.31
indene	563	1.60E+07	0.50
4,5-dimethyl-2,6-octadiene	570	1.60E+07	0.50
1-methyl-3-propyl-benzene	580	9.50E+06	0.30
butyl-benzene	588	1.80E+07	0.56
2-methyl-phenol	593	1.00E+07	0.31
bicyclo(3.3.1)nonane	602	2.10E+07	0.65
2,2-dimethyl-5-methylene-bicyclo(2.2.1)-heptane	618	1.00E+07	0.31
2,4,4-trimethyl-2-pentenal	631	9.50E+06	0.30
1-hexadecyne	639	1.00E+07	0.31
4-dodecen-2-yne	647	1.20E+07	0.37
1-dodecene	652	9.10E+07	2.84
3-nonen-1-ol	661	9.10E+06	0.28
5-undecene	674	1.60E+07	0.50
4-undecene	686	1.50E+07	0.47
methyl ester-12,15- octadecadienoic acid	704	1.60E+07	0.50
1,10-undecadiene	708	1.80E+07	0.56
4-methylindan	719	7.50E+06	0.23
1,5-diethenyl-2,3-dimethylcyclohexane	728	9.10E+06	0.28
3-methylindene	733	1.40E+07	0.44
2-methyl-5-(1-methylethenyl)-cyclohexanone	738	1.20E+07	0.37
pentyl-benzene	752	2.45E+07	0.76
1,1-dimethyl-propyl-benzene	776	5.00E+06	0.16
napthalene	790	1.40E+07	0.44
1,11-dodecadiene	797	1.20E+07	0.37
1-tridecene	812	8.90E+07	2.77
1,15-pentadecanediol	817	1.20E+07	0.37
cyclododecene	861	1.50E+07	0.47

6,9-pentadecadine-1-ol	869	1.30E+07	0.41
5,7-dodecadiene	879	1.30E+07	0.41
cyclobuta[1,2:3,4]dicyclopentene	906	2.05E+07	0.64
2,4-dodecadiene	912	1.30E+07	0.41
3-pentylfuran	922	1.40E+07	0.44
3-decen-1-ol	949	1.80E+07	0.56
8-nonenoic acid	964	1.50E+07	0.47
hexadecanoic acid	969	1.50E+07	0.47
alpha.,4-dimethyl-3-cyclohexene	1016	9.00E+06	0.28
3-hexadecene	1099	1.10E+08	3.43
1-tetradecanol	1100	2.80E+07	0.87
decanoic acid	1131	4.40E+07	1.37
1-propenylcyclohexane	1174	1.80E+07	0.56
1-undecenoic acid	1218	2.40E+07	0.75
9-eicosene	1227	6.80E+07	2.12
hexadecane	1236	3.25E+07	1.01
1,13-tetradecadiene	1324	3.80E+07	1.18
oleyl alcohol	1330	3.30E+07	1.03
dodecanoic acid	1337	1.40E+07	0.44
1-octadecene	1350	7.10E+07	2.21
1-decyl-cyclohexene	1364	1.30E+07	0.41
heptadecane	1438	2.40E+07	0.75
1-heptadecene	1466	2.20E+07	0.69
heneicosane	1474	1.50E+07	0.47
hexadecanal	1491	2.20E+07	0.69
tetradecanoic acid	1564	3.60E+07	1.12
1-nonadecene	1576	1.10E+07	0.34
cyclononanone	1654	2.20E+07	0.69
9-octadecenal	1682	1.30E+07	0.41
2-pentadecanone	1690	1.70E+07	0.53
15-octadecanal	1709	9.00E+06	0.28
9-hexadecenoic acid	1800	1.20E+08	3.74
hexadecanoic acid methyl ester	1715	3.00E+06	0.09
4-octyldodecyl-cyclopentane	1835	9.00E+06	0.28
1-docosene	1865	3.70E+07	1.15
2-nonadecanone	1890	1.10E+07	0.34
9-12-octadecadienoic acid	1899	1.28E+07	0.40
2-(9-12-octadecadienyloxy)-ethanol	1908	1.28E+07	0.40
oleic acid	1934	1.08E+08	3.37
stearic acid	1971	1.00E+08	3.12
1-cyclopentyl-4-(3-cyclopentylpropyl)-dodecane	2025	2.40E+07	0.75
oxacyclohexadecan-2-one	2037	1.60E+07	0.50
2-propenyl ester octadecanoic acid	2050	1.90E+07	0.59
octahydro-4,8a-dimethyl-4a(2H)-Naphthalenol	2158	1.45E+07	0.45
octadecanedioic acid	2076	7.90E+06	0.25
2-octyl-cyclopropaneoctanal	2083	9.00E+06	0.28
cyclotetracosane	2129	8.30E+06	0.26

diisooctyl ester,1,2-benzenedicarboxylic acid	2256	3.90E+07	1.22
	Total	3.21E+09	100.00

Table F-3 Compounds Identified in GC/MS for the liquid product obtained during pyrolysis of lard at 650^{o}C, carrier gas flow rate of 10 cm^{3}/min, quartz chips packing height of 70 mm and size 1.7-2.4 mm

Components	scan no	peak area	% area
2-methyl-3-buten-1-ol	58	1.60E+07	0.55
1,3-cyclopentadiene	62	3.00E+07	1.03
1-hexene	68	5.65E+07	1.95
trans-hexa-2,4-dienyl acetate	80	6.80E+07	2.34
ethenylmethyl-benzene	488	2.90E+07	1.00
benzene	84	1.00E+08	3.45
1-heptene	93	7.75E+07	2.67
1-ethyl-cyclopentene	110	2.40E+07	0.83
2,4 heptadiene	121	3.40E+07	1.17
1-decyne	130	1.90E+07	0.65
1,5-heptadien-3-yne	171	1.40E+07	0.48
toulene	140	9.60E+07	3.31
1,4-octadiene	153	3.55E+07	1.22
1-octene	162	7.00E+07	2.41
spiro[2.5]octane	199	1.50E+07	0.52
2-methyl-5-(1-methylethenyl)-2--cyclohexen-1-one	217	2.10E+07	0.72
1-ethenyl-3-methylene-cyclopentene	254	4.20E+07	1.45
p-Xylene	270	4.20E+07	1.45
12-heptadecyn-1-ol	278	7.50E+06	0.26
1,8-nonadiene	292	1.30E+07	0.45
styrene	301	9.10E+07	3.14
1-nonene	309	7.40E+07	2.55
cyclooctene	314	2.10E+07	0.72
1-propenyl-benzene	394	2.00E+07	0.69
(7S)-Trans-bicyclo(4.3.0)-3-nonen-7-ol	407	3.00E+07	1.03
1-ethyl-3-methyl-benzene	420	2.20E+07	0.76
1,3,5-trimethyl-benzene	425	2.00E+07	0.69
1,2,4-trimethyl-benzene	449	2.10E+07	0.72
alpha.-methylstyrene	456	1.35E+07	0.47
phenol	468	1.80E+07	0.62
1-decene	481	1.00E+08	3.45
bicyclo(2.2.1)-5-heptene-2-carboxaldehyde	513	2.30E+07	0.79
1-ethenyl-3-methyl-benzene	535	3.35E+07	1.15
2,2-dimethyl-5-methylene-bicyclo(2.2.1)-heptane	547	2.20E+07	0.76
Indene	561	4.70E+07	1.62
1-methyl-2-propyl-benzene	575	1.60E+07	0.55

butyl-benzene	582	2.80E+07	0.97
2-methyl-phenol	590	1.90E+07	0.65
3,4-diethenyl-cyclohexene	614	2.70E+07	0.93
1-ethenyl-3-ethyl-benzene	628	1.90E+07	0.65
2-norbornene	650	8.80E+07	3.03
3-methyl-1H indene	729	4.10E+07	1.41
1-methyl-1H indene	734	3.90E+07	1.34
pentyl-benzene	747	3.00E+07	1.03
1,2 -dihydro-naphthalene	754	4.90E+07	1.69
1-dodecene	800	8.40E+07	2.90
1-methyl-naphthalene	954	7.95E+07	2.74
1-ethylidene-1H indene	972	3.90E+07	1.34
biphenyl	1068	1.70E+07	0.59
hexadecene	1093	9.50E+07	3.27
decanoic acid	1119	4.00E+07	1.38
2-ethenyl-naphthalene	1135	1.60E+07	0.55
acenaphthylene	1156	1.80E+07	0.62
undecenoic acid	1211	2.25E+07	0.78
1-pentadecene	1221	5.00E+07	1.72
hexadecane	1231	3.40E+07	1.17
cyclododecene	1318	2.35E+07	0.81
2-propyl-1,1'-bicyclohexyl	1323	3.20E+07	1.10
1-octadecene	1344	5.40E+07	1.86
1-hexadecenoic acid	1432	2.10E+07	0.72
1,22-docosanediol	1440	1.30E+07	0.45
octadecene	1460	2.35E+07	0.81
octadecane	1469	2.05E+07	0.71
hexadecanal	1485	1.80E+07	0.62
phenanthrene	1550	2.70E+07	0.93
tetradecanoic acid	1555	2.90E+07	1.00
2-nonadecanone	1684	1.95E+07	0.67
hexadecanoic acid	1760	1.00E+08	3.45
2-propenyl ester octadecanoic acid	1858	1.70E+07	0.59
9-hexadecenoic acid	1925	6.20E+07	2.14
4-nonyn-1-ol	1940	5.10E+07	1.76
octadecanoic acid	1963	9.00E+07	3.10
diisooctyl ester,1,2-benzenedicarboxylic acid	2250	5.10E+07	1.76
2-propenyl-benzene	542	3.20E+07	1.10
		2.90E+09	100.00

Table F-4 Compounds identified in GC/MS for the liquid product obtained during pyrolysis of lard at 550^{o}C, carrier gas flow rate of 10 cm^{3}/min, quartz particles packing height of 70 mm and size 1.7-2.4 mm

Components	scan no	peak area	% area
2-methyl-1-propene	58	2.20E+07	1.4
1-pentene	62	4.90E+07	3.0
1,3 pentadiene	67	3.70E+07	2.3
hexane	73	8.10E+07	5.0
4-methyl-1-pentene	79	4.00E+07	2.5
acetic acid	82	3.40E+07	2.1
4-methyl-cyclopentene	85	3.40E+07	2.1
benzene	88	3.30E+07	2.0
1,7-octadiene	156	4.30E+07	2.6
cycloheptane	98	7.50E+07	4.6
ethylidenecyclopentane	114	1.30E+07	0.8
3-methyl-cyclohexene	124	2.50E+07	1.5
toulene	143	3.20E+07	2.0
1-octene	165	5.70E+07	3.5
1-nonene	308	3.40E+07	2.1
cyclooctene	318	6.80E+07	4.2
1-decene	482	6.00E+07	3.7
bicyclo(2.2.1)-5-heptene-2-carboxaldehyde	515	2.00E+07	1.2
methyl ester-11- octadecynoic acid	600	8.60E+06	0.5
1-undecene	650	5.80E+07	3.6
1-dodecene	808	5.50E+07	3.4
1-tridecene	955	4.50E+07	2.8
1-tetradecene	1095	8.20E+06	0.5
decanoic acid	1128	2.60E+07	1.6
13-heptadecyn-1-ol	1171	9.20E+06	0.6
1-pentadecene	1223	3.30E+07	2.0
hexadecane	1234	2.30E+07	1.4
1,13-tetradecadiene	1321	2.10E+07	1.3
1-octadecene	1347	4.30E+07	2.6
Oleyl alcohol	1435	1.38E+07	0.9
8-heptadecene	1443	1.32E+07	0.8
1-tetradecanol	1451	5.70E+06	0.4
1-nonadecene	1463	1.22E+07	0.8
heptadecane	1471	1.12E+07	0.7
tetradecanal	1489	2.32E+07	1.4
tetradecanoic acid	1560	2.32E+07	1.4
(Z)6-pentadecene-1-ol	1612	6.00E+06	0.4
octadecanedioic acid	1651	8.90E+06	0.5
9-octadecenal	1680	1.54E+07	0.9
2-heptadecanone	1688	2.40E+07	1.5
hexadecanal	1706	9.80E+06	0.6
1-docosene	1863	3.90E+07	2.4

2-nonadecanone	1888	1.54E+07	0.9
1-mono-Olein	1948	1.20E+08	7.4
octadecanoic acid	1978	1.20E+08	7.4
1-cyclopentyl-4-(3-cyclopentylpropyl)-dodecane	2023	3.10E+07	1.9
ally ester stearic acid	2047	1.90E+07	1.2
octahydro-4,8a-dimethyl-4a(2H)-Naphthalenol	2157	2.50E+07	1.5
		1.62E+09	100

Appendix G: Simulated Distillation Data

Table G-1 Simulated distillation data for the liquid product of lard pyrolysis and steam reforming at quartz chips packing height of 70 mm and size 0.7-1.4 mm

Mass (wt%)	Pyrolysis Carrier gas flow rate 50 cm^3/min			Steam Reforming steam to lard ratio 1:1		
	T: 500°C	T: 550°C	T: 600°C	T: 500°C	T: 550°C	T: 600°C
	Boiling point (°C)					
IBP	168.3	167.6	167.3	166.4	165.9	166.5
10	264.4	177.7	168.3	240.4	170.0	170.8
20	344.0	258.8	172.0	334.0	185.1	177.7
30	363.8	344.7	182.4	355.2	246.3	192.9
40	368.3	354.6	221.8	371.3	297.2	251.5
50	410.1	371.8	275.4	378.4	344.1	313.5
60	513.7	377.2	345.7	382.6	361.5	350.5
70	548.0	381.9	352.2	393.3	369.4	370.5
80	591.6	428.6	370.7	504.3	401.3	400.5
90	600.2	531.7	401.2	591.8	523.8	582.4
FBP	634.2	612.3	540.2	666.8	605.2	689.1

Table G-2 Simulated distillation data for the liquid product of lard pyrolysis at quartz chips packing height of 70 mm and size 1.7-2.4 mm

Mass (wt%)	Temperature 600°C			Temperature 800°C		
	N_2: 30 cm^3/min	N_2: 50 cm^3/min	N_2: 70 cm^3/min	N_2: 30 cm^3/min	N_2: 50 cm^3/min	N_2: 70 cm^3/min
	Boiling point (°C)					
IBP	169.6	170.3	170.6	170.8	170.3	170.7
10	170.8	171.7	171.9	177.2	171.4	174.0
20	171.7	173.3	173.7	178.2	172.2	177.4
30	174.1	180.4	177.2	178.8	173.3	178.2
40	182.7	199.6	189.3	179.3	174.7	178.8
50	209.3	252.8	230.9	180.0	177.9	184.6
60	261.6	318.5	283.5	186.4	178.9	195.1
70	352.4	362.9	359.7	198.9	179.4	204.7
80	367.1	404.3	382.7	208.4	180.2	273.8
90	403.4	464.3	432.7	288.8	195.8	372.0
FBP	537.5	568.4	549.5	458.9	284.1	501.0

Table G-3 Simulated distillation data for the liquid product during steam reforming of lard at quartz chips packing height of 70 mm and size 0.7-1.4 mm

Mass (wt%)	Steam Reforming steam to lard ratio 0.5:1		Steam Reforming steam to lard ratio 1.5:1	
	T: 500°C	T: 600°C	T: 600°C	T: 800°C
	Boiling point (°C)			
IBP	166.5	165.8	167.3	167.1
10	244.6	166.8	169.1	168.0
20	338.9	168.8	173.5	169.1
30	348.7	173.3	189.4	169.9
40	366.1	182.8	257.7	173.6
50	371.2	214.3	341.5	181.8
60	374.7	259.7	353.2	184.0
70	401.3	313.7	372.3	184.8
80	522.9	353.3	377.6	221.6
90	590.6	375.6	500.9	294.8
FBP	652.0	590.5	605.3	459.3

Appendix H: Energy Balance Calculation

Appendix H-1: Energy balance for the pyrolysis experiment

Properties of tristearin are readily available in the literature. It is thus chosen to represent the lard for the purpose of energy balance. The energy balance calculations are based on the following simplified cracking reaction.

$$\begin{array}{l} H_2C\text{-}OCO(CH_2)_{16}CH_3 \\ HC\text{-}OCO(CH_2)_{16}CH_3 \\ H_2C\text{-}OCO\,(CH_2)_{16}CH_3 \end{array} \quad = \quad 3C_{16}H_{34} + 2C_2H_4 + CO_2 + 4CO \qquad \text{(H-1)}$$

Basis: 1mole of tristearin (TS)

The feed is assumed to be at 25 ^{o}C and products at 600 ^{o}C

The properties of TS are given in Table H-1.

Calculation of heat required to preheat the feed to reaction temperature Qp

Heat required to take TS from 25^{o}C to melting point:
Q_1 = 1 mol x 1288.4 J/mol ^{o}C x (54.7-25)^{o}C = 38266.1 J

Heat required to melt TS at the melting point:
Q_2 = 1 mol x 93838.8 J/mol = 93838.8 J

Assuming the heat capacity is constant from melting point to boiling point,

Heat required to take TS from melting point (54.7^{o}C) to boiling point (505.8^{o}C):
Q_3 = 1 mol x 2201.3 J/mol ^{o}C x (505.8 -54.7^{o}C) = 993006 J

Heat required to vaporize TS at its boiling point:

Q_4 = 1 mol x 174900 J/mol = 174900 J

Heat required to take TS vapour from 505.8^{o}C to the reaction temperature (600^{o}C)

Q_5 = 1 mol x 2010.5 J/mol ^{o}C x (600 -505.8 ^{o}C) = 189389.1 J

Total energy required to preheat the feed to the reaction temperature:

$Q_p = Q_1 + Q_2 + Q_3 + Q_4 + Q_5$

Q_p = 1489400 J

Table H-1 Properties of Tristearin

Heat of vaporization, J/mol[a]	174900
Molecular wt[a]	890
Heat capacity as solid J/mol ^oC (22-mp)[b]	1288.4
Heat of fusion J/mol[b]	93838.8
Activation energy kJ/mol[a]	170.7
Heat capacity as liquid J/^oC mol[a]	2201.3
Heat capacity as gas J/^oC mol[a]	2010.5
Melting point[b] ^oC	54.7
Boiling point[a] ^oC	505.8

[a]Kishore and Shobha (1990) [b]O'Brien et al(2000)

Determination of the heat of reaction, Q_R

The specific heat capacities and heats of formation at 25^{o}C of CO, CO_2, C_2H_4 and $C_{16}H_{34}$ were obtained from Chemical Properties handbook by Yaws (1999). The data were used to evaluate the heat of reaction as stated below. The integration was done over $T_1 = 273$ K and $T_2 = 873$ K

$$\Delta H_r(C_{16}H_{34}) = 3*[\Delta H_f(C_{16}H_{34}) + \Delta C_p dT]$$

$$= 3x\ [-493 + \int (131.75 + 6.7397x\ 10^{-1}\ T + 8.777\ x\ 10^{-4}T^2 - 1.243\ x\ 10^{-6}T^3 + 3.9785x10^{-10}T^4)\ dT]$$

$$= 1053621\ J$$

$$\Delta H_r(C_2H_4) = 2*[\Delta H_f(C_2H_4) + \Delta C_p dT]$$

$$= 2\ x\ [52.3 + \int (32.083\ -1.4831x\ 10^{-2}\ T + 2.4774\ x\ 10^{-4}T^2 - 2.3766\ x\ 10^{-7}T^3 + 6.8274x10^{-11}T^4)dT]$$

$$= 78244.6\ J$$

$$\Delta H_r\ (CO_2) = 1*[\Delta H_f\ (CO_2) + \Delta C_p dT]$$

$$= 1\ x\ [-393.51 + \int (27.437 + 4.231x\ 10^{-2}T\ -1.9555\ x\ 10^{-5}T^2 + 3.9968\ x\ 10^{-9}T^3 - 2.9872x10^{-13}T^4)dT]$$

$$= 26006.5J$$

$$\Delta H_r\ (CO) = 4*[\Delta H_f\ (CO) + \Delta C_p dT]$$

$4 \times [-110.54 + \int (29.556 - 6.5807 \times 10^{-3}T + 2.013 \times 10^{-5}T^2 - 1.2227 \times 10^{-8}T^3 + 2.2617 \times 10^{-12}T^4)\, dT]$

$= 69714.8$ J

$\Delta H_r\,(TS) = 1*[\Delta H_f\,(TS) + \Delta C_p dT]$

The standard heat of formation of TS is obtained from its heat of combustion as follows

$57C(s) + 57O_2(g) = 57CO_2(g)$ $\quad \Delta H^o_{298} = (57)(-393{,}509)$ J

$55H_2(g) + 27½O_2(g) = 55H_2O(l)$ $\quad \Delta H^o_{298} = (55)(-285{,}830)$ J

$57CO_2(g) + 55H_2O(l) = C_{57}H_{110}O_6\,(s) + 81½O_2(g)$ $\quad \Delta H^o_{298} = 37760000$ J

$57C(s) + 55H_2(g) + 3O_2 = C_{57}H_{110}O_6\,(s)$ $\quad \Delta H^o_{298} = -390663$ J

And its $\Delta C_p dT$ is the same as Q_P calculated above less heat of fusion and vaporization

Thus

$(\Delta C_p dT)_{TS} = QP - Q2 - Q4$

$= 1489400 - 93838.8 - 174900 = 1220662$ J

Therefore,

$\Delta H_r\,(TS) = 1*(-390663 + 1220662) = 829998.6$ J

$\Delta H_r(\text{reaction}) = Q_R = \sum(\Delta H_r)_{product} - \sum(\Delta H_r)_{reactants}$

$= 78244.6 + 26006.5 + 69717.8 + 1053621 - 829998.6$

$= 397591.3$ J (endothermic)

The positive heat of reaction is confirmed by the TG/DTA analysis.

Total energy required is

$Q_T = Q_P + Q_R$

$= 1489400 + 397591.3$
$= 1886992$ J/mol TS

Accounting for 15% heat loss

$Q_{Tactual} = 2170040$ J/mol TS $= 2170.0$ kJ/mol TS

The enthalpies of combustion of the products at 25^{o}C are given by Yaws (1999) as:

CO (g): 283 kJ/mol
CO_2 (g): 0
C_2H_4 (g): 1322.6 kJ/mol
$C_{16}H_{34}$ (g): 9952.8 kJ/mol

Based of equation (H-1), total energy available in the product is:

Q_A= 3*(9952.8) + 2*(1322.6) + 4*(283) = 33635.6 kJ/ mol TS = 2.44 kJ/g

Therefore,
for the pyrolysis reaction, the net energy gain is
33635.6 – 2170.0 = **31465.6 k**J/ mol TS (Based on stoichiometry)

Evaluation of heat obtainable from products from material balance

From the material balance (Appendix B-1),

Total mole of ethylene produced per 2.79 g of lard was
= 7.26E-03 gmole

Assuming all lard is TS, mole of TS in lard fed
=2.79 g/ 891g/gmole
= 0.003131 gmole

Therefore mole of ethylene produced per mole of lard fed was
2.32 mole ethylene/mol lard

Similarly for CO,

Mole produced from material balance = 3.23E-03 mole
Mole of CO produced per mole of lard fed is
1.03 mole CO/mole lard
Using the enthalpy of combustion of these compounds, heat recoverable from the gas products is
2.32 x 1322.6 kJ/mol +1.03 x 283 kJ/mol =3358.4 kJ/mol lard = 3.8 kJ/g of lard fed

The liquid product obtained was not analyzed so the energy recoverable from the liquid is based on the heating value of the liquid.

From Appendix B-1, 1.48 g of liquid was produced per 2.79 g of lard fed
i.e. 1.48 / 2.79 g = 0.530466g of liquid/ g of lard fed

From Appendix C-2, the heating value of this liquid is (Run #23) 38.44 kJ/g
Therefore heat recoverable from the liquid is

0.530466g of liquid/ g of lard fed x 38.44 kJ/g of liquid
20.4 kJ/g of lard fed

Total heat recoverable from products = 3.8+20.4 = **24.2kJ/g of lard**

The net heat gain
24.2 – 2.4 = **21.8 kJ/g lard**

Appendix H-2: Energy balance for steam reforming of lard for the case of steam to lard ratio (S/L) of 1 (Basis 1 mol TS)

1 mole tristearin = 891 g
Therefore for S/L of 1,
891 g of water = 49.5 moles is fed.

The energy balance is done for the reaction

$$\begin{array}{l} H_2C\text{-}OCO(CH_2)_{16}CH_3 \\ HC\text{-}OCO(CH_2)_{16}CH_3 + 49.5\ H_2O = 3C_{16}H_{34} + 2C_2H_4 + CO_2 + 4CO + 49.5\ H_2O \\ H_2C\text{-}OCO\ (CH_2)_{16}CH_3 \end{array}$$

Calculation of the heat required for the feed water

Boiling temperature of water is 100^{o}C at 1 atm

Heat capacity of liquid water is given by the expression,
$Cp_L = 8.712 + 1.25x\ 10^{-3}T - 1.8x\ 10^{-7}T^2$ J/mol.K

Energy required to take liquid water from 25^{o}C to 100^{o}C is:
$Q6 = 49.5\ mol \times \int Cp_L dT = 33825.33$ J

Heat of vaporization of water at 1 atm is 40656 J/mol

Energy required to vaporise the water at 100^{o}C is
Q7 = 49.5 mol x 40656J/mol = 2012472 J

Heat capacity of water vapour is given by the expression
$Cp_g = 32.24 + 1.924x10^{-3}T + 1.055x10^{-5}T^2 - 3.596x10^{-9}T^3$

Energy required to take water from 100^{o}C to reaction temperature of 600^{o}C is
$Q8 = 49.5\ mol \times \int Cp_g\, dT = 909315$ J

Total energy required to take liquid water to the reaction temperature is
$Q_W = Q_6 + Q_7 + Q_8$
$= 33825.33 + 2012472 + 909315 = 2955612$ J

Assuming water did not take part in the reaction,

Total heat required for this reaction is
$Q_{TW} = Q_T + Q_W$
$= 1886992 + 2955612 = 4842604$ J/mol TS = **4842.6 kJ/mol TS**

Accounting for 15% heat loss

$Q_{TWactual}$ = 5569.0 kJ/ mol TS

As calculated in Appendix H-1, total energy available in the product is:
Q_A= 3*(9952.8) + 2*(1322.6) + 4*(283) = 33635.6 kJ/ mol TS = 6.25 kJ/g

Therefore,
for the steam reforming reaction, the net energy gain is
33635.6 – 5569.0 = **28066.6 k**J/ mol of TS (based on stoichimetery)

Calculation of heat obtainable from the steam reforming products from material balance

From the material balance Appendix B-2,
Total mole of ethylene produced per 2.68 g of lard was = 6.77E-03gmole

Assuming all lard is TS, mole of TS in lard fed
=2.68 g/ 891g/gmole
= 0.003008 gmole

Therefore mole of ethylene produced per mole of lard fed was
2.25 mole ethylene/mol lard
Similarly for CO,

Mole produced from material balance = 3.17E-03mole
Mole of CO produced per mole of lard fed is 1.05 mole CO/mole lard

Using the enthalpy of combustion of these compounds, heat recoverable from the gas products is
2.25 x 1322.6 kJ/mol +1.05 x 283 kJ/mol =3275.13 kJ/mol lard =3.7 kJ/g

The liquid product for this condition was not analyzed so the energy recoverable from the liquid is based on the heating value of the liquid.

From Appendix B-2, 1.48 g of liquid was produced per 2.79 g of lard fed
i.e. 1.65 / 2.68 g = 0.615672 g of liquid/ g of lard fed

From Appendix C-2, the heating value of this liquid is (Run #39) 39.7 kJ/g
Therefore heat recoverable from the liquid is
0.615672 g of liquid/ g of lard fed x 39.7 kJ/g of liquid

24.45 kJ/g of lard fed

Total heat recoverable from products = 3.7+24.5 = 28.2 kJ/g of lard
The net heat gain
28.2 – 6.3 = **21.9 kJ/g lard**